EPRI | ELECTRIC POWER RESEARCH INSTITUTE

2008-131 BWR Vessel & Internals Project (BWRVIP)

April 23, 2008

Document Control Desk
U. S. Nuclear Regulatory Commission
11555 Rockville Pike
Rockville, MD 20852

Attention: Vanice Perin

Subject: Transmittal of NEDO 10174 to Support NRC review of a revision to Section 4.0 of BWRVIP-06A

The purpose of this memo is to provide a copy of GEH NEDO-10174 "Consequences of a Postulated Flow Blockage Incident in a Boiling Water Reactor" in response to a request from NRC during a conference call on March 10, 2008.

The BWRVIP has previously submitted a revision to Section 4.0 of BWRVIP-06A for NRC review. NRC has provided Requests for Additional Information (RAIs) on this document and BWRVIP has provided responses to these RAIs.

A conference call between BWRVIP and NRC representatives was conducted on March 10, 2008 to discuss BWRVIP responses to NRC RAIs on Section 4.0 of BWRVIP-06A (a list of participants is provided in Attachment 1). During the conference call, NRC requested that BWRVIP provide a copy of GEH NEDO-10174 "Consequences of a Postulated Flow Blockage Incident in a Boiling Water Reactor" to support their review of Section 4.0 of BWRVIP-06A.

In response to this request, copy of NEDO-10174 is provided (Attachment 2). This is a non-proprietary report.



**PALO ALTO OFFICE**
3420 Hillview Avenue, Palo Alto, CA 94304-1338 USA • 650.855.2000 • Customer Service 800.313.3774 • www.epri.com

T008
Add: Vanice Perin

If you have any questions regarding the transmittal discussed above, please contact Charles Wirtz at First Energy by telephone at 440.280.7665 or by e-mail at cjwirtz@firstenergycorp.com or Randy Stark at EPRI by telephone at 650.855.2122 or by e-mail at rstark@epri.com.

Sincerely,

Rick Libra

Rick Libra, Exelon
Chairman, BWR Vessel and Internals Project

c: BWRVIP Technical Chairs
BWRVIP EPRI Task Managers
Randy Bunt (SNOC)
Sharon Eldridge (Exelon)

Attachment 1
List of Participants in
BWRVIP-NRC Conference Call on BWRVIP-139
March 10, 2008

| Name | Organization |
|---|---|
| Chakrapani Basavaraju | NRC |
| Bob Carter | EPRI |
| Ganesh Cheruvenki | NRC |
| Ron Horn | GEH |
| John Hosler | EPRI |
| Dan Pappone | GEH |
| Vanice Perin | NRC |
| Patrick Sekerak | NRC |
| Tom Scarbrough | NRC |
| Jon Thompson | NRC |
| Chuck Wirtz | FENOC |

J. KLAPROTH
JL Castillo

NEDO-10174
Revision 1
CLASS I
OCTOBER 1977

LICENSING TOPICAL REPORT

# CONSEQUENCES OF A POSTULATED FLOW BLOCKAGE INCIDENT IN A BOILING WATER REACTOR

GENERAL ELECTRIC

NEDO-10174
Revision 1
Class I
October 1977

LICENSING TOPICAL REPORT

# CONSEQUENCES OF A POSTULATED FLOW BLOCKAGE INCIDENT IN A BOILING WATER REACTOR

Approved: J. Jacobson / N. J. Bigliani
J. Jacobson, Manager
Reactor Design

Approved: F. D. Judge
F. D. Judge, Manager
Systems Design

Approved: R. A. Proebstle
R. A. Proebstle, Manager
Applied Metallurgy and Chemistry

BOILING WATER REACTOR PROJECTS DEPARTMENT • GENERAL ELECTRIC COMPANY
SAN JOSE, CALIFORNIA 95125

GENERAL ELECTRIC

## DISCLAIMER OF RESPONSIBILITY

*This document was prepared by or for the General Electric Company. Neither the General Electric Company nor any of the contributors to this document:*

A. *Makes any warranty or representation, express or implied, with respect to the accuracy, completeness, or usefulness of the information contained in this document, or that the use of any information disclosed in this document may not infringe privately owned rights; or*

B. *Assumes any responsibility for liability or damage of any kind which may result from the use of any information disclosed in this document.*

TABLE OF CONTENTS

TABLE OF CONTENTS (Continued)

TABLE OF CONTENTS (Continued)

# LIST OF ILLUSTRATIONS

LIST OF ILLUSTRATIONS (Continued)

LIST OF ILLUSTRATIONS (Continued)

LIST OF TABLES

*ABSTRACT*

*The effects of a fuel bundle flow blockage in a boiling water reactor have been investigated. The consequences in terms of fuel damage, fission product release, local high-pressure production, and possible propagation to adjacent assemblies have been evaluated. The conclusions reached are that a flow blockage incident will not result in local high-pressure production, propagation to adjacent assemblies, or off-site doses in excess of small fractions of 10CFR100 guidelines.*

*ACKNOWLEDGMENTS*

*This report originally prepared by G. J. Scatena, has been revised by B. J. Gitnick, K. W. Holtzclaw, R. J. Pederson, A. S. Rao, J. R. Redding, P. J. Savoia, O. S. Wang, and D. G. Weis to reflect changes in more recent products.*

*The authors wish to express their appreciation for valuable contributions by J. S. Armijo, W. R. DeHollander, J. D. Duncan, T. Y. Fukushima, E. W. Giambalvo, C. S. Heller, H. R. Helmholz, N. R. Horton, J. D. James, J. E. Jones, C. C. Lin, M. O. Marlowe, S. L. Mather, L. D. Noble, E. Plaza-meyer, J. C. Rawlings, D. R. Rutkin, D. R. Shiflett, J. S. Wiley, and R. D. Williams.*

# 1. INTRODUCTION

## 1.1 BACKGROUND AND PURPOSE

In 1967, the Advisory Committee on Reactor Safeguards in a report on Browns Ferry Units 1 and 2 indicated a concern relative to the potential of melting and subsequent disintegration of a portion of a fuel assembly due to inlet orifice flow blockage. It was indicated in that report that information should be developed to show that such an incident would not lead to unacceptable fission product release, local high pressure production, and possible propagation of failure to adjacent fuel assemblies. The basis for the concern evolved from the intentional destructive transients imposed on the BORAX-1 and SPERT-1 nuclear test reactors, along with the accident that occurred at the SL-1 reactor. In both BORAX-1 and SPERT-1 multi-thousand psi pressure pulses occurred which damaged portions of the cores. In the SL-1 reactor core, there was no direct evidence to indicate whether a pressure pulse of comparable magnitude occurred; however, a water-hammer pressure pulse did occur when the core water impacted the pressure vessel head.

In response to the ACRS request, General Electric Company provided the report, "Consequences of a Postulated Flow Blockage Incident in a Boiling Water Reactor" NEDO-10174, May 1970. This report addressed the coolant thermal hydraulic and nuclear effects resulting from a flow blockage, fuel rod and channel thermal effects, the potential for molten $UO_2$/Zr-2-water interaction, and the radiological aspects associated with a flow blockage incident.

In early 1977, as a result of NRC review of NEDE-20944-P[1.1], the applicability of NEDO-10174 to more recent fuel designs was questioned. General Electric committed to revising NEDO-10174 (which addressed 7x7 fuel- the standard product line design at that time) with particular consideration of the following items:

(1) Geometric features of 8x8 fuel with bypass holes drilled in the lower tie plate casting,

(2) Present approved GE thermal-hydraulic correlation GEXL,

(3) Coolant fallback from top of core or steam separators,

(4) Higher power in a voided bundle as suggested by INEL calculations for the PBF program (roughly 70% vs. 48%), and

(5) The response of the main steam line instrumentation in detecting the postulated fuel failures, thereby furnishing the assurance that the failures will not propagate into adjacent bundles or cause problems with control rod insertion.

It is the purpose of this report to revise NEDO-10174 by addressing these items.

## 1.2 GENERAL DESCRIPTION OF APPROACH

Generally there are two ways in which the suggested incident could be initiated. One way would be through a loss of coolant in a fuel channel, while the other way would be through a nuclear excursion. With regard to nuclear excursions, which are discussed in Section 7, the inherent reactor design, combined with engineered safeguards, limits the peak fuel enthalpies during the worst control rod drop accident to below 425 cal/gm, which is estimated to be the threshold for immediate rupture of fuel rods due to $UO_2$ vapor pressure. Therefore, it does not appear that design basis nuclear excursion accidents could lead to any kind of a propagation event. The only damage expected would be failed fuel rods. Thus, partial or complete blockage of inlet coolant flow to a fuel bundle during normal power operation can be hypothesized as the only possible mechanism for initiating conditions where molten metal and water may interact.

A flow blockage accident is very unlikely. In the 260 reactor years of light water reactor operation, no fuel damage attributable to bundle flow blockages have occurred. However, flow blockages have occurred in other types of reactors. The Enrico Fermi Reactor[1.2] in 1966 experienced a blockage which resulted in fuel melting. Another incidence of a flow blockage was reported in the Materials Test Reactor (MTR) in 1962[1.3]. In the Engineering Test Reactor (ETR),[1.4] a partial flow blockage caused cracks in six fuel elements. Thus, experience indicates that flow blockages are a possibility. However, this report will show that flow blockages will not lead to unacceptable conditions in a BWR.

In assessing the consequences of a flow blockage incident, several different aspects of a "cause and effect" type have to be examined to fully explain the possible sequence of events. Figure 1-1 is a block diagram describing the scope of the analytical and test work performed in meeting the objectives of this report. The diagram can also serve as a description of the chain of phenomenological events that may occur during a flow blockage. As can be seen, the complete evaluation of a flow blockage incident is a complex and detailed task. In many cases, the state of the art prevented an accurate determination of the results. However, in circumstances such as these, conservative assumptions were made in the analyses and, where possible, experimental results from tests performed by either the General Electric Company or by other investigators were used.

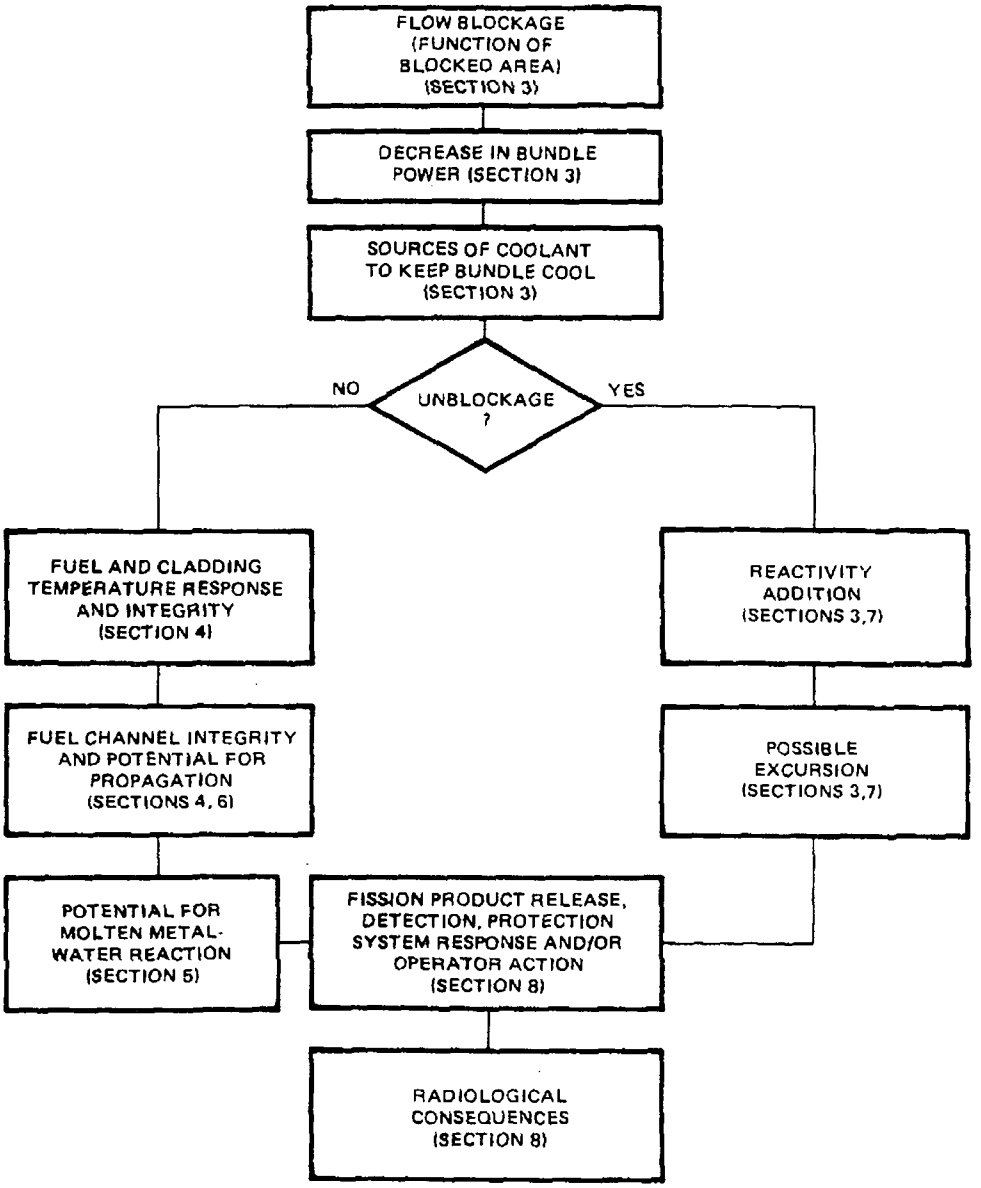


Figure 1-1. Scope of Flow Blockage Investigation

## 2. SUMMARY OF CONCLUSIONS

The only mechanism capable of causing a major flow blockage is that induced by a foreign object. Fragmentation, crudding or fuel swelling cannot cause major flow blockages. Even though it is possible for minor blockages to occur by small objects entering the fuel bundle and affecting the life of the fuel, it is unlikely that a blockage which would induce a significant flow reduction will occur. A fuel assembly is capable of withstanding very severe blockages before losing adequate cooling. The consequences of the full range of postulated flow blockage incidents are summarized in Table 2-1.

For orifice blockages greater than 98%, fuel and cladding melt are expected to occur, however this will not result in:

a. failure propagation to adjacent assemblies,

b. Local high pressure production, or

c. offsite doses in excess of small fractions of 10CFR100 guidelines.

For this postulated worst case event, no action is required of the Reactor Protection System to ensure the above results. However, the reactor will be scrammed by the Main Steam Line Radiation Monitor.

For orifice blockages between 95 and 98%, cladding melting is expected but fuel melting is not calculated. For this case, the Offgas Radiation Monitor will provide an alarm to the reactor operator. Depending on the conditions of the event, the Main Steam Line Radiation Monitor may provide a reactor scram. For this degree of blockage the consequences are less severe than for the postulated worst case described above.

For orifice blockages between 79 and 95%, boiling transition and attendant cladding heatup is calculated to occur. No cladding and/or fuel melting is

Table 2-1

CONSEQUENCES OF POSTULATED
FLOW BLOCKAGES

| Percentage of Orifice Blockage | Percent of Rated Flow | Cladding State/Environment | Fuel State | Detection System Response |
|---|---|---|---|---|
| >98 | > 5 | melt | melt | Main Steam Line Radiation Monitor trip resulting in reactor scram |
| >95 | <14 | incipient melt | solid | Offgas Radiation Monitor resulting in Control Room Alarm<br><br>Potential Main Steam Line Radiation Monitor trip resulting in reactor scram |
| >79 | <41 | subject to boiling transition | solid | Potential Offgas Radiation Monitor resulting in Control Room Alarm |
| <79 | >41 | nucleate boiling | solid | No action required |

calculated, however, cladding failure is not precluded. The offgas Radiation Monitor will provide an alarm to the reactor operator if fission product release are significant.

For orifice blockages less than 79%, nucleate boiling is maintained, therefore the fuel and cladding are unaffected.

# 3. COOLANT THERMAL HYDRAULICS AND NUCLEAR EFFECTS AS A RESULT OF A FLOW BLOCKAGE

The effect of a flow blockage on the coolant flow and the nuclear channel power in a BWR fuel assembly will be evaluated in this section. The magnitudes of coolant flow and power decrease resulting from various degrees of blockages as well as the mechanisms that may be responsible for such blockages will be investigated. Other pertinent factors such as detection by in-core instrumentation and the possibility of downflow into the channel will also be discussed. The effects of the blockage on the cladding and fuel integrity will be discussed in Section 4.

## 3.1 MECHANISMS CAPABLE OF INDUCING A FLOW BLOCKAGE

In discussing the mechanisms which are capable of restricting the flow of coolant to a fuel assembly, it is first necessary to describe the geometrical configuration of a fuel bundle. This will indicate the most probable blockage locations and the degree of difficulty involved in blocking the coolant flow path.

Figure 3-1 is a schematic of a typical boiling water reactor (BWR). Coolant to the flow channels is provided by two recirculation pumps which circulate water via a jet pump system. The flow exits from the jet pump diffuser and enters the lower plenum (Figure 3-2) which contains a forest of control rod guide tubes.

These tubes, approximately 10.9 inches in diameter, are spaced on a 12-inch pitch. The guide tubes support four individual fuel assemblies, except for the guide tubes on the periphery of the core, which support only one assembly. The configuration is depicted in Figure 3-3. The flow from the lower plenum enters the fuel channel through an orifice located in the support piece. This orifice is typically 1.5 to 2.5 inches in diameter. The fuel assembly which rests on the support piece consists of a fuel bundle and a channel which surrounds it as shown in Figure 3-4. The fuel bundle itself contains 62 fuel rods and 2 water rods which are spaced and supported in a square 8x8 array by the lower and upper tie plates. The lower tie plate has a nosepiece which fits into fuel support piece and distributes coolant flow from the fuel support piece to the fuel rods. Both tie plates are fabricated from Type-304 stainless steel.

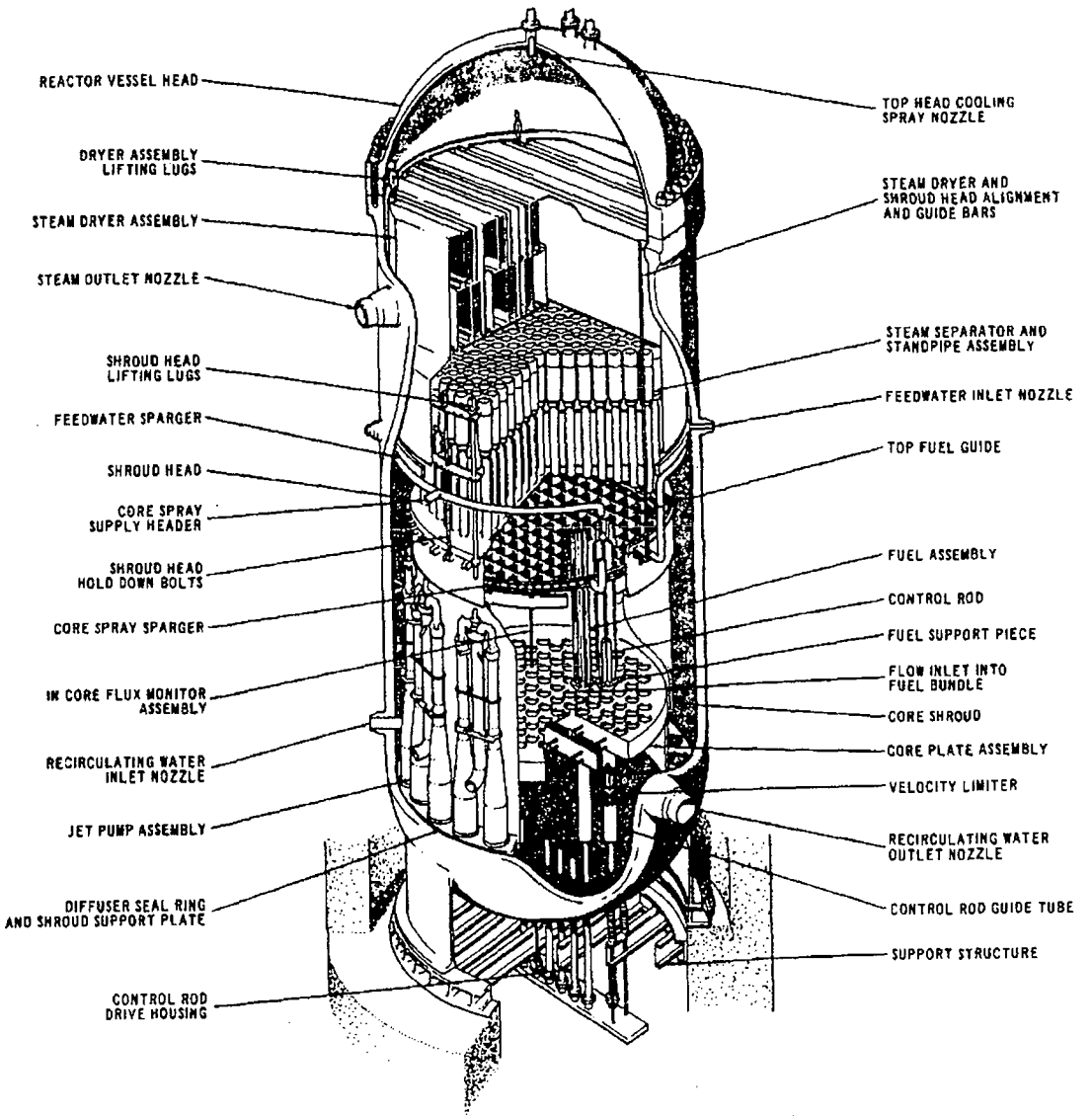


Figure 3-1. General Electric Boiling Water Reactor

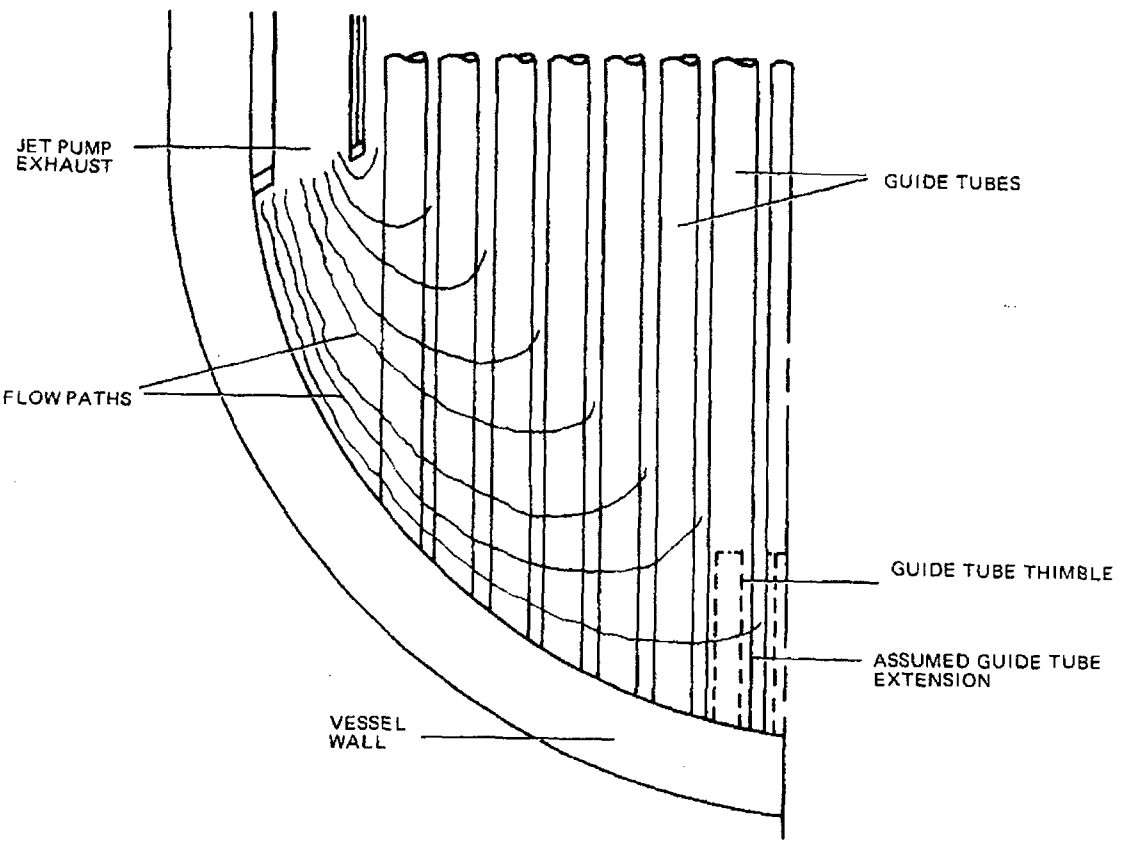


Figure 3-2. Lower Plenum Configuration

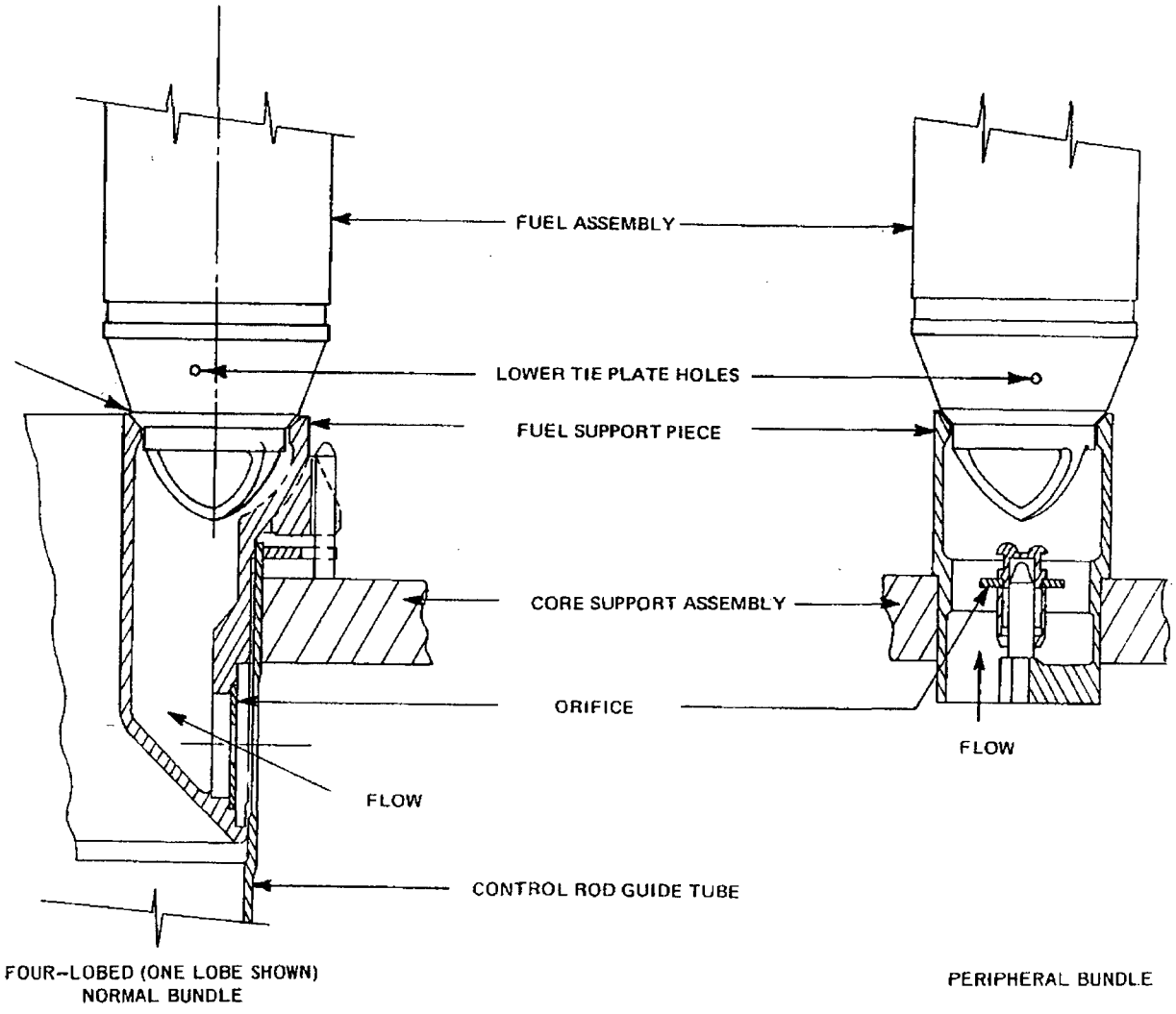


Figure 3-3. Fuel Support Pieces

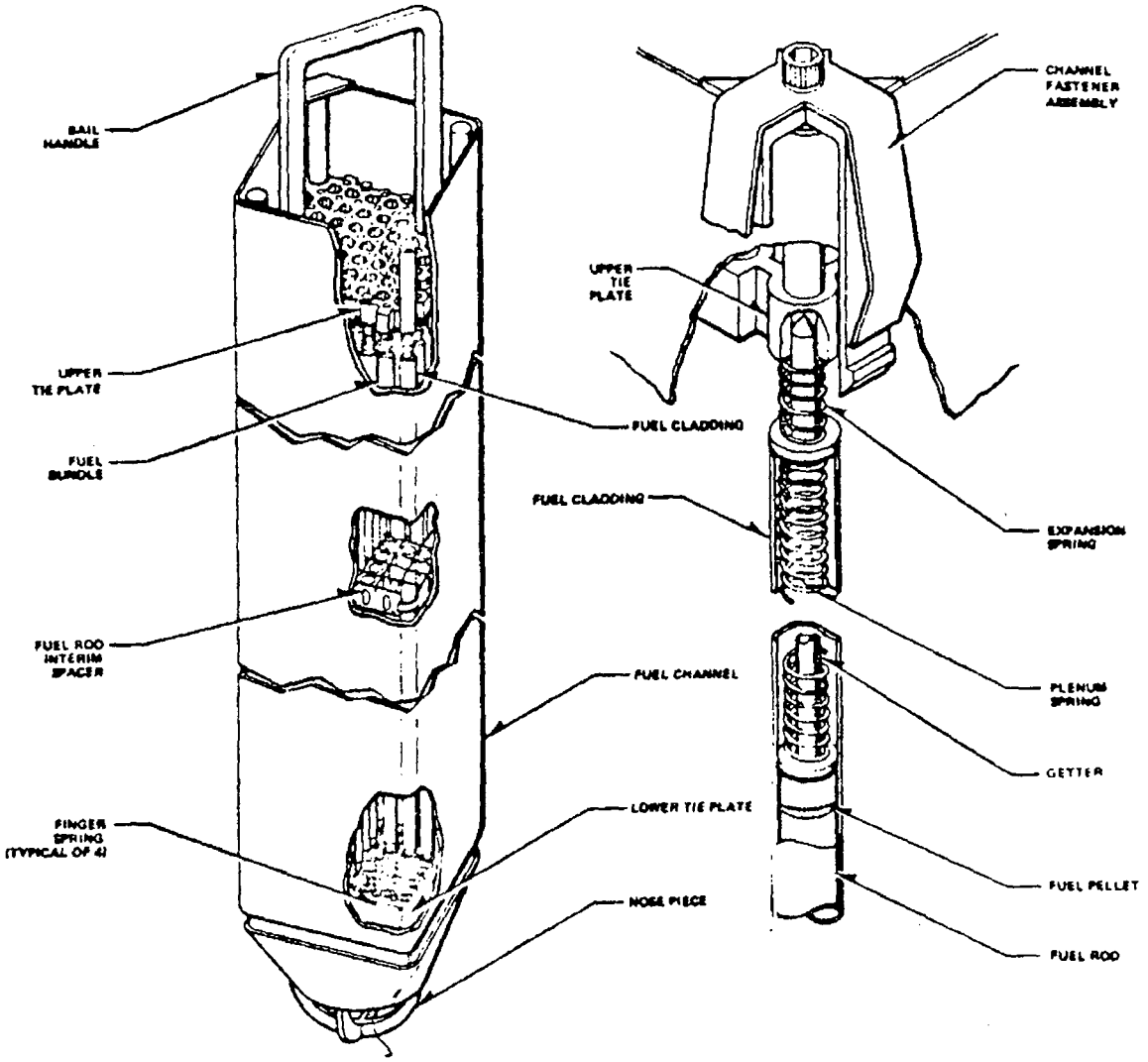


Figure 3-4. Fuel Assembly

Three types of rods are used in the bundle: tie rods, water rods, and standard rods. The third and sixth rod along each outer edge of a bundle are tie rods. The eight tie rods in each bundle have threaded end plugs which thread into the lower tie plate casting and extend through the upper tie plate casting. Two central rods in each fuel bundle are water rods, one of which is used to position seven Zircaloy-4 fuel rod spacers vertically in the bundle. The standard rods are 0.483 inch in diameter located on a typical pitch of 0.640 inches.

### 3.1.1 Foreign Objects

One of the most obvious ways in which coolant flow could be restricted is for some foreign object to become lodged in the flow path of a channel. This can occur only in certain locations: the orifice could become partially restricted, an object could become lodged between the fuel support piece and the lower tie plate nosepiece or an object could enter the fuel bundle and become lodged between the fuel rods. This latter type of blockage is of less consequence than the former two because any one single object cannot restrict enough flow to pose a serious threat to the integrity of bundle. The reason for this is the maximum size of an object capable of getting through the lower tie plate is only 0.410 inch (0.132 $in.^2$) in diameter (this is the size of the hole provided in the tie plate for flow distribution) compared to a total flow area of 15.82 $in.^2$ It would take a great many objects to block the flow area significantly to cause concern. This subject is discussed in more detail below. The other two locations, the orifice and the lower tie plate nosepiece, offer a more probable location in which objects can become lodged and cause a more significant reduction in flow.

In the normal reactor, great care is taken to remove and prevent any objects from entering the reactor system through strictly controlled operating and startup procedures. However, there does exist the possibility, remote as it may seem, that some object could either escape detection or break loose from the vessel internals. Such an object would have to make its way into the lower plenum through the jet pumps that have a typical nozzle diameter of 3 inches for BWR/2, 3, and 4 product lines. BWR/5 and 6 designs have five nozzles of 1.3 inches diameter. The throat diameter of a jet pump is 8 inches for the BWR/2, 3, and 4's and is 6.5 inches for the BWR/5 and 6 product lines. Once the object enters

the lower plenum (if it was not there to begin with), it has to proceed along the tortuous path through the guide tubes before reaching the channel inlet. The guide tubes leave a minimum gap of 1.125 inches and a maximum gap of 6.096 inches between guide tubes.

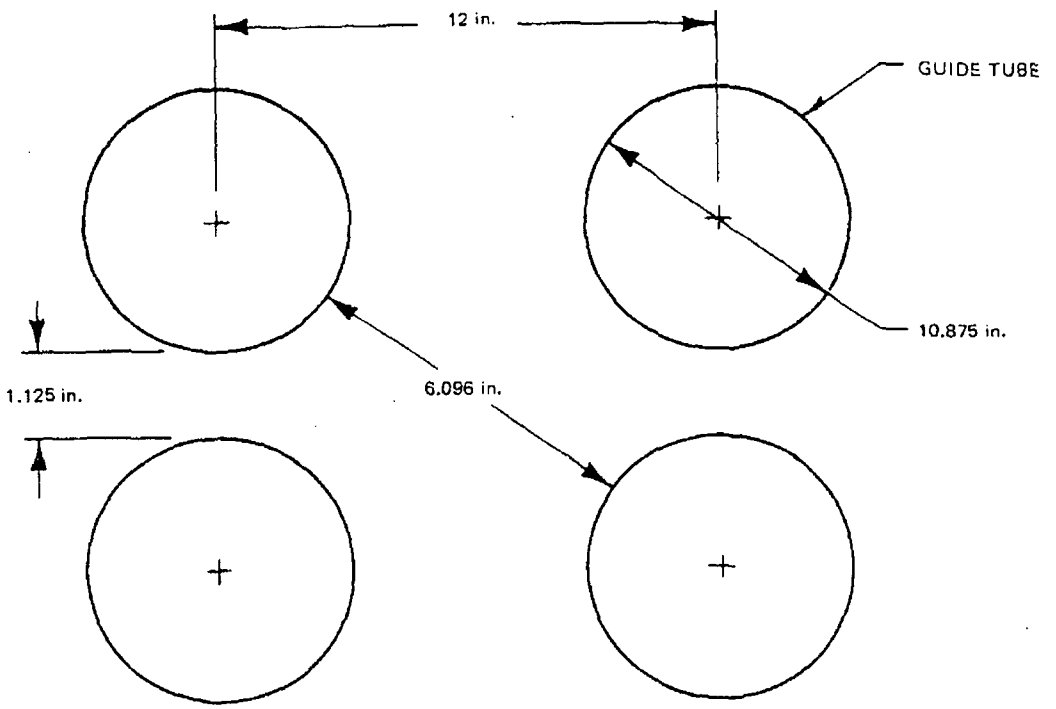


If the object is initially in the lower plenum it will be resting on the bottom of the vessel or if it is brought in through the jet pumps the high downward velocity component will tend to keep it on the bottom. The factor that will determine whether the object will be swept up off the bottom is dependent on the radial component of the velocity. Calculations of the average vertical and radial velocity components were made for typical plants at rated flow. These are given in Table 3-1 for a symmetrical wedge representing 1/8 of the guide tube field as shown in Figure 3-5.

Table 3-1

LOWER PLENUM VELOCITY COMPONENTS

| Row | Average Radial Component (fps) Maximum | Minimum | Average Vertical Component (fps) |
|---|---|---|---|
| I | 7 | <1 | 6 |
| II | 6 | <1 | 10 |
| III | 5 | . | . |
| IV | . | . | . |
| . | . | . | . |
| . | . | . | . |
| VII | <1 | <1 | 10 |

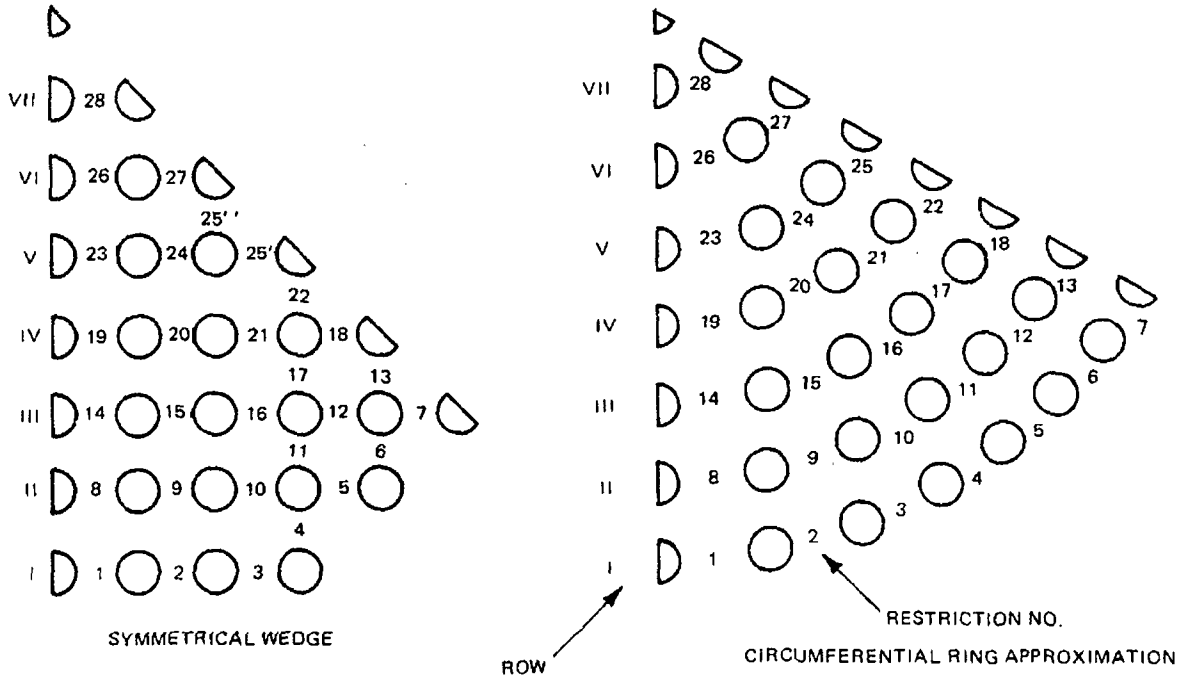


Figure 3-5. Geometrical Approximation for Control Rod Guide Tube Field

The maximum radial velocity is that which occurs in the 1.125 inch gap between guide tubes, whereas the minimum is that which occurs between rows. As can be seen, as the flow proceeds toward the center of the core the coolant has very little radial velocity and for all practical purposes is flowing vertically.

Figures 3-6 and 3-7 show the terminal velocity for sideways motion of cylindrical and flat-plate-type objects in water at 1000 psia and 520°F. If the vertical fluid velocity is greater than the terminal velocity, the object may be lifted by the drag forces from the fluid. Thus it is seen that most objects of reasonable size are capable of being swept up off the bottom of the vessel by the radial component and up toward the core by the vertical component.

However, while it is possible for certain size objects to be swept upward toward the bundle entrance, the following factors tend to reduce this possibility:

a. There are very few locations where the radial velocity would be high enough to sweep the piece off the floor of the narrow 1.125 inch gap between guide tubes.

b. If an object fell to the bottom of the vessel, it would tend to drift toward the vessel centerline where horizontal velocities are low and the boundary layers on the vessel may be thicker than the object. Thus, the boundary-layer effect would reduce the capability of the fluid to sweep the piece up off the floor of the vessel so that the vertical components could carry it upward.

c. Even if the object were somehow swept upward, it seems unlikely that it could completely block the orifice holes, which are vertically oriented.

d. If the object were small enough to pass through the orifice, it would have to pass through the lower tie plate nosepiece and the lower tie plate to enter into the fuel channel, which would require very unlikely alignment of the object and the passage through holes of only 0.410 inch diameter.

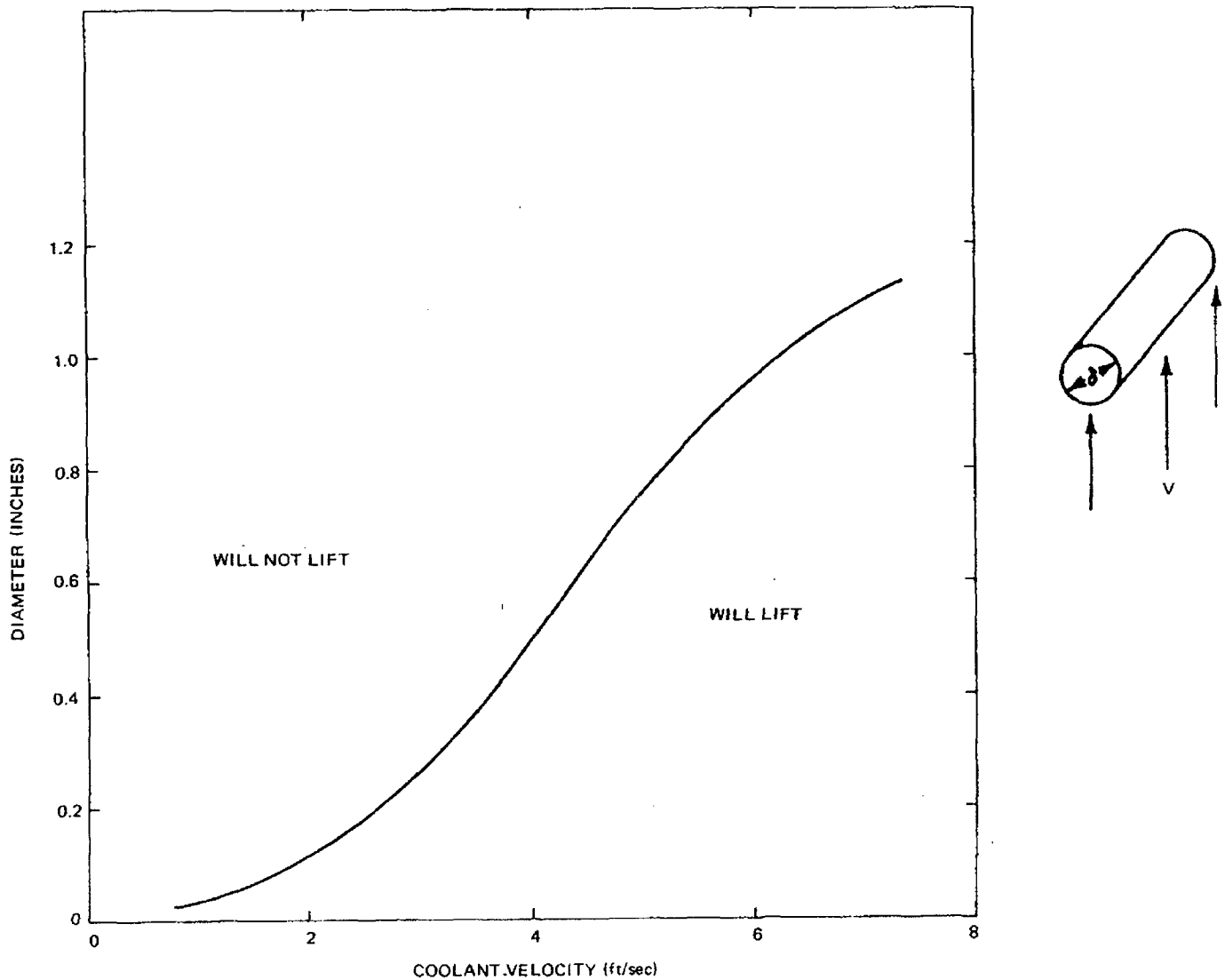


Figure 3-6. Criteria for Lift of a Cylindrical Steel Rod

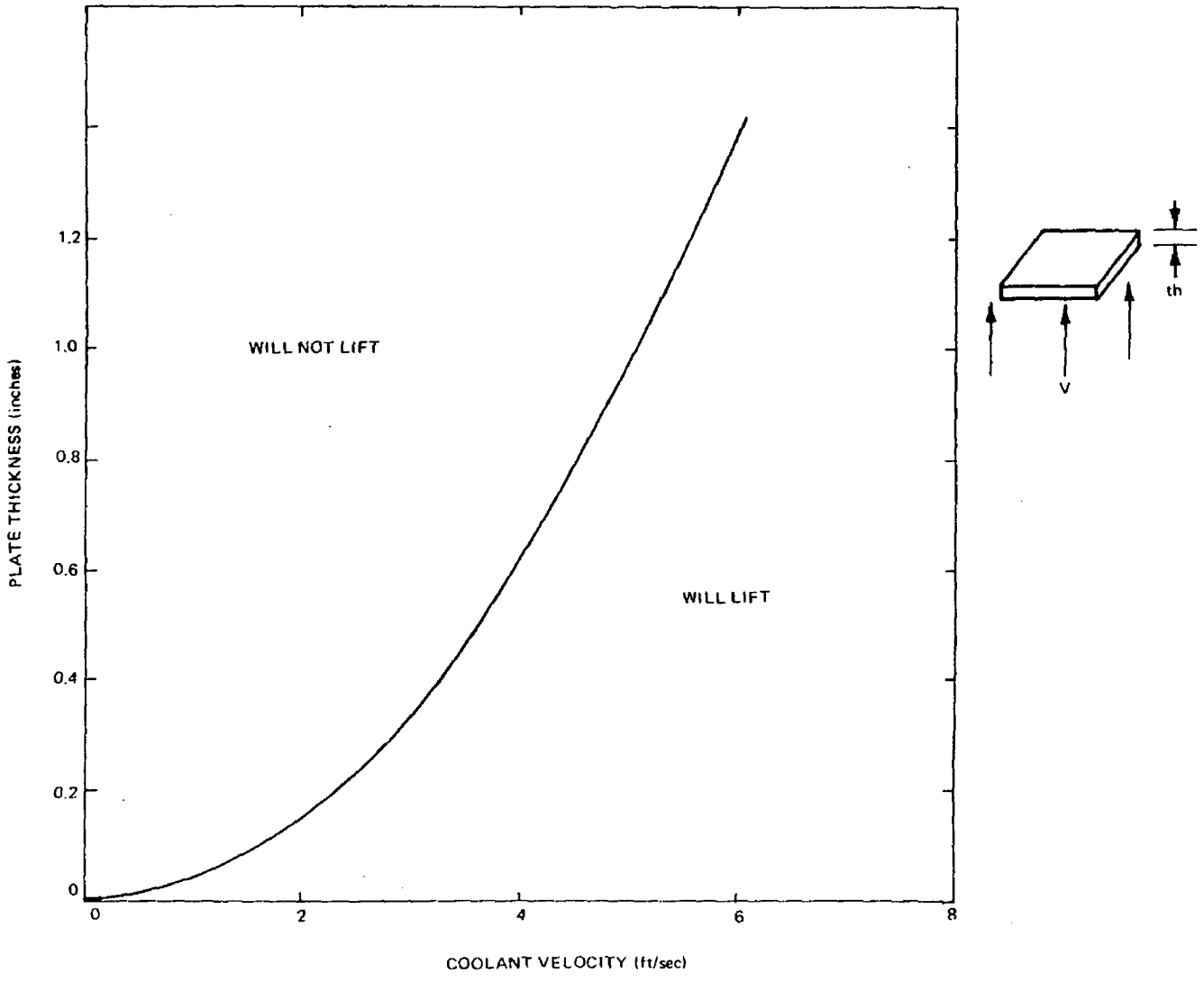


Figure 3-7. Criteria for Lift of a Flat Steel Plate

e. If the object were to make it through the lower tie plate, it would be stopped by the first spacer, which would probably cause local boiling transition and overheating. Depending on the size and shape, the object will most likely remain in a vertical position since the maximum distance between fuel rods is only 0.422 inch. The object would not significantly reduce the flow in one bundle and cause serious degradation of the heat transfer conditions in other areas of the fuel assembly.

Therefore, even though it is possible for minor blockages to occur by small objects entering the fuel bundle and affecting the life of the fuel, it is very unlikely that a blockage which would induce a significant flow reduction will occur. This is in part supported by the thermal shield vibration failure at Consumers Big Rock Point Reactor.[3.1] One-inch-diameter bolts on the thermal shield holddown assembly failed due to vibration. During the shutdown, debris was found on the bottom of the reactor vessel but there was no evidence that any had been swept up into the core.

Another possibility for flow blockage occurs during reactor fueling operations. It is remotely possible for an object to be dropped on top of the fuel support piece prior to loading a fuel bundle. Subsequently, when a fuel bundle is loaded into this location, the object if undetected, could become lodged between the fuel support piece and the bundle's lower tie plate nosepiece. This type of blockage would, in most cases, result in improper seating of the bundle, which presents another opportunity for detection during the subsequent core loading verification checks. Therefore, the opportunity for detection is present: (1) at the time the object is dropped, (2) during fuel loading, and (3) after fuel loading verification, - - - making this an unlikely mechanism to cause a flow blockage.

### 3.1.2 Core Crudding

Fuel channel crudding also can be considered as a potential mechanism causing flow blockage. This problem is normally eliminated by the reactor water cleanup system which provides continuous purification of a portion of the recirculation flow. The reactor water cleanup system maintains high reactor water purity to limit

chemical and corrosive action, thereby limiting fouling and deposition on heat transfer surfaces. If fouling did occur, all the bundles, rather than a preferential few, would generally experience this uniformly. As a result of this, the monitored core pressure drop will show an increase which would, in turn, cause the operator to take appropriate action. This would occur before the flow becomes reduced sufficiently to cause boiling transition to occur on the cladding. Thus, flow starvation caused by fouling can be considered a less severe condition than blockage by a foreign object.

### 3.1.3 Fuel Swelling

Fuel swelling as a consequence of a nuclear excursion is also a possible mechanism that may induce a limited degree of flow blockage in a channel. This is discussed in detail in Section 7.2.

## 3.2 FLOW REDUCTION AS A FUNCTION OF THE DEGREE OF BLOCKAGE

In subsection 3.1 the potential mechanisms capable of causing a flow blockage were discussed. The consequences of these blockages are, of course, inconsequential unless the blockage is capable of causing a significant decrease in channel flow which would cause a degradation of the convective heat transfer process.

In order to assess the consequences and severity of such a flow blockage it is first necessary to determine the decrease in flow as a function of the degree of blockage.

It was pointed out above that the two locations where a major blockage is most likely to occur are: (1) at the orifice entrance, and (2) at the lower tie plate nosepiece. Tests were performed at GE in which entrance loss coefficients were measured for various orifice sizes attached in a fuel support piece similar to that shown in Figure 3-3. This in effect simulated a blockage at the orifice location by some foreign object which partially covered the entrance. The loss coefficients are shown in Figure 3-8.

The decrease in flow of an operating channel can now be assessed for various blockages with the information provided by Figure 3-8. This has been done for

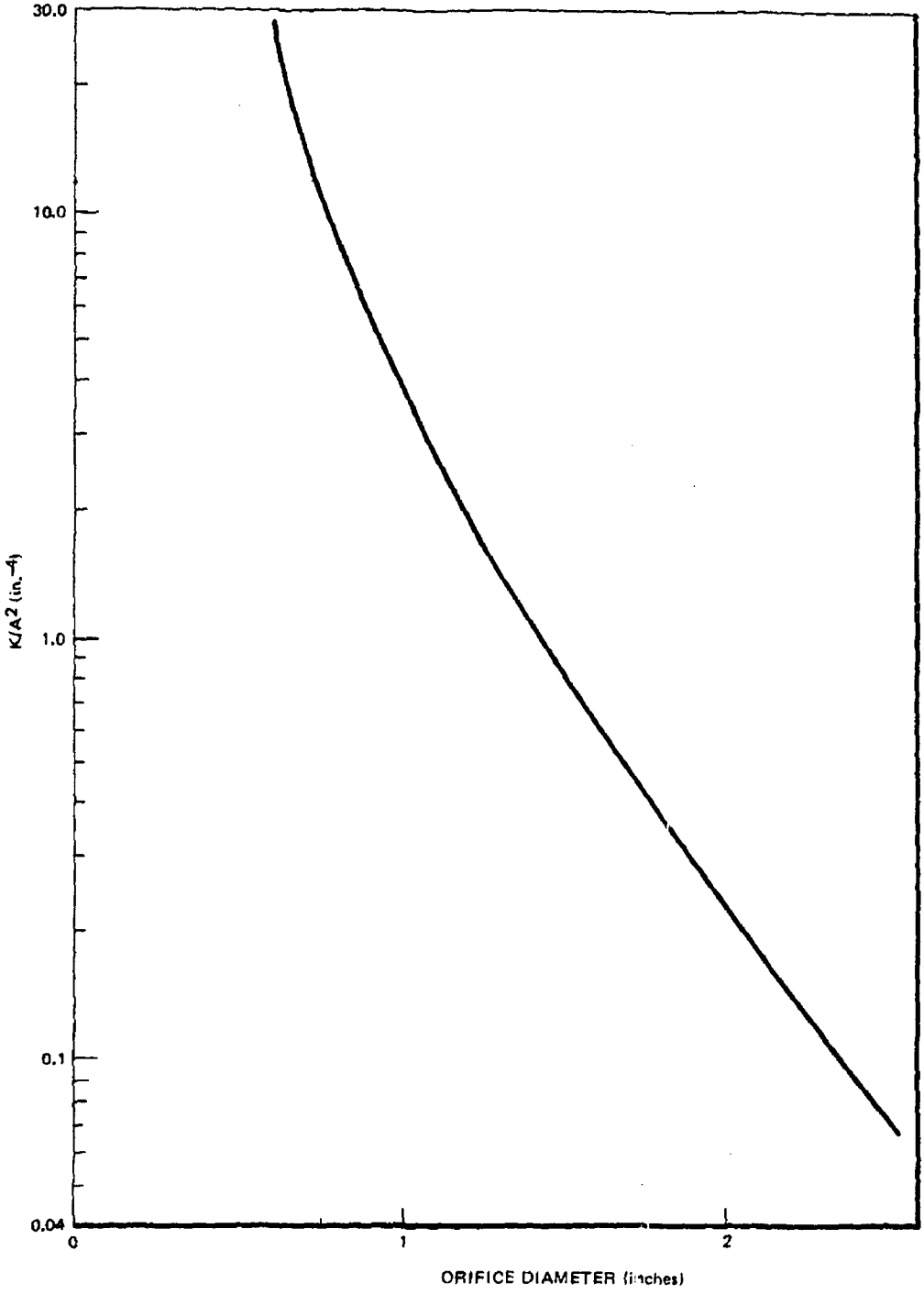


Figure 3-8. Hydraulic Loss Coefficients

the highest power bundle in the core and the results are shown in Figure 3-9. Both types of blockages were evaluated; that for the lower tie plate nosepiece and at the orifice entrance. The decrease in bundle power due to the increase in void content of the channel was also considered in this analysis. In Section 4 it will be shown that boiling transition will occur in a high-power bundle only when the flow has been decreased by more than 59% its rated value. From Figure 3-9, this reduction in flow is seen to occur only for area blockages greater than 79%. There is relatively little difference in whether the channel is blocked at the orifice entrance or at the lower tie plate. For a blockage at the orifice entrance, boiling transition will occur only when the entrance area has been blocked by more than 79% and if the blockage is at the lower tie plate this will occur for area restrictions greater than 86%.

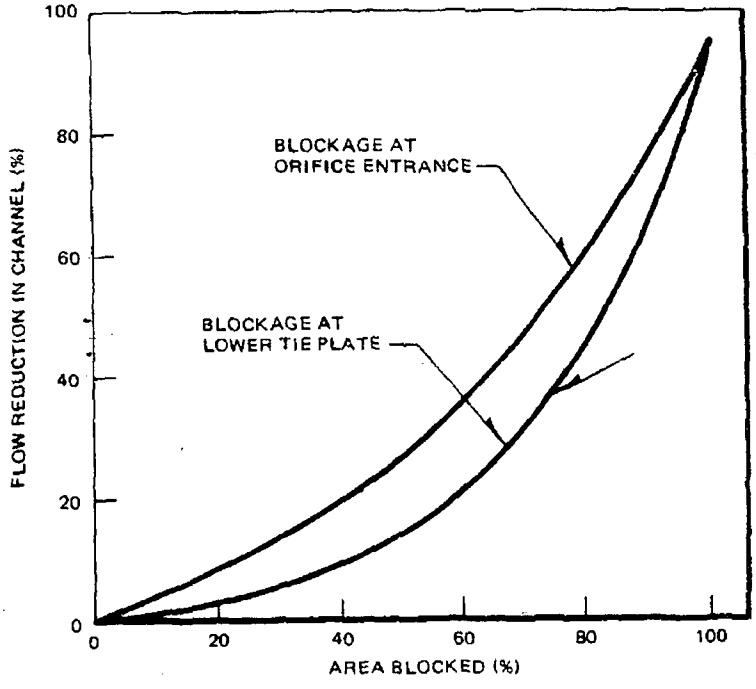


Figure 3-9. Flow Reduction in a High Power Bundle That Has Experienced a Flow Blockage.

## 3.3 NUCLEAR POWER REDUCTION RESULTING FROM A FLOW BLOCKAGE INCIDENT

Due to the loss of neutron moderation, the relative power in a flow-restricted bundle decreases as shown in Figure 3-10. This figure depicts a bounding curve of relative bundle power as a function of relative bundle flow. These results are considered realistic, yet because of the reactor conditions assumed, conservative and applicable to all BWRs.

In the event that a blocked channel suddenly becomes unblocked, the resultant positive reactivity insertion is minimal and will pose no problems.

### 3.3.1 Description of Calculational Methods

The worst conditions for a flow-blockage were identified by doing survey calculations with the BWR Simulator Code.[3.2] Results indicate that the reduction in relative bundle power as a function of flow reduction is smallest for an unexposed, low-enriched, first core bundle in a large plant. This was inferred from Figure 3-11 which contains the results of calculations for low, medium and high enriched bundles at different exposures, in different size plants, at conditions of low flow. It was assumed that by drawing straight lines through the calculated power-flow points and the point of 100% power and 100% flow, that the bounding straight line identified the most conservative case. This result is reasonable because lower-enriched bundles have smaller void coefficients than higher-enriched bundles and, therefore, the multiplication factor of the bundle does not diminish with void fraction as much as a higher enrichment bundle.

The BWR Simulator Code uses several assumptions which must be examined for the extreme conditions of flow blockage. A major modelling assumption is a one-group approximation based on the use of the infinite lattice neutron energy distribution. When a blocked bundle with a large void fraction is surrounded by others at about 40% voids, the neutron energy spectrum in the blocked bundle is expected to be affected through in-leakage from the neighboring bundles, which tends to violate the assumption above. Thus, a practical difficulty in using the BWR Simulator Code is to extrapolate values of nuclear data for normal operating conditions to the extreme condition of flow blockage.

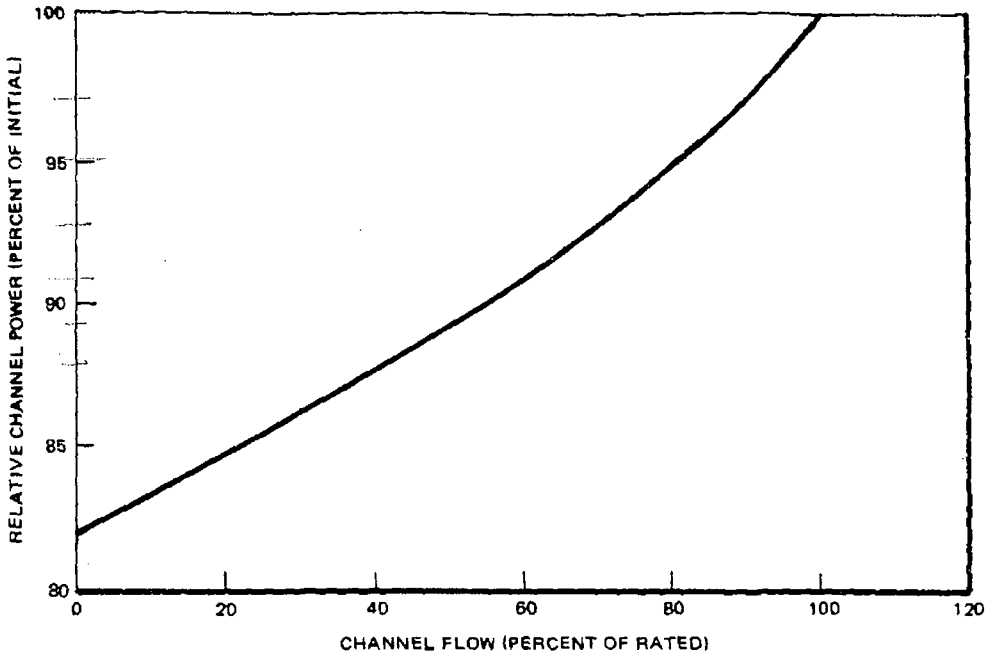


Figure 3-10. Power Reduction in a Blocked Channel

For the conditions of flow blockage, a more accurate tool is the four-bundle version of the BWR Lattice Physics Code[3.3] This code is more analytically correct because it uses three-group, fine-mesh, transport-corrected diffusion theory with self-generated cross sections to predict power and reactivity. Consequently, this code was used to calculate the power in the flow restricted bundle for several void fractions. Figure 3-10 was constructed by using the results of these calculations (see Table 3-2) and by assuming 100% bundle power for 100% channel flow.

It is worthwhile to note the assumptions made in order to construct Figure 3-10. First, as already noted, the low enriched bundle in a high power density BWR first core will give conservative results. This belief is based on calculational results shown in Figure 3-11 and the recognition that all of the above-mentioned factors contribute to a small void coefficient in the blocked bundle. Secondly, since Figure 3-10 indicates that bundle power is not sensitive to small changes in channel flow, zero flow was conservatively assumed to result in 100% voids (i.e., 100% steam quality) in the blocked bundle. Next, it was assumed that rising temperatures in the blocked bundle do not reduce the bundle power via Doppler feedback. In

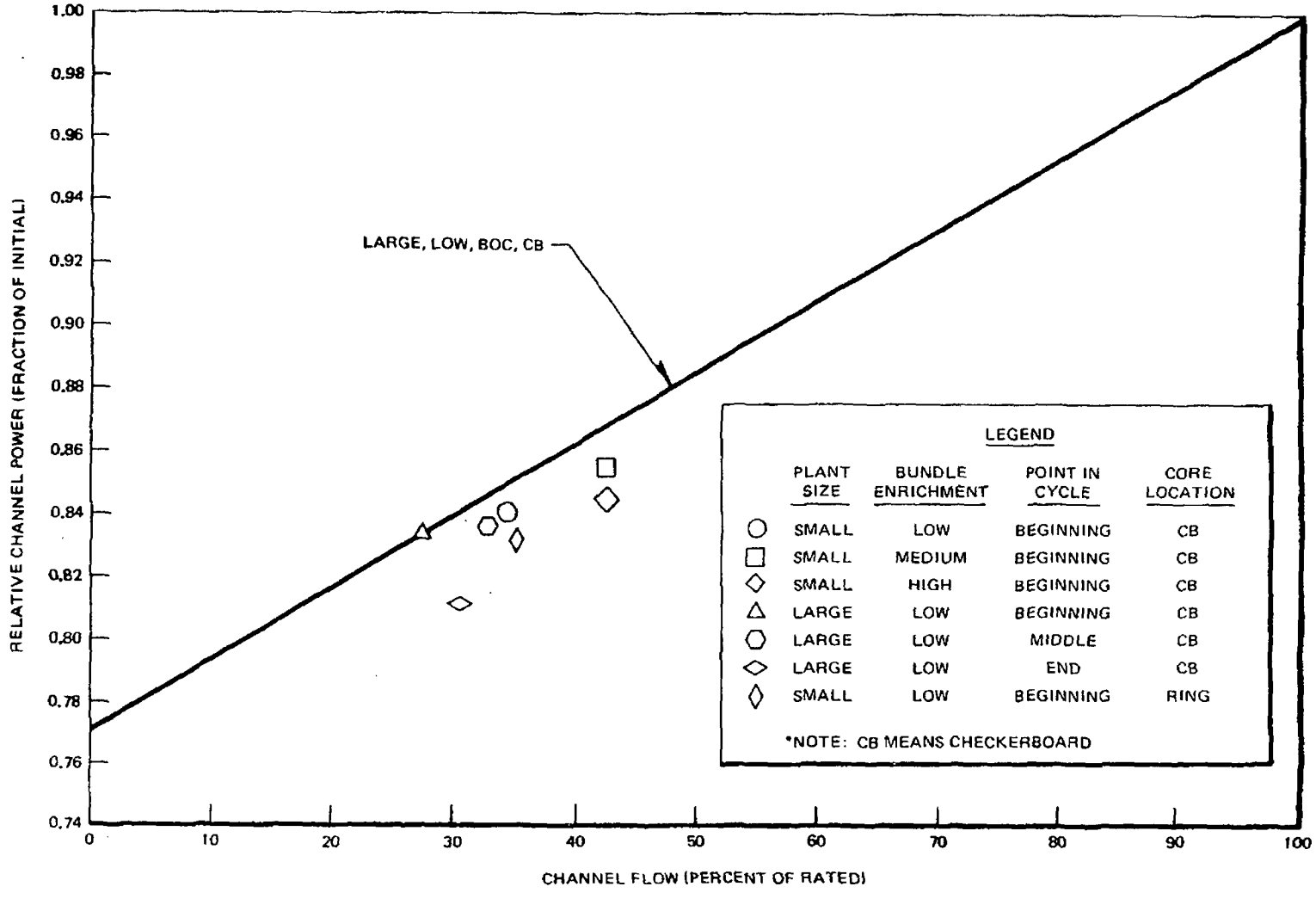


Figure 3-11. Power Reduction Versus Flow Reduction

Table 3-2

| Void Fraction of Surrounding Bundles | Void Fraction of Blocked Bundles | Power in Blocked Bundle, % of Original |
|---|---|---|
| 0.00 | 1.00 | 74 |
| 0.40 | 1.00 | 82 |
| 0.70 | 1.00 | 90 |

addition to being a conservative assumption, calculations with the four-bundle version of the BWR Lattice Physics Code[3.3] confirm that this is the case.

Finally, the decrease in power is dependent upon the void fraction in the surrounding bundles, which is to say, the decrease is axially dependent (see Table 3-2). A value of 82% was chosen because, for the worst case of an uncontrolled group of bundles surrounding and including the blocked bundle, the axial power will peak in the bottom half of these bundles where the void fraction ranges from 0.0 to 0.4, and is typically 0.4 at the peak power bundles.

In the event that a blocked channel suddenly becomes unblocked, a positive reactivity insertion will occur due to the rapid flooding of the voided channel. If this reactivity insertion were large enough it could lead to a prompt critical transient. Therefore, a conservative analysis was done by calculating the reactivity insertion due to reflooding of the blocked channel. The flow in 12 center channels of a high-power-density core was reduced to 10% of rated; the reactivity added due to complete reflooding of these channels was only 0.0028$\Delta$k. This reactivity addition will therefore not lead to a prompt critical transient since the delayed neutron fraction at the beginning and end of life are approximately 0.007 and 0.0055, respectively. Since the reactivity addition of one channel will be many times less than 0.0028$\Delta$k, the sudden unblockage of a blocked channel will not pose any problems.

## 3.4 DETECTION OF A FLOW BLOCKAGE BY IN-CORE INSTRUMENTATION

To assure optimum operation of the reactor system, several plant parameters are continuously monitored during operation. Upon investigation the detectability of a flow blockage is found to be remote. The core pressure drop will not alter noticeably because of the blockage of one channel since many other channels are controlling. The only feasible in-core detection could be made by the neutron monitoring system. The Local Power Range Monitor Subsystem (LPRMS) is capable of detecting a flow blockage by the resulting decrease in neutron flux; however, during normal operation these are not usually monitored individually and therefore in most cases it would be strictly fortuitous that a flow blockage would be detected. The Average Power Range Monitor Subsystem (APRMS), which provides a continuous indication of average reactor power, is continuously monitored. However the APRMS uses input signals from a number of LPRM channels located in different parts of the core and since it measures the average core power to within $\pm 2\%$ the decrease in power of a single channel due to a flow blockage is not even noticeable.

Hence even though a flow blockage is detectable with the LPRMS it is unlikely that such detection will occur during normal operating.

## 3.5 COOLANT LEAKAGE PATHS INTO A BLOCKED BUNDLE

During a flow blockage, any leakage flow coming into the fuel channel could have a significant effect on the consequences of the accident. As shown in Figure 3-12, there are several locations whereby coolant may potentially back-flow or leak into the channel. These locations are:

1. At the channel - lower tie plate interface.

2. At the lower tie plate - fuel support interface.

3. Through bypass flow holes located in the lower tie plate.

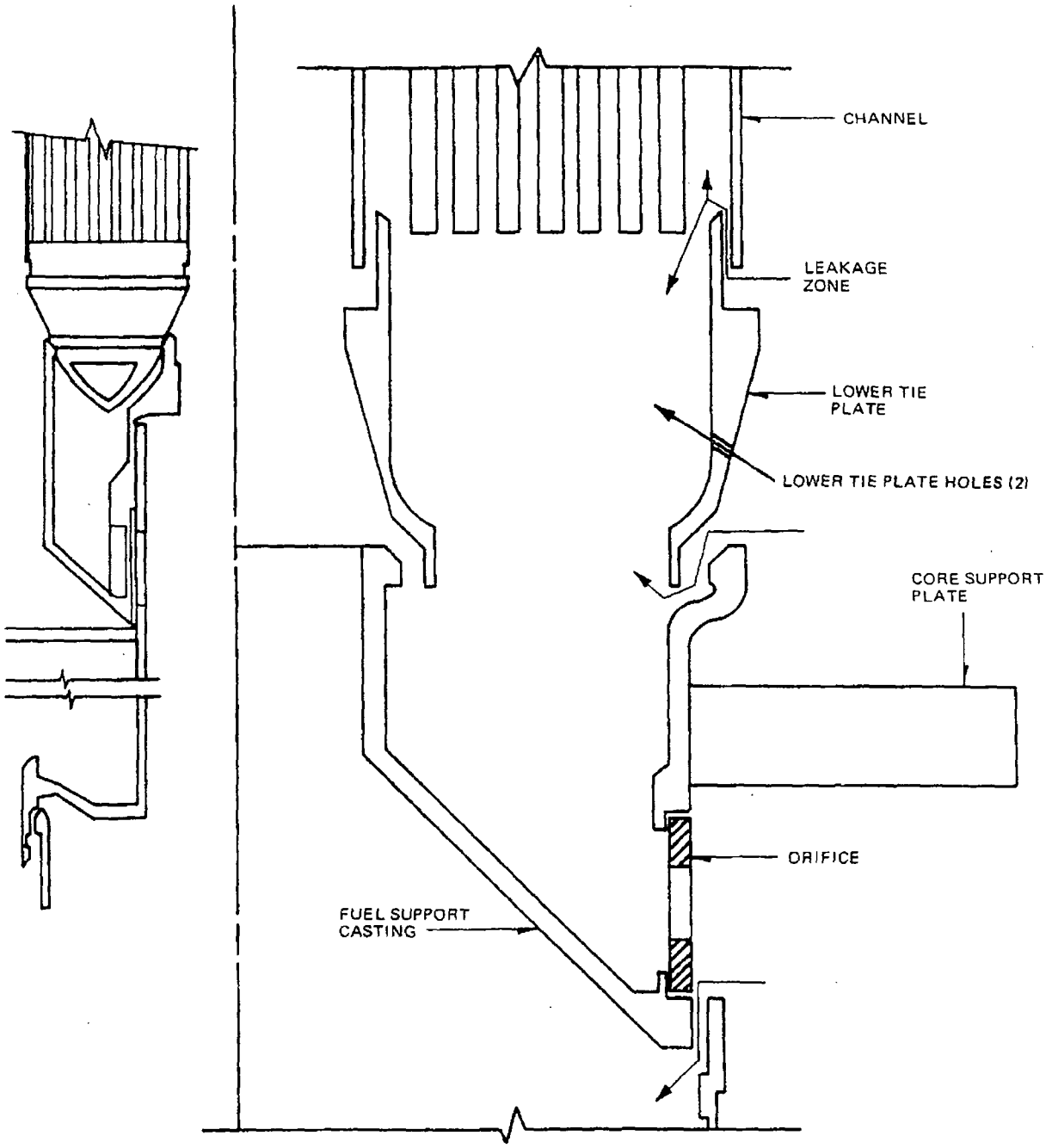


Figure 3-12. Fuel Channel Leakage Locations

In the event of a high degree of blockage, the flow within the fuel assembly decreases to approximately 5%, and the bundle pressure drop becomes negligible. However, because of the elevation head of the bypass region, there is a 4.3 psi driving pressure which will force core bypass coolant through the above mentioned paths and into the blocked channel. Realistically, the backflow through the lower tie plate-fuel support interface is essentially zero. The backflow through the channel-lower tie plate interface (with or without finger springs) is about $3 \times 10^3$ lbm/hr. The two 9/32 inch diameter lower tie plate holes provide an additional $3.2 \times 10^3$ lbm/hr. Therefore, a total of about $6.2 \times 10^3$ lbm/hr will be available for cooling the bundle even in the event of a complete blockage of either the orifice or lower tie plate nosepiece. This flow corresponds to about 5% of the normal bundle flow.

Another possible source from which coolant may enter the channel is from the top of the fuel assembly. It can be hypothesized that for high degrees of blockage, coolant could flow down the sides of the channel thereby providing a limited amount of cooling. This counter-current flow of water and steam is only possible for a certain limited range of upward steam velocities. For a given set of conditions there is usually a critical steam velocity above which no counter-current flow of the liquid can take place and the water film is torn from the surface of the wall. This breakdown of the liquid film is known as "flooding" from the analogous phenomenon that occurs in packed beds and columns in the chemical industry. The upper tie plate counter-current flow model, as described in Reference 3.4, shows that down flow will occur only at extremely low inlet channel flows. At total channel flows of 5500 lb/hr or greater, there is no counter-current flow.

## 3.6 CONCLUSIONS

In this section the mechanisms capable of inducing flow blockages and the resulting effects on the channel coolant were investigated. The following conclusions can be drawn:

a. The most likely mechanism capable of inducing a flow blockage is some foreign object.

b. The vertical velocities in the lower plenum are high enough to lift most reasonable size objects up toward the fuel bundle inlet. Even though it is possible for minor blockages to occur by small objects entering the fuel bundle and affecting the life of the fuel it is unlikely that a blockage which would induce a significant flow reduction will occur because of the tortuous path, narrow spacing, vertical orientation of the orifice in the inlet, and low radial velocities. The chances of a large object being swept up off the bottom seem to be very remote.

c. Partial blockage at the orifice entrance results in a more severe flow reduction per unit area blocked than at the lower tie plate nose piece. However, for complete blockage both cases result in greater than 5% of rated coolant flow.

d. For blockages both at the orifice entrance and at the lower tie plate nose piece the flow area must be restricted by more than 79% before boiling transition conditions are reached.

e. For a complete blockage the bundle power will be reduced by a nominal 18%.

f. Detection of a flow blockage by in-core instrumentation is possible but not very likely.

g. A negligible amount of coolant will re-enter the bundle from the top during partial flow blockages.

# 4. FUEL ROD THERMAL EFFECTS FOLLOWING A FLOW BLOCKAGE

Investigation of the potential consequences of a flow blockage accident requires that the fuel and cladding temperatures be known for various degrees of blockage. In this section the fuel and cladding temperatures are determined for various degrees of blockage.

## 4.1 MODEL DESCRIPTION

### 4.1.1 Thermal-Hydraulic Model

The analysis calculates the coolant conditions which occur axially in a fuel bundle under varying conditions of inlet flow, enthalpy, pressure, and power generation. The local heat flux (among other parameters) is determined through the simultaneous solution of coupled, time-dependent partial differential equations satisfying mass and energy conservation, considering the local power generation and rod time constants, heat transfer coefficients, and the effects of the energy addition to the fluid.

The onset of boiling transition is determined through application of the GEXL correlation[4.1] as a function of the predicted coolant mass flow rate, quality, boiling length, and rod to rod power distribution. The major outputs are the bundle critical power ratio, the axial values of heat flux, mass flow rate, fluid temperature, quality, void fraction, and fuel rod temperatures.

For calculational purposes, a single fuel rod is considered which has an average power generation rate for the bundle being analyzed and time independent axial and radial power shape. Only radial heat transfer in the fuel rod is considered in the calculations, axial and circumferential heat transfer being negligible. The thermal properties of the fuel and cladding are functions of temperature and are, therefore, continuously calculated and modified throughout the transient.

### 4.1.2 Fuel Bundle Heatup Model

The thermal-hydraulic model described above is used in calculating the coolant conditions as well as the cladding and fuel temperatures. If the convective heat transfer conditions have degenerated significantly (i.e., for high degrees of blockage) the cladding temperatures become high enough that the effects of thermal radiation and metal-water reaction become important. For these conditions the fuel temperatures, cladding temperatures, channel temperature, and the amount of cladding and channel oxidation are calculated. In this analysis the power generation and the chemical energy released by metal water reactions are included as heat sources.

The power distribution is assumed to be symmetrical along the diagonal of the bundle and the rods are then divided into various groups (References 4.2 and 4.3). A one dimensional heat balance is then written for each group of fuel rods. Heat is transferred from the surface of the fuel rods by convection to the fluid. In addition, thermal radiation between fuel rods and from the rods to the channel is accounted for in the over-all heat balance.

A typical fuel rod consists of uranium dioxide fuel with a Zircaloy cladding. An 8x8 fuel bundle consists of 62 fuel rods and 2 water rods grouped together to form a square array which is surrounded by a metal channel. Each fuel rod is divided into nine equal radius radial temperature zones for the numerical calculations as shown in Figure 4-1. The cladding, on the other hand, is divided into two nodes and the cladding temperature presented is the average for these two nodes. As the temperature difference across the metal oxide is small the oxide is assumed to be at the temperature calculated for the cladding surface. The channel (Figure 4-1) is considered to be at a uniform temperature circumferentially. For each rod group a transient radial conduction calculation is performed at one axial plane. Axial conduction is not significant for the fast transients considered here as the radial conduction overshadows any axial effects, hence it is ignored. Resistance to heat flow through the fuel-cladding gap is taken into account.

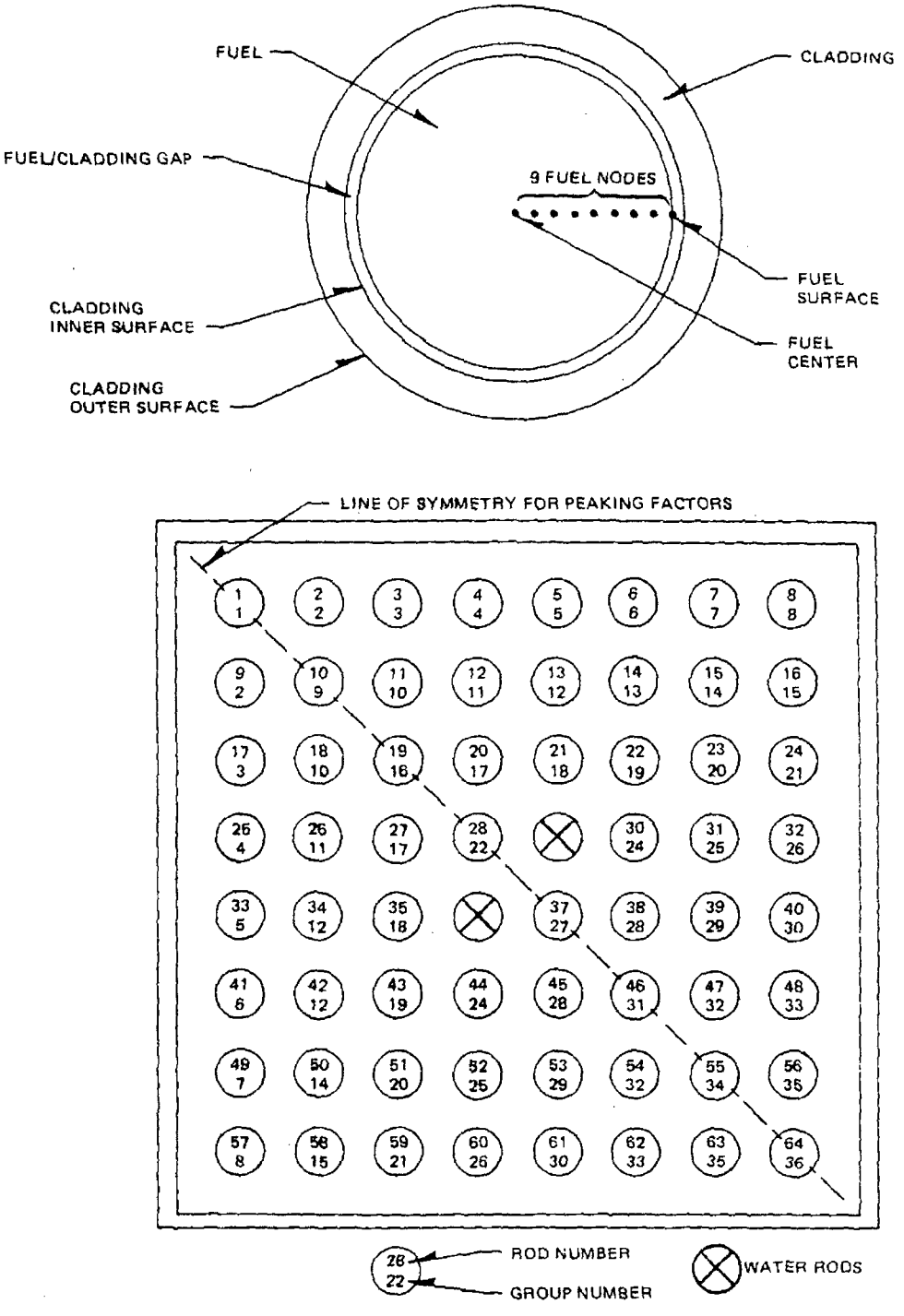


Figure 4-1. Fuel Rod and Fuel Bundle Details

The reduction in power in a flow restricted bundle, due to voiding and loss of neutron moderation is discussed in section 3.3. The relative power reduction used in the heatup calculations is shown in figure 3-10. The bounding calculations for the highest power assembly assumed that this assembly operated at the technical specification maximum linear heat generation rate (MLHGR) of 13.4 kw/ft. The chemical energy released by the metal-water reaction is described by the parabolic rate law given by Baker,[4.4] where the rate of change of the metal oxide thickness is written as

$$\frac{d\delta}{dt} = \frac{K}{\delta} \exp\ (-D/T_c) \qquad (4.1)$$

where

$K$ = rate coefficient,
$T_c$ = cladding temperature,
$D$ = activation coefficient, and
$\delta$ = oxide thickness.

The heat generation rate and hydrogen release rate are proportional to the rate of change of oxide generated. The chemical heat liberated is given as follows:

$$\frac{dQ_c}{dt} = \frac{d\delta}{dt} \Delta H \rho_c A_s \qquad (4.2)$$

where

$\Delta H$ = heat of reaction,
$\rho_c$ = density of metal, and
$A_s$ = exposed surface area of oxide.

The mass rate of hydrogen generated is

$$\frac{dW_H}{dt} = 2 \frac{d\delta}{dt} \rho_c A_s \frac{N_{H_2}}{N_{METAL}} \qquad (4.3)$$

where

$W_H$ = mass of hydrogen generated and
$N$ = molecular weight.

The above reaction considers that there is an unlimited source of saturated steam available for the reaction. The empirical reaction constants, K and D, are based upon experimental data obtained under conditions where the metal and water are at the same temperature.

Heat is transferred from the cladding and channel to the surrounding fluid by thermal radiation and convection. During conditions where nucleate boiling exists, the Jens-Lottes correlation for boiling heat transfer is used.

$$h = \frac{e^{P/900}}{1.9} Q_s^{0.75} \qquad (4.4)$$

where

$P$ = pressure, and
$Q_s$ = surface heat flux.

For conditions where boiling transition takes place film boiling or single phase convection are calculated. These are functions of flow rate and quality.

Thermal radiation between fuel rods and the fuel channel box is permitted if they are not covered with water. To simplify calculations, the fuel rods are divided into groups. Radiation view factors are calculated for each group of rods. The view factors together with the emissivity and relative areas are converted to radiation coefficients used in the Stephen-Boltzmann equation for obtaining the radiant heat transfer.[4.3] The fuel, cladding, and channel temperature are calculated at each time step by considering the aforementioned energy consideration.

## 4.2 PEAK FUEL AND CLADDING TEMPERATURE FOR VARIOUS DEGREES OF BLOCKAGE

A rapid decrease in channel flow will result the moment a blockage occurs in a fuel assembly. This rapid reduction in flow will cause the fuel rods to undergo a thermal transient if the flow reduction is enough to cause boiling transition to occur. Soon after the blockage has occurred the flow will settle out to some steady-state value depending on the degree of flow area that has been restricted. This initial transient that the fuel bundle undergoes is depicted in Figure 4-2 for two distinct types of blockages: (a) those for which the rate of flow reduction causes a momentary departure from nucleate boiling but the net flow reduction is not sufficient to allow the rod surface to remain in this state long enough to cause a significant heatup of the cladding, and (b) those for which the flow is reduced below the point where sustained departure from nucleate boiling can occur and cause cladding heatup. For the types of blockages that cause flow transients such as that shown in Figure 4-2a the fuel cladding will undergo a momentary heatup but this will be terminated quickly when the flow recovers. This 1 to 2 second period is not considered significant since the ultimate consequences for these degrees of blockage are negligible and the bundle will not undergo any permanent damage.

The philosophy adopted in assessing the consequences of a flow blockage incident is one of determining the ultimate or final consequences of the blockage. The initial phases of the transient (Region I in Figure 4-2) will not alter the ultimate consequences of the incident. For this reason the thermal-hydraulic analysis has been performed on a steady-state basis, i.e., the degree of blockage for which the MCPR becomes less than 1.0 has been determined. The analysis has neglected the minimal effects of Region I and has concentrated upon the effects resulting from the conditions in Region II of Figure 4-2. The important factor is not the mechanism by which the actual blockage induces a flow reduction but the degree of flow reduction which has occurred and the consequences.

By incorporating the flow and power reduction for various degrees of blockage (shown in Figures 3-9 and 3-10) into the thermal hydraulic model the flow reduction necessary to cause boiling transition to first occur can be determined. The results of such an investigation for a reactor operating at 100% of rated

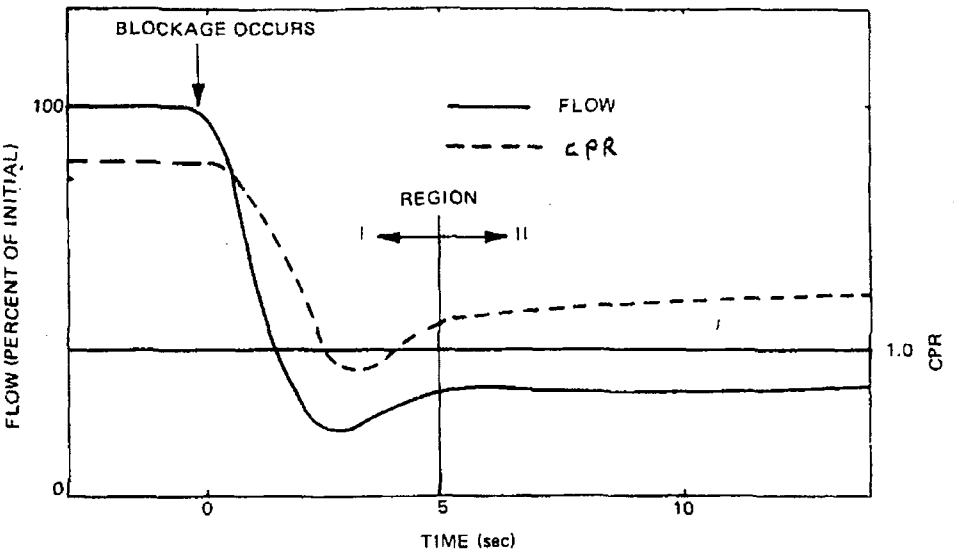


a. BLOCKAGES FOR WHICH NO SIGNIFICANT HEAT-UP OCCURS

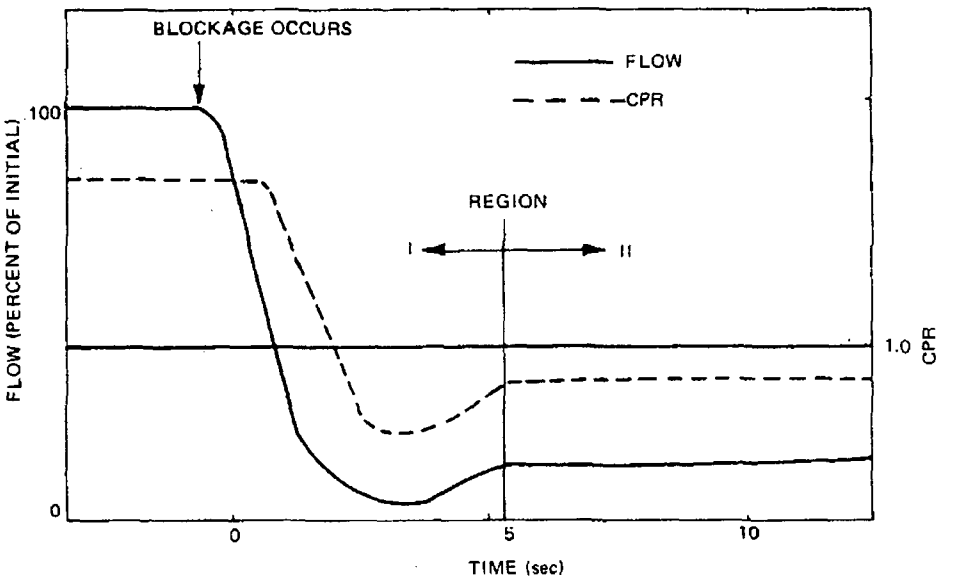


b. BLOCKAGES FOR WHICH HEAT-UP OCCURS

Figure 4-2. Typical Flow CPR Responses

power are shown in Figures 4-3 and 4-4 for both an average and a high-power channel. These figures, together with Figure 3-9, indicate the conditions for which nucleate boiling is lost on the hottest (highest Power) rod in the average and highest power bundle in the core. The other rods in the bundle would experience these conditions at higher degrees of blockage. It is significant to note that for an average channel, which is the type for which a blockage is more likely to occur, the area must be 90% restricted before nucleate boiling is lost and the fuel rods show any thermal effects of the blockage. For blockages at the lower tie plate the bundle can withstand 93% blockage. Because of the higher operating power, the hot channel will experience a loss of nucleate boiling conditions for lower degrees of blockage than an average channel. However, the differences are not significant and even for a hot channel the entrance area of the bundle has to be 79% blocked before the onset of boiling transition. The results shown in Figures 4-3 and 4-4 are for the hottest rod in the channel. Even on the rods which have exceeded the critical power, only a small portion of the rod is in boiling transition.

For flow blockages greater than those at which significant steam superheat was calculated, the fuel bundle heatup model was used to assess the cladding and fuel temperatures reached in the fuel assembly. Based on the results of this analysis and the criterion that the melting point of $UO_2$ is $5000^{\circ}F$ and that of Zircaloy is $3371^{\circ}F$, the amount of bundle damage can be determined. It should be noted that although the melting point of Zircaloy is $3371^{\circ}F$, the Zircaloy cladding will undergo a chemical reaction with the water, commonly referred to as a "metal-water reaction" or,

$$Zr + 2H_2O \rightarrow ZrO_2 + 2H_2 + \text{heat} \qquad (4.5)$$

The oxide layer formed, $ZrO_2$, is very brittle and does not possess much strength. The melting point of this oxide is approximately $4600^{\circ}F$; however, the conservative assumption was made that once the cladding surface reached $3371^{\circ}F$ the zircaloy was considered melted although the cladding may have been oxidized.

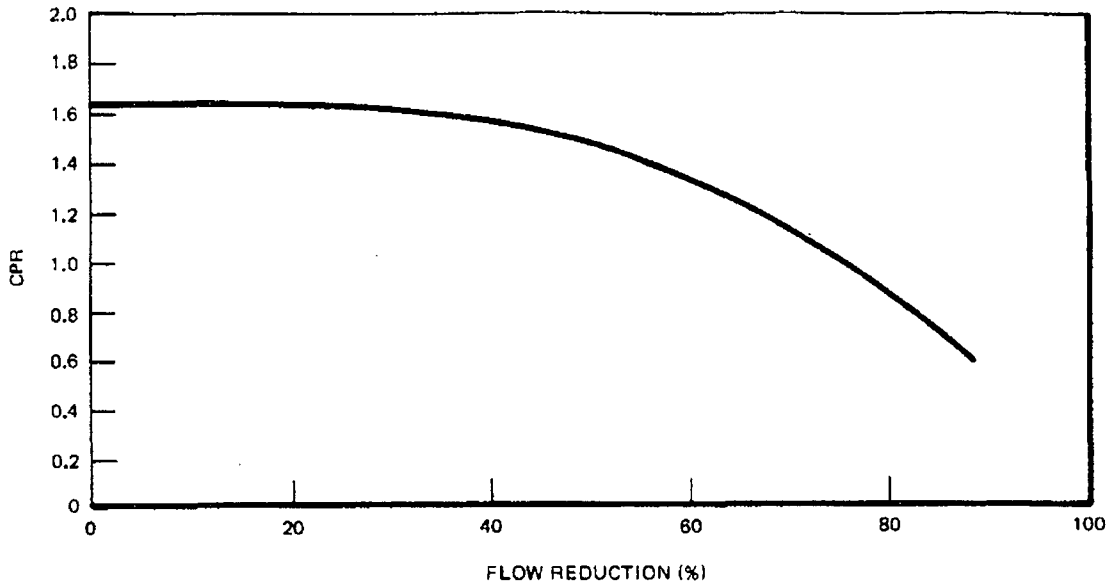


Figure 4-3. Hot Channel CPR for Various Degrees of Blockage

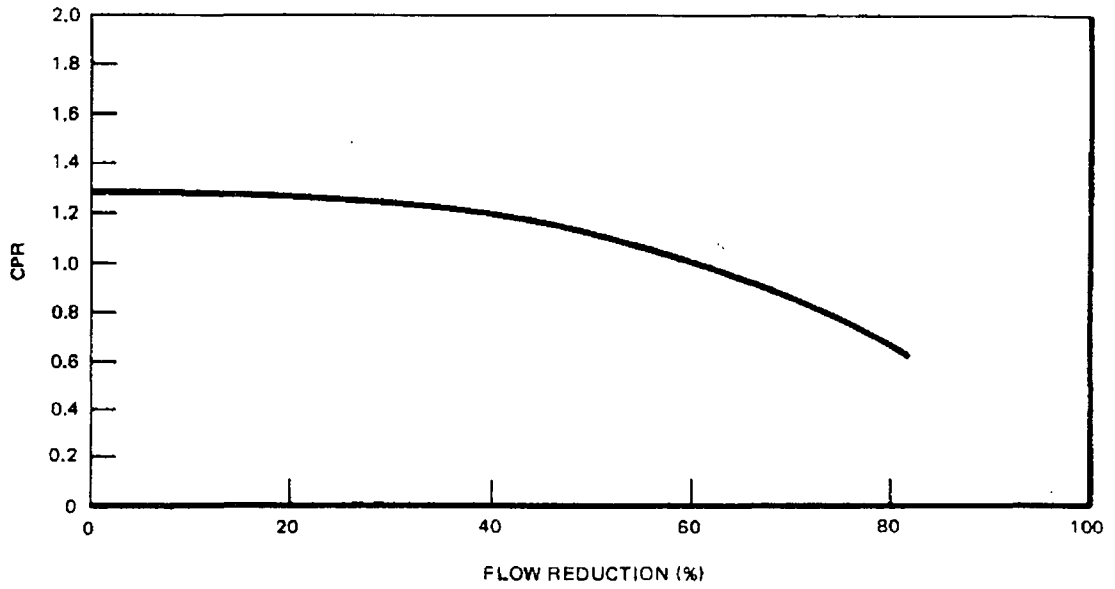


Figure 4-4. Average Channel CPR for Various Degrees of Blockage

During film boiling conditions (CPR $\leq$ 1.0), the Dougall-Rohsenow[4.5] heat transfer correlation was used with saturated fluid properties:

$$h = 0.023 \frac{K_g}{D_H} \left[ \frac{\rho_g D_H}{3600\mu} \left( \frac{G(1 - X)}{\rho_\ell} + \frac{G(X)}{\rho_g} \right) \right]^{0.8} Pr_{SAT}^{0.4} \qquad (4.6)$$

where,

$X$ = quality
$G$ = mass flow rate (lbm/hr-ft$^2$)
$D_H$ = hydraulic diameter (ft)
$\rho_g$ = density of vapor (lb/ft$^3$)
$\rho_\ell$ = density of liquid (lb/ft$^3$)
$K_g$ = conductivity of vapor (Btu/hr-ft-$^\circ$F)
$\mu$ = viscosity of vapor (lbm/ft-sec)
$Pr$ = Prandtl number

For superheated steam conditions, the commonly known Dittus-Boelter relation was used, or

$$Nu = 0.023\ Re^{0.8}\ Pr^{0.40} \qquad (4.7)$$

Figure 4-5 is a histogram of the range of fuel cladding temperatures for a range of flow blockages up to and including a complete blockage of the orifice for the highest power bundle with the reactor operating at full power. This histogram has been generated for the condition of no reactor scram.

In Section 8 the response of the radiation monitoring systems to the fission product release from cladding failure and fuel melt is evaluated. Reactor scram is shown to occur within about 13 seconds from the time fuel melt first occurs for a complete orifice blockage. The scram (and also reactor vessel isolation) is initiated by trip of the main steam line monitoring channels which input to the reactor protection system. Even though reactor scram will occur

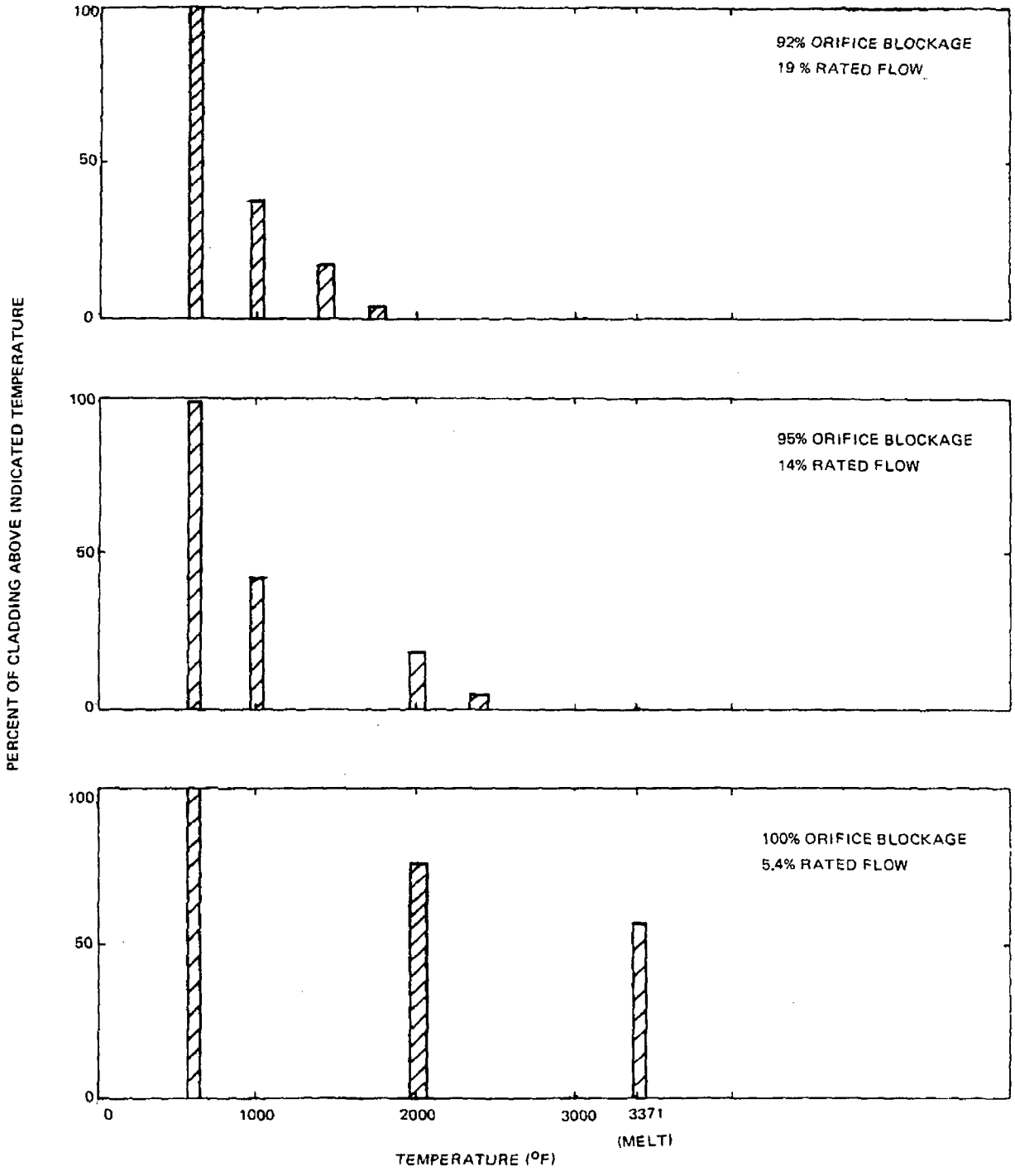


Figure 4-5. Cladding Temperature Distribution in a Hot Fuel Assembly

it will be shown in Section 4.4 that the potential for blockage propagation does not exist even for the condition of the reactor scram.

Figure 4-5 indicates the amount of cladding above a given temperature in a fuel assembly. The results in the figure are for the highest power bundle in a typical high-power-density core operating at 100% power. At 19% flow (92% blockage) no cladding has melted and most temperatures are below 2000°F. At 14% flow, (95% blockage) 15% of the cladding is above 2000°F and well oxidized. For a complete blockage in which very little coolant enters the channel, all the cladding in the bundle will either have melted or fragmented, assuming that reactor scram has not already occurred. Although a complete blockage of the orifice is highly unlikely it is the most severe condition which the bundle can experience. This melted or fragmented Zircaloy will be in the form of fairly large particles. The range of particle sizes and their effect on the fuel assembly is discussed in the following paragraphs.

The range of estimated $UO_2$ temperatures for various flow conditions is shown in Figure 4-6, assuming the geometrical relationships between the fuel rods and the channel do not change once incipient melting first occurs in the $UO_2$. Fuel center melt is first experienced at approximately 10% flow (98% blockage). However, even though the center of the fuel is molten the outer surface of the fuel, indicated by the outer fuel mode, is relatively cool and well below the molten condition. Significant amounts of molten fuel is not expected to be expelled into the fuel channel until the outer fuel nodes have reached the melting point. This condition occurs for rated flows lower than 7% (>98% blockage). However, although it is difficult to analyze, it is expected that prior to the outer fuel node becoming molten, the strength of the fuel rod will rapidly diminish as the fuel center heats up and the fuel pellets will simply crumble and fall to the bottom of the channel in a solid state.

For a complete blockage, fuel center melting first occurs at approximately the axial midpoint of the hottest rod in the bundle. The tops of the rods are not restrained (except for the tie rods described in Section 3) and are free to expand; thus as the center of the rod loses strength, due to the incipient melting, the top half can no longer be supported and will eventually fall toward the bottom of the channel, possibly making contact with the channel wall.

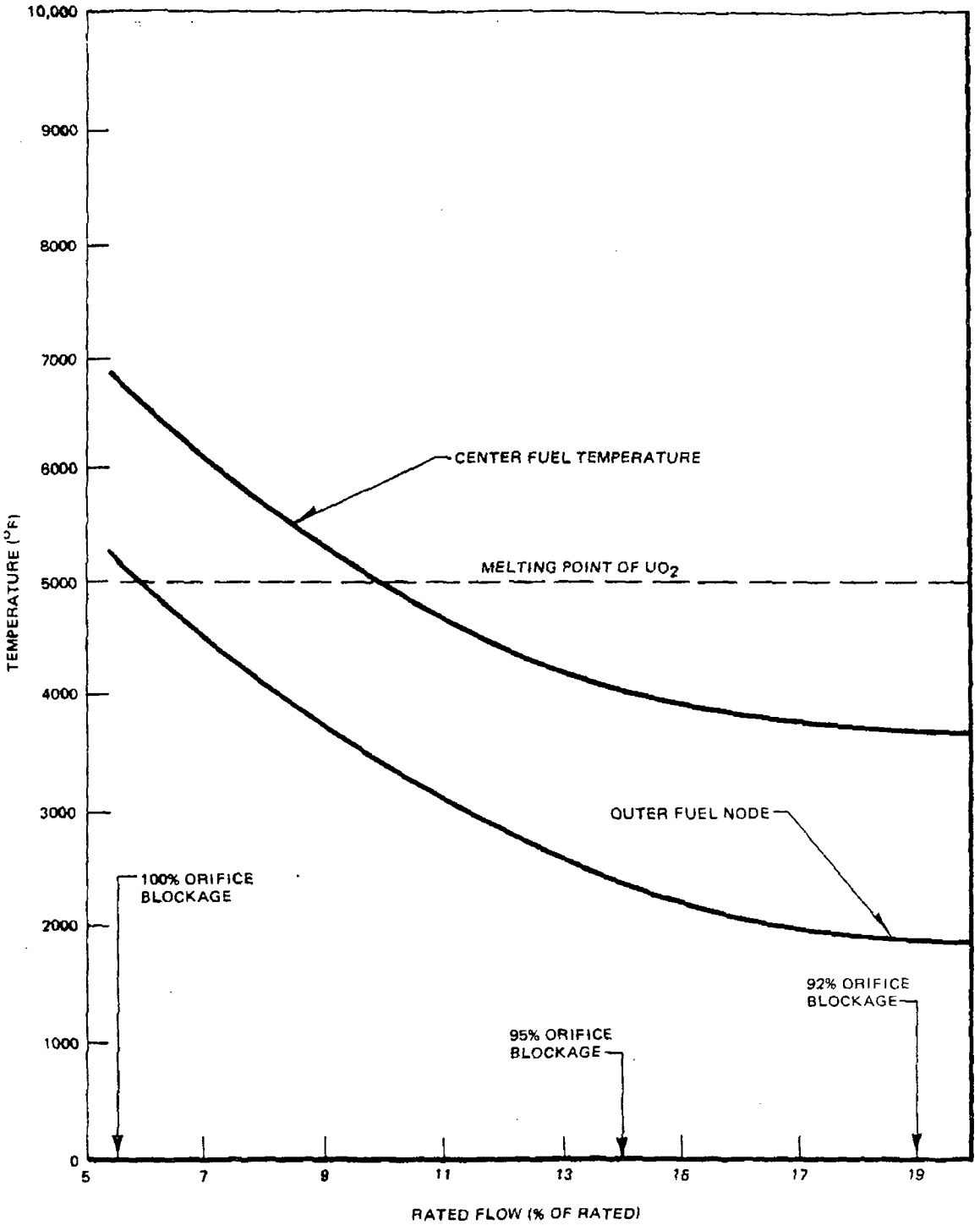


Figure 4-6. Peak Fuel Temperatures in a High Power Fuel Assembly

The important conclusion to be drawn from Figure 4-6 is that no molten fuel will be expelled into the channel except for an almost complete flow restriction. A complete blockage is highly unlikely. For the more likely case of a partial blockage enough cooling will be available so that no molten fuel will be expelled into the assembly. For the most severe condition of a complete blockage and using the criteria that the melting point of $UO_2$ is 5000°F, and that molten fuel is not released to the channel environment unless the outer fuel node reaches 5000°F, the amount of $UO_2$ that will melt (for the no scram case) and be released into the channel, for a high power bundle, is approximately 270 pounds or 60% of the fuel contained in the fuel assembly. This will occur shortly after the blockage has occurred. With this amount of fragmented fuel in the channel the chances are very high that contact with the channel wall will be made very quickly. The integrity of the channel subjected to this high temperature is discussed below. The possibility of a significant pressure generation is discussed in Section 5.

The estimated temperatures resulting from a complete blockage and no scram at different reactor power levels is shown in Figure 4-7. For a completely blocked channel, cladding melting will occur for power levels greater than 75% and the outer fuel node will reach melting for power levels greater than 98%.

## 4.3 ABILITY TO COOL MOLTEN $UO_2$ DROPLETS

It was shown above that for degrees of blockage greater than 98% and no reactor scram, fuel rods will experience limited amounts of melting. Once this melting has started it is difficult to predict analytically the course of subsequent events since the geometry of the bundle can no longer be well defined. It is possible, though, to bracket the consequences by combining a parametric study and experimental results.

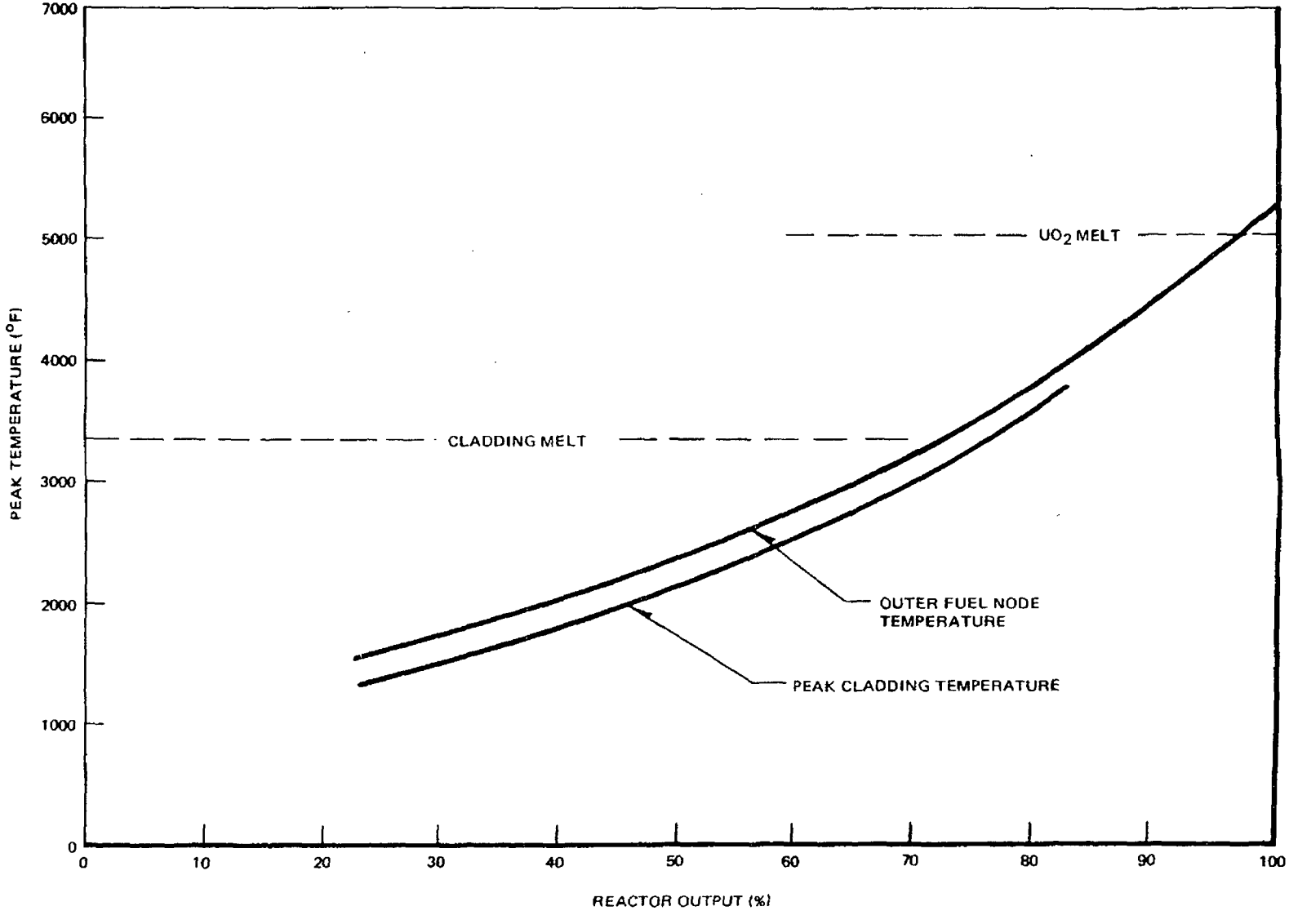


Figure 4-7. Cladding and $UO_2$ Temperatures at Various Reactor Operating Powers for a Completely Blocked Channel

As the fuel rods melt due to the lack of coolant, gradual amounts of molten $UO_2$ and Zircaloy will drip along the rods and eventually coalesce at the bottom of the channel. In addition, the rods will tend to crumble apart and fall to the bottom once they lose their strength.[4.6]

Once the molten fuel enters the channel the ability to cool these pieces of $UO_2$ is of course dependent on the heat transfer environment. A conservative approximation of the amount of internal heat generation present in a $UO_2$ droplet can be obtained from the following expression:

$$q''' = GN\sigma_f\phi \tag{4.8}$$

where

$q'''$ = volumetric heat generation,
$G$ = energy per fission,
$N$ = number of fissionable nuclei/$cm^3$,
$\sigma_f$ = microscopic fission cross section,
$\phi$ = neutron flux.

For typical thermal fluxes that exist in BWR's, the volumetric heat generation rate is,

$$q''' = 3.5 \times 10^7 \text{ Btu/hr-ft}^2\text{°F} \tag{4.9}$$

In Figure 4-8, the minimum surface heat transfer coefficient required to remove the internal heat generation from spherical $UO_2$ droplets of various sizes is shown. The two curves shown are for the droplets transferring heat to a saturated mixture of 550°F water and superheated steam of 2000°F. As can be seen, particle solidification will occur if coefficients of 20 to 40 Btu/hr-ft$^2$°F exist. Once the blockage has been detected by the steam line radiation monitors (discussed in Section 8) and the reactor is scrammed the power generation in the

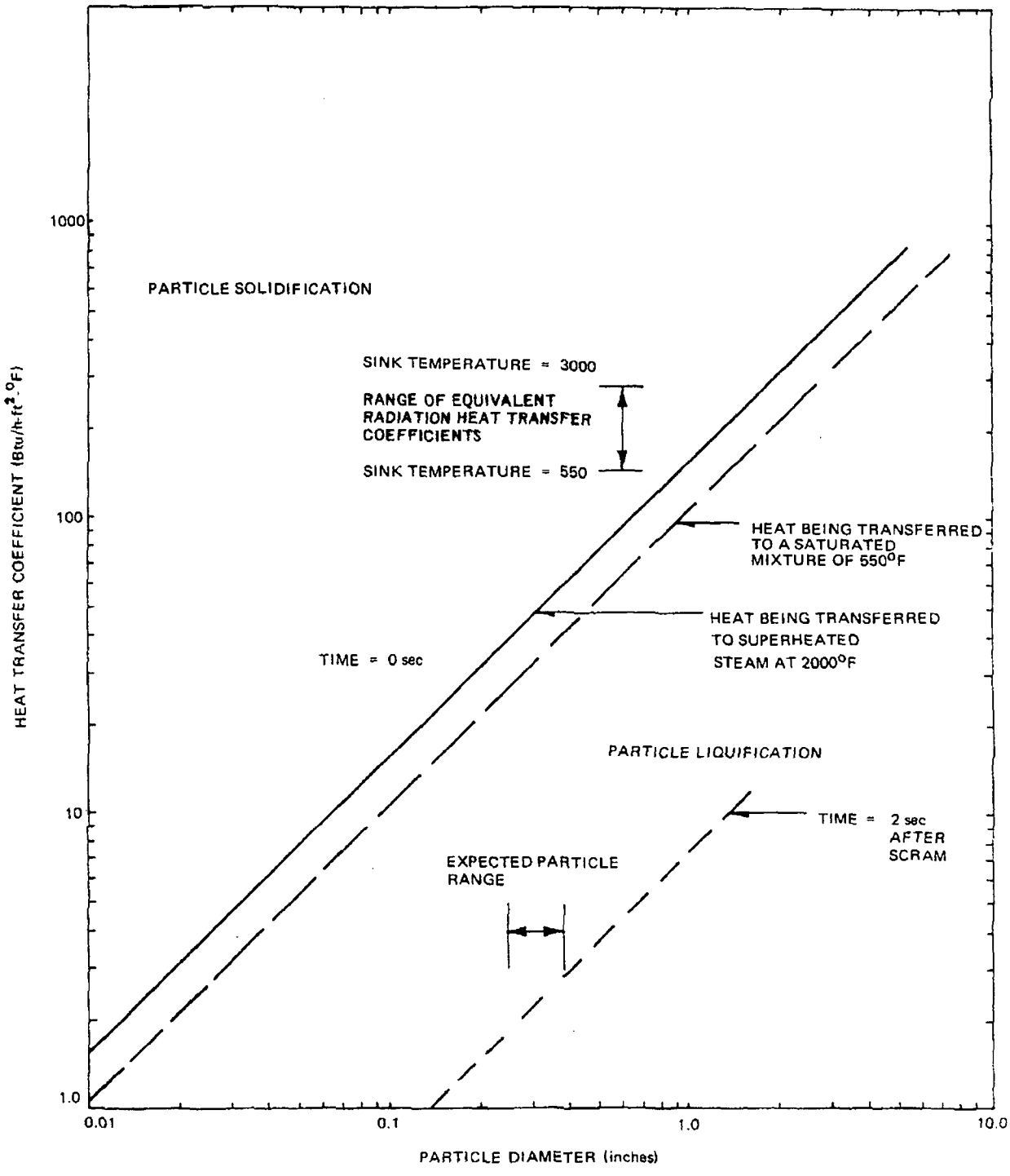


Figure 4-8. Minimum Heat Transfer Coefficient Required to Remove Internal Heat Generation from a Molten Spherical Particle

droplets will decay very rapidly. This decay rate is shown in Figure 4-9 and the effect of this on the required heat transfer coefficient to remove the internal heat generation is shown for 2 seconds after scram in Figure 4-8.

The availability of adequate heat transfer coefficients for cooling of these $UO_2$ particles can be assessed by examining the equivalent radiation and convective coefficients under various conditions. An equivalent radiation coefficient for a small gray body radiating to black surrounding can be expressed as

$$h_r = \epsilon\sigma \frac{(T_F^4 - T_S^4)}{T_F - T_S} \tag{4.10}$$

where

$\epsilon$ = emmissivity,
$T_F$ = temperature of $UO_2$ particle,
$T_S$ = sink temperature,
$\sigma$ = Stefan-Boltzman constant.

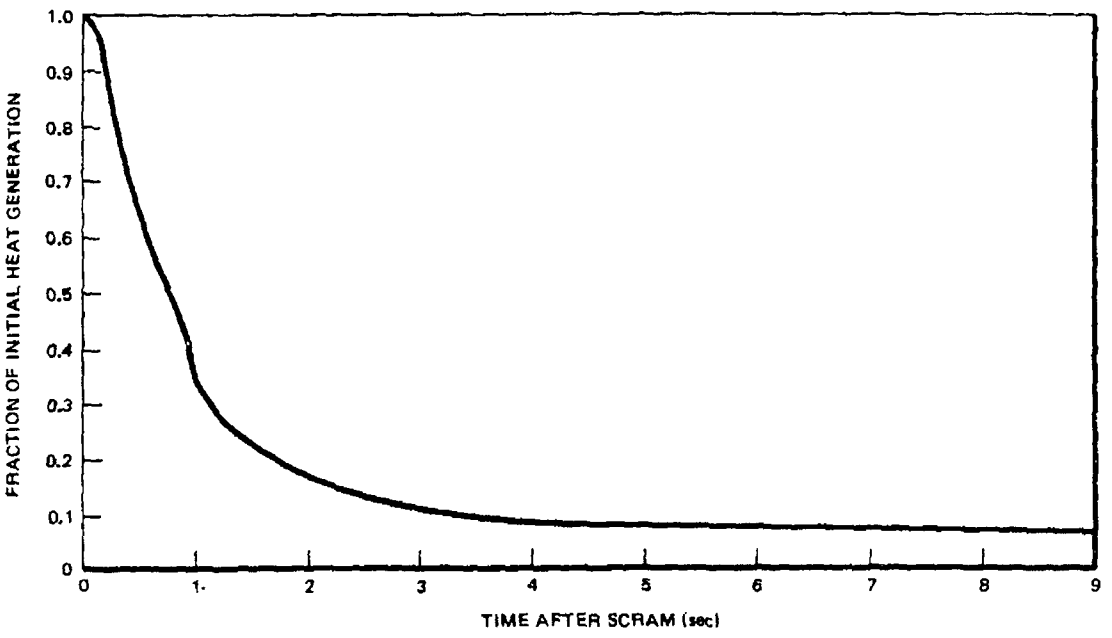


Figure 4-9. Decay Heat Rate of $UO_2$

Equation 4.10 is plotted in Figure 4-10 for various sink temperatures; and the results indicate that radiation alone is adequate to solidify the $UO_2$ particles. A conservative estimate of the available convective heat transfer coefficients can be obtained by evaluating the coefficients for pure steam. This is shown in Figure 4-11 for various degrees of blockage.

From this it is obvious that for most reasonable degrees of blockage, convective heat transfer provides a more than adequate amount of cooling for solidification of the $UO_2$ or Zircaloy particles. For complete blockage radiation is adequate in cooling the droplets. Thus once the fuel has melted and left the rods it will not remain in a molten state.

## 4.4 FUEL CHANNEL INTEGRITY

The fuel channel during normal plant operation serves to control and "channel" the coolant flow past the fuel rods. In this manner, more-than-adequate convective heat transfer conditions are maintained upon the surfaces of the heat-generating fuel rods. The channel is constructed of Zircaloy-4 and has an 0.080-inch to 0.120-inch thick wall depending on the product line. In addition to flow passing through the inside of the channels, flow is also circulated on the outside of the channel wall. This flow is normally referred to as the "core leakage flow" and usually amounts to approximately 10% of the rated core flow. The configuration of this leakage path in relation to the fuel assemblies and control rods is shown schematically below.

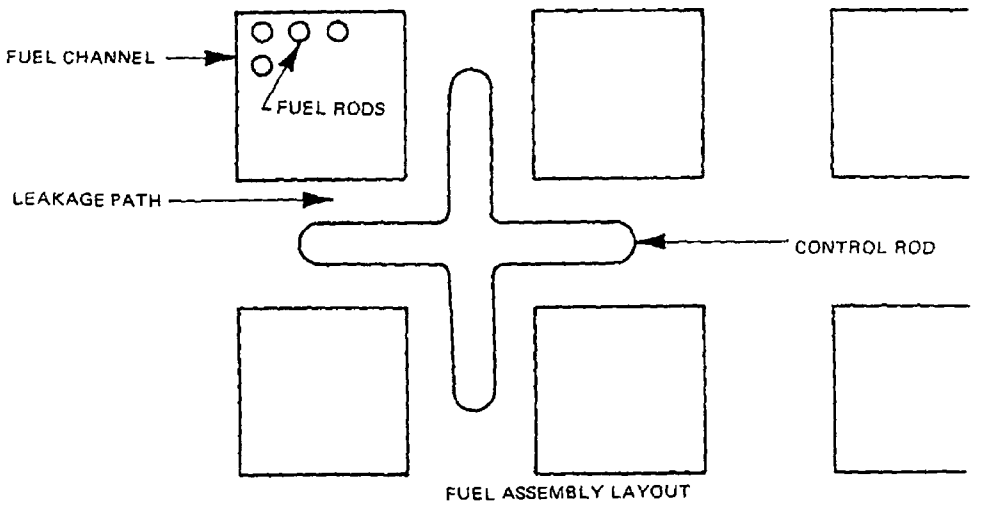


FUEL ASSEMBLY LAYOUT

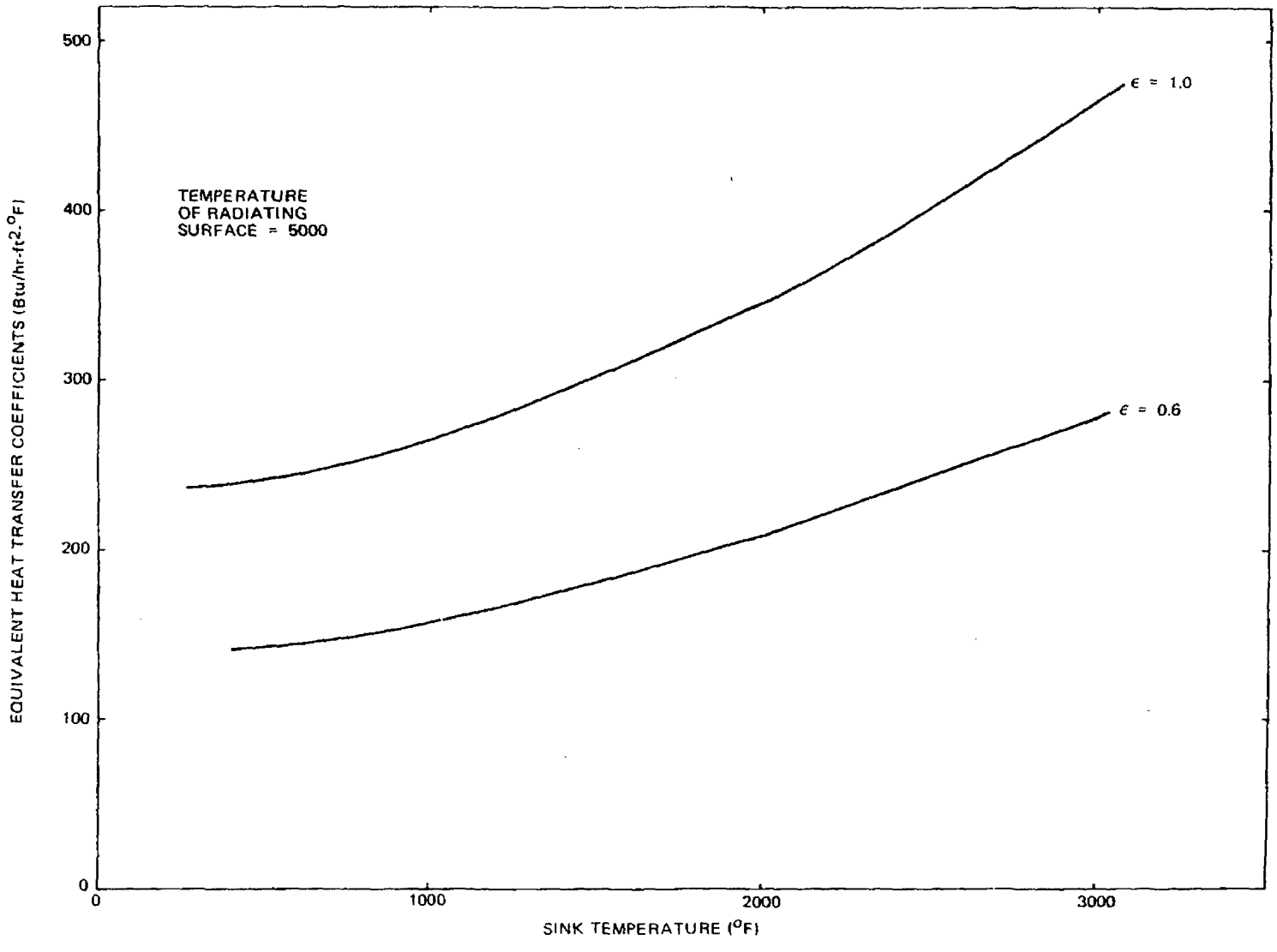


Figure 4-10. Equivalent Radiation Heat Transfer Coefficient for a Gray Body Radiating to a Black Surface

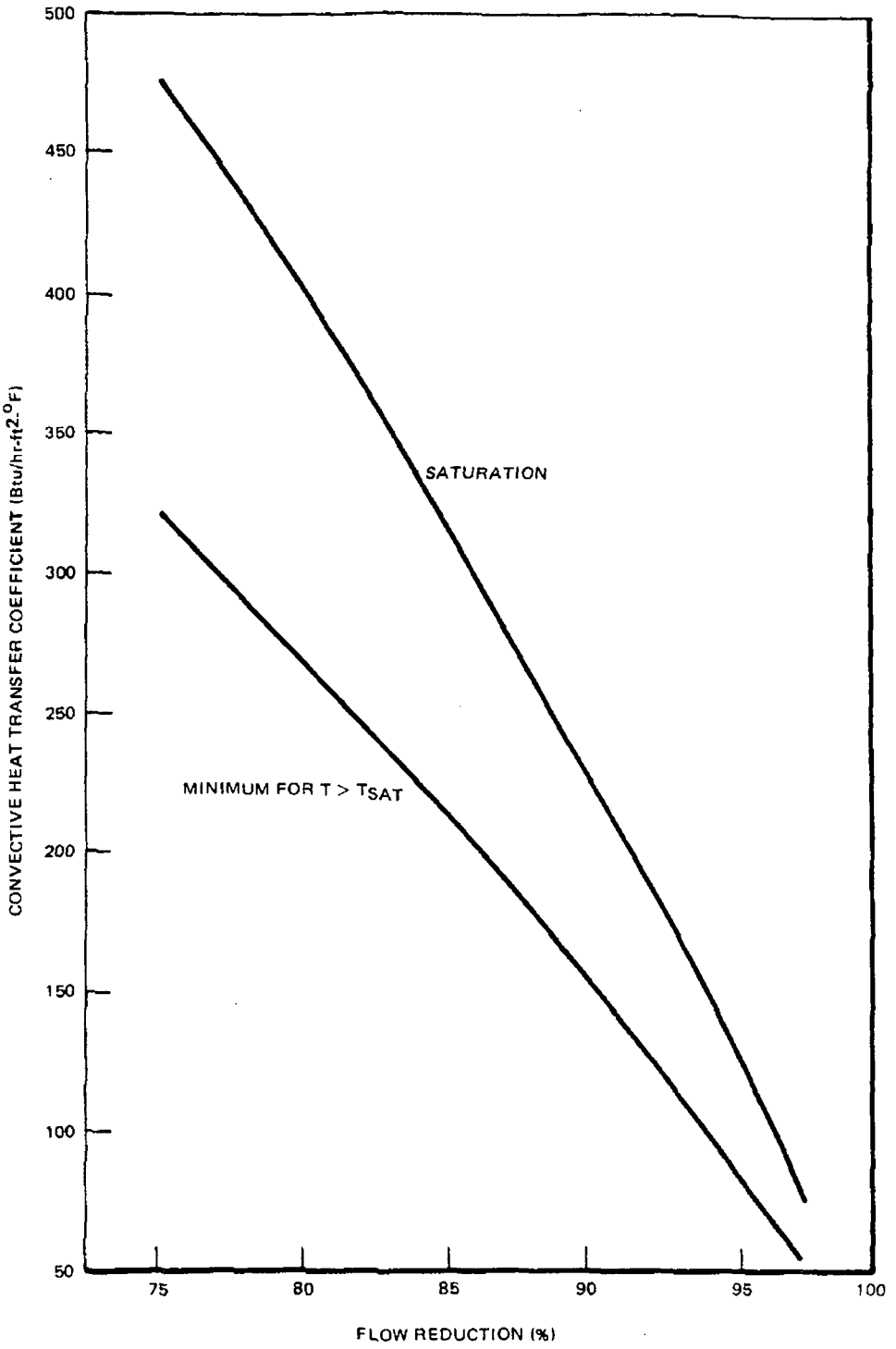


Figure 4-11. Dittus-Boelter Convective Heat Transfer Coefficient

Normally the channel provides a useful function by channeling the coolant flow past the rods; however, in the case of a flow blockage the channel tends to increase the severity of the consequences by acting as a barrier and prohibiting the leakage flow from coming into contact with the rods.

The temperature of the leakage side of the channel wall is expected to be at or near the saturation temperature of the coolant. Nucleate boiling will be maintained on the outer surface even for a complete blockage where large amounts of heat are being radiated to the channel wall. That this is so can be shown by examining the critical heat flux at the outer surface.

Considering the worst case of a complete blockage (5% Flow) and assuming that all the heat is radiated out through the channel walls, the peak heat flux at the channel midpoint is approximately $1.15 \times 10^6$ Btu/hr-ft$^2$. The narrow spacing between the adjacent channels or the channel and the control rod will not significantly reduce the critical heat flux. Applying the pool boiling critical heat flux correlation by Zuber[4.7] to the channel wall shows the channel wall critical heat flux to be $1.22 \times 10^6$ Btu/hr-ft$^2$. Thus, even under the worst conditions, nucleate boiling conditions will exist on the leakage side of the channel. However, on the interior of the channel high-temperature steam will add to the deterioration of the channel wall by oxidation. For high degrees of blockage the steam in the channel becomes superheated. The calculated coolant temperature at various axial locations in the blocked bundle is provided in Figure 4-12.

For very high degree of blockage the fuel cladding and fuel will melt. Once this melting is initiated the molten fuel will tend to drip to the bottom of the channel. As the damage of the bundle continues one of two things is most likely to occur: (1) at some point in time the strength of the rods will diminish to the point where they can not adequately support themselves and the rods will either bow or crumble and possibly make contact with the

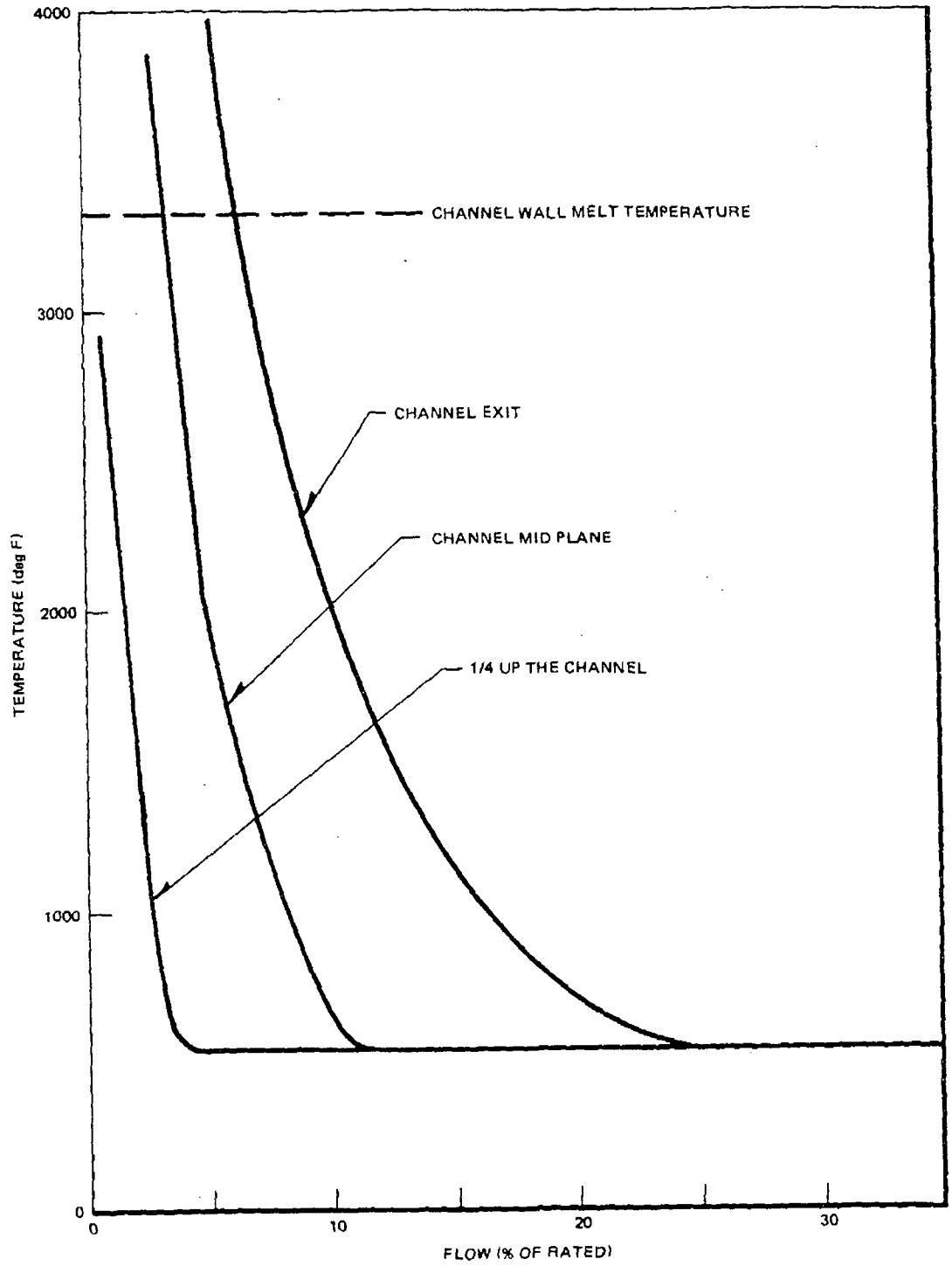


Figure 4-12. Axial Coolant Temperature Profile

wall or (2) the hot $UO_2$ will collect at the bottom of the channel and at some point will make contact with the channel wall. It is probable that the bulk of the molten material will fall toward the bottom of the bundle. Some of this material will be cooled sufficiently to solidify, and if coarse enough will accumulate on spacers and the lower tie plate. Solidified material and any remaining molten material will accumulate in the flow blockage region. Depending on the amounts and temperatures of this accumulated material and the properties of the blocking materials (metallic, ceramic, organic) the debris will either accumulate or melt through the blockage. If it melts through, the blockage will be relieved and coolant will enter the channel and terminate the incident.

Some of the molten material may contact the channel wall. Once contact is made with the wall the molten material may melt through the wall very rapidly, and allow coolant to re-enter the bundle and will also terminate the incident. An analysis was performed to determine the temperature response of the wall when subjected to contact with molten $UO_2$. The results and the model used are shown in Figure 4-13 for a typical case as a function of channel wall to bypass flow heat transfer coefficient. Once molten fuel makes contact with the channel it can be seen that the channel wall may be melted through in less than 1 second, Assuming that the critical heat flux has been exceeded in the bypass region. At this point the leakage coolant re-enters the bundle providing cooling for the bundle. This same coolant freezes the exiting fuel-metal mixture, prevents transport of the molten material across the interchannel gap and thus prevents propagation of the flow blockage failure to adjacent bundles.

If the molten material should penetrate the channel wall adjacent to the control blade, the control blade-to-channel wall clearance may be reduced. However, it is unlikely that this clearance would be reduced to the extent necessary to prevent insertion of the control blade. Nevertheless, the reactor is designed to be

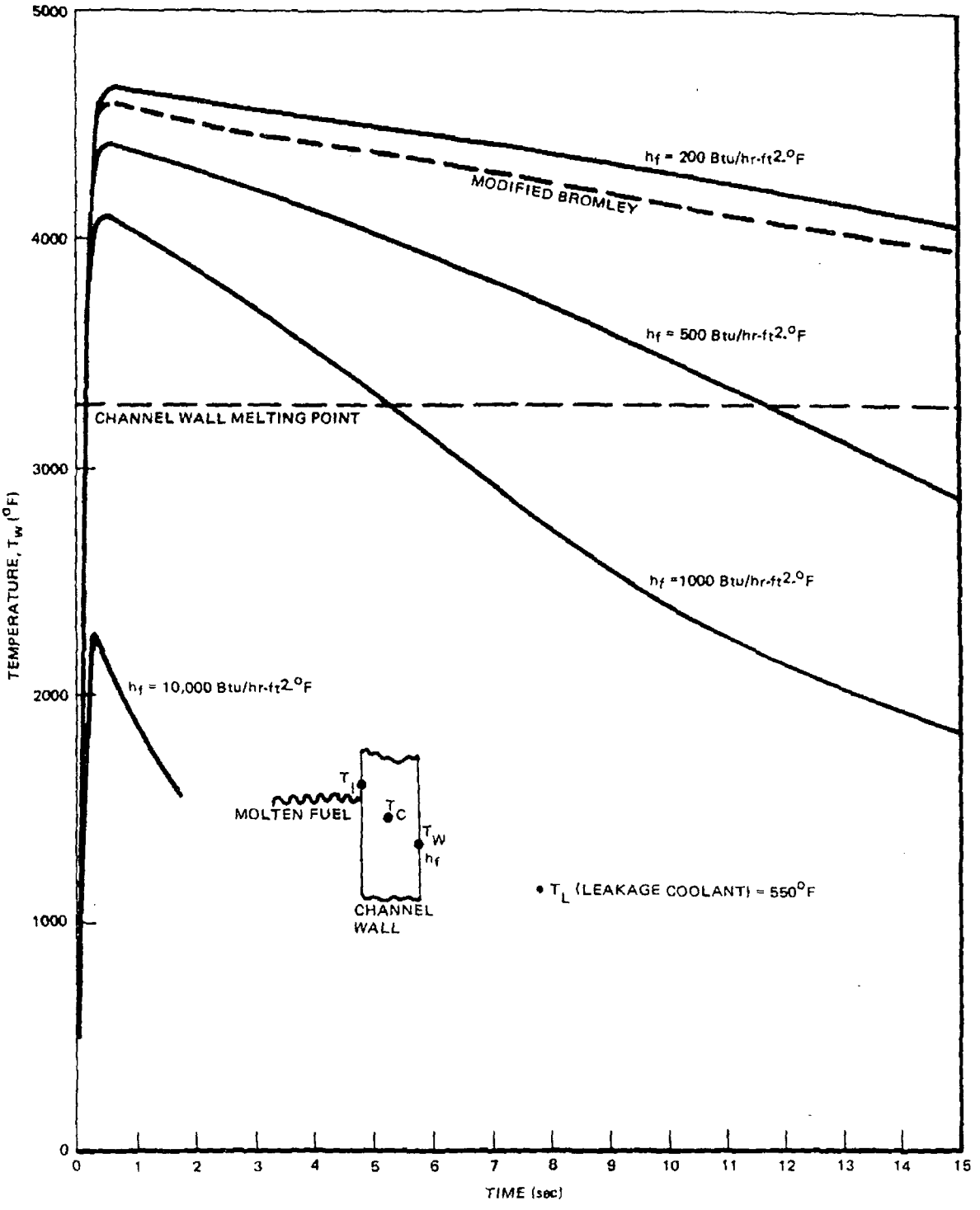


Figure 4-13. Channel Wall Response, $T_W$, to Contact With Hot Molten Fuel for Various Bypass Film Coefficients, $h_f$.

shut down, in the cold condition, with the highest worth control blade fully withdrawn. Therefore, since only one control blade would be affected by the flow blockage event, and since the reactor will be in the hot condition at the time the shutdown is required, there will be more than sufficient reactivity control to safely shut down the reactor.

## 4.5 CONCLUSIONS

In this section the thermal effects of a flow blockage on the cladding, $UO_2$, and channel wall were investigated. The significant conclusions reached were:

a. Loss of nucleate boiling conditions in high power density fuel assemblies will occur only for blockages in which the flow area has been blocked by more than 79%.

b. Cladding melting will occur for blockages greater than 95%. Molten $UO_2$ will be expelled into the channel only for blockages greater than 98% neglecting the effects of a reactor scram that would normally be initiated by the reactor protection system and for the highly unlikely condition of a complete flow restriction all of the cladding in the assembly will either have melted or fragmented and approximately 60% of the fuel will have melted.

c. Convective and radiative modes of heat transfer are adequate for rapid solidification of the molten particles that may exist in the channel.

d. If molten fuel makes contact with the channel wall, the wall will very quickly melt allowing leakage water to enter the assembly, and terminate the thermal transient. The molten material will freeze before being transported across the interchannel gap thereby preventing propagation of failure to adjacent bundles. The ability to safely shutdown the core will not be impaired.

# 5. MOLTEN $UO_2$/ZIRCALOY - WATER INTERACTION

As was shown in Section 4, a certain amount of cladding and fuel melting will occur for high degrees of flow blockage. Even though these high degrees of blockage are unlikely to occur and reactor scram will be initiated by the reactor protection system, it will be shown that the consequences of introducing molten materials into a BWR environment are minimal. This will eliminate the concern that has been predicated upon evidence that interactions between molten metals and water have exhibited the potential for destructive pressure pulses. As discussed in the introductory section of this report, considerable interest has been generated in molten metal/coolant interaction as a result of the intentionally destructive transients imposed upon BORAX-1 and SPERT-1, along with the accidental explosion of the SL-1 reactor. The interest has been concentrated primarily upon the mechanisms that were responsible for these destructive transients and, as a result of this, a large amount of experimental information concerning the interaction of water with molten materials has been generated. The consequences of molten $UO_2$/Zircaloy-water interaction during a flow blockage incident will be considered based on the wealth of this experimental information. From these it will then be possible to assess whether a flow blockage incident is capable of propagating widespread damage throughout the core.

The consequences of molten metal/water interaction are strongly dependent on the initiating mechanism and the environment in which this interaction is taking place. To thoroughly explore every aspect of this phenomenon, thereby assuring ourselves of the conclusions, a systematic approach has been taken in this study. First, a review of all the mechanisms which have been responsible for generating a pressure pulse will be discussed. This includes hot solid surfaces as well as molten materials. The applicability of these mechanisms to a flow blockage incident will be discussed and conclusions drawn regarding their consequences. In reviewing these mechanisms it becomes evident that the one ingredient necessary for destructive pressure generation is dispersal. Therefore, secondly, a review is made of the mechanisms known to be responsible for the dispersal of molten materials. Next, the consequences of actual flow blockages that have occurred in the nuclear industry are discussed, and lastly an analytical estimate is made in determining the pressure rise that may occur in the channel for conditions of high flow starvation.

## 5.1 OBSERVED MECHANISMS FOR PRESSURE PULSE GENERATIONS

### 5.1.1 BORAX-1, SL-1, SPERT-1

In each of the events that occurred at BORAX-1, SL-1 or SPERT-1, the experimental or accidental event was initiated by a power burst on a millisecond time scale resulting from a reactivity addition to above prompt critical. Each of these events involved an aluminum-uranium plate core in water which was at ambient temperature and pressure at the time of the incident. In BORAX-1 and SL-1 the experimental evidence indicated that the destructive pressure pulses that occurred in the reactor cores were produced by vaporization of the fuel near the time of peak power.[5.1,5.2] In these cases the vaporization aided considerably in the fine dispersal of aluminum into the water. This dispersal augmented the heat transferred to the coolant, thereby generating the pressure pulse. In the SL-1 accident the major damage to the primary system was produced by a water-hammer impact upon one head of the pressure vessel and not by the actual pressure pulse generated in the core by the molten fuel. The water slug was accelerated by a rapid void formation in the core from the heat liberated by the finely dispersed molten material. The impact of this slug against the vessel head caused the damage.[5.3]

In the destructive test performed with the SPERT-1 core, vaporization temperatures were not reached and no destructive pressure pulse occurred at the time of peak power before the fuel plates were molten. The core used for the SPERT-1 program was comprised of a 5 x 5 array of 3-in. x 3-in. x 24-in. fuel assemblies each containing 12 plates. The core was mounted in a 10-foot-diameter open tank facility which contained no provision for forced coolant circulation. On November 5, 1962, the core was subjected to a power excursion resulting in a 3.2 millisecond period. Data obtained during the power excursion indicated " . . .a peak power of 2300 MW, a nuclear energy release to the time of peak power of 14 MW-sec, a total burst energy of 31 MW-sec and an initial pressure pulse at about the time of peak power of about 35 psi".[5.4] A data plot for the 3.2-millisecond-period destructive transient is shown in Figure 5-1 which is reproduced from IDO-16883.[5.5]

Distinct from the transient pressure observed during the power excursion was a large amplitude pressure burst of about 2800 psi. This destructive pulse occurred 15 milliseconds after peak power. However, at the time when the power excursion had effectively been terminated by steam void formation, about one-third

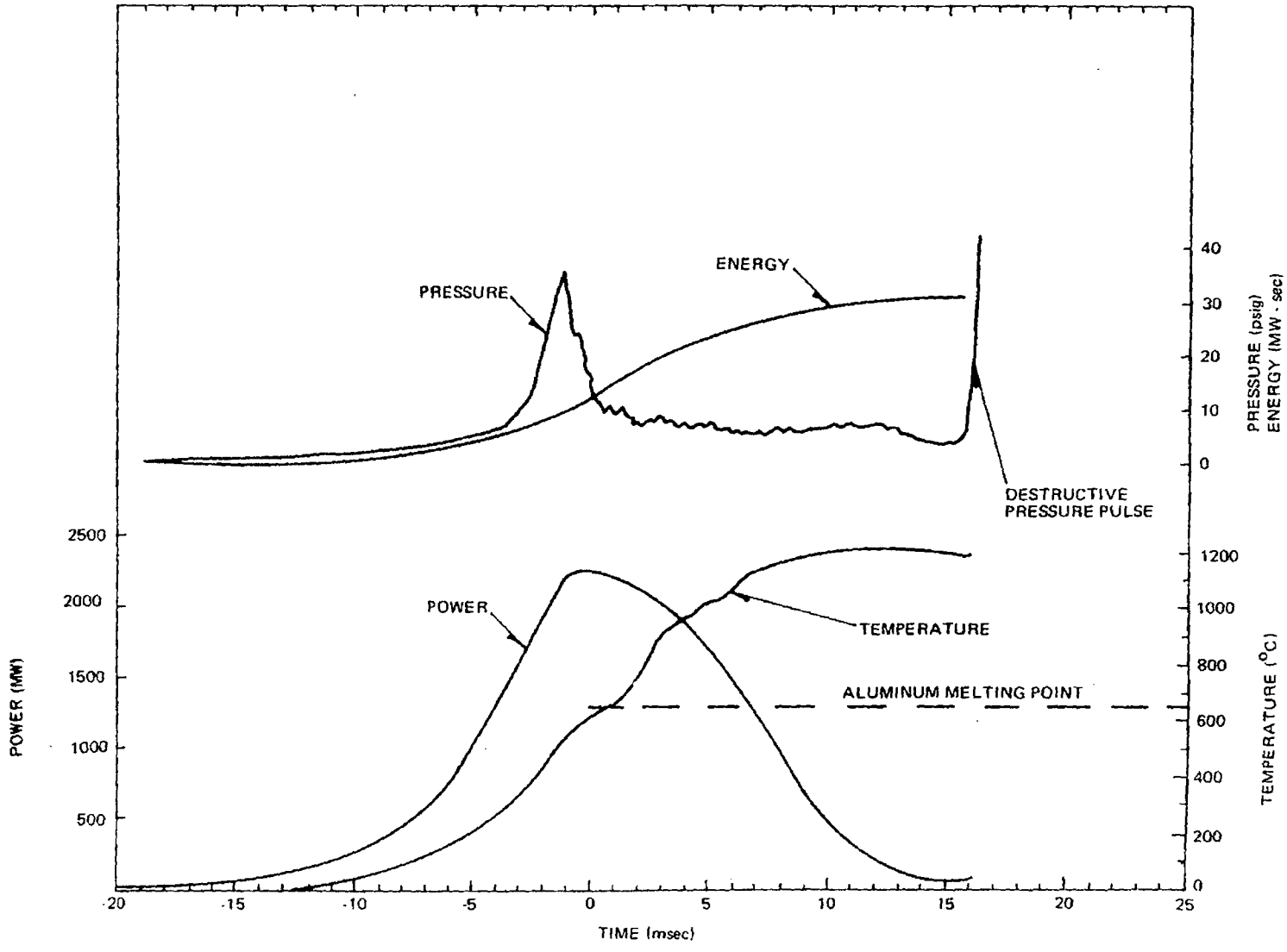


Figure 5-1. Data Plot From SPERT-ID Destructive Tests

of the fuel plate surface was molten. Extensive core damage resulted from this destructive pulse. Approximately 20 kg of metallic debris recovered from the reactor tank revealed particles ranging in size from a few inches to less than 0.003 inch in diameter.

The primary pulse of 35 psi that occurred was a consequence of the heat transferred to the coolant during the time in which peak power was reached. The causes of this mild pulse are easily explained and its consequences were not of any particular importance. The important aspect of this incident was of course the mechanisms which triggered the delayed 2800 psi pulse that resulted in extensive damage to the core.

Chemical analysis of the debris showed that an aluminum-water chemical reaction could have augmented the nuclear energy release by about 15%.[5.2,5.5] However, it is generally accepted that chemical reaction rates are too slow to have contributed significantly to generation of the destructive pressure pulse[5.6] In the absence of a rapid and energetic chemical reaction as the mechanism for generating destructive pressures, it was hypothesized that this pressure pulse was generated from steam generation by rapid heat transfer through the dispersal of the molten fuel plates into the water throughout the core. Two major questions remained unanswered as to the cause of the destructive pulse: (1) What was the mechanism for dispersal? and (2) Once dispersal occurred, what was the mechanism for large pressure generation?

TRW Space Technology Laboratories initiated an experimental program under a USAEC contract (Contract No. AT(04-3)-372) in an effort to find the answers to these questions. Transient in-pile experiments were performed[5.7,5.13] on a capsule containing an aluminum clad uranium molybdenum fuel disc immersed in water. The disc was fission heated in the reflector of the KEWB reactor with reactor periods as short as 1 millisecond. Reactor power, fuel disc temperature, capsule pressure, and steam-void volume were measured as a function of time. Simulation of the hydrostatic head above the reactor core was accomplished by a piston whose mass could be varied. Results of these experiments indicated that during rapid heating of a surface surrounded by a solid liquid, large destructive pressure pulses did not occur. However, the experiments did show that vapor blanket collapse upon the surface of the disc occurs about 10 milliseconds after the initial nucleate

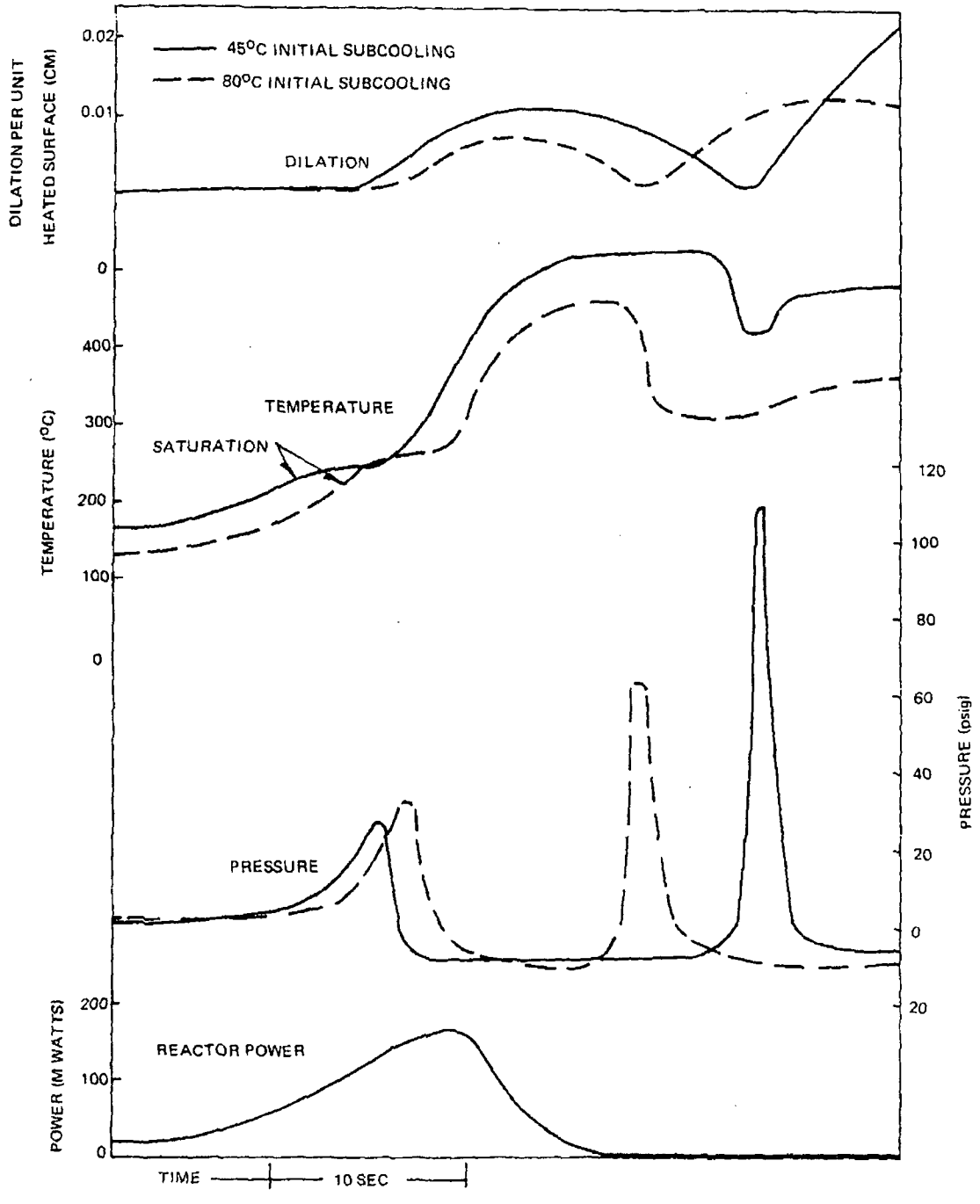


Figure 5-2. Reproduction from STL 372-30 of In-Pile Capsule Measurements of Transient Steam-Void Growth and Collapse for a 5-Millisecond Period

boiling phase and this collapse reproduces a water-hammer impact pressure pulse of about 100 psi under ambient conditions.[5.9,5.14,5.15] Figure 5-2, which was reproduced from STL 372-30,[5.9] shows the resulting water-hammer impact caused by the void collapse on the heater surface (dilation/$cm^2 \rightarrow 0$).* This was performed with a 120 gram piston loading which simulated a hydrostatic head of approximately 50 inches of water. It was hypothesized that this delayed mechanism dispersed the molten aluminum core into the water in SPERT-1.

A shock tube experiment[5.11] was devised to simulate this process and to see whether this mechanism would disperse the molten aluminum into the impacting water and generate a sufficient pressure to account for the SPERT-1 results. In this experiment a slug of water was allowed to impinge on a pool of molten aluminum at impact pressures comparable to those seen in the transient in-pile experiments. Figure 5-3 is a schematic drawing of the molten-aluminum water shock tube.

The results of these tests were affirmative in that the largest pressures observed were 2900 psia. This resulted from water impacting upon 950°C aluminum (melting point of aluminum is 650°C). The large impact pressures, which were on the order of 200 psia forced the dispersal of molten aluminum into fine particles thereby augmenting the heat transfer to produce high-pressure steam. An interesting conclusion of this experiment was that if the assumption was made that the pressure pulse was produced by the generation of high-pressure steam, only the sensible heat of the molten aluminum was needed to produce the pressure pulse; the latent heat and sensible heat of the solid aluminum are not necessary. Also the efficiency with which the sensible heat of the molten aluminum is converted into steam energy and mechanical energy increased with increases in the aluminum temperature above melting. This is shown in Figure 5-4 which is reproduced from STL 372-30.

Another important characteristic of the interaction between water and molten materials was revealed in this experiment. In one of the methods of diaphragm rupture, a solenoid-driven sharp needle was used at the center of the diaphragm. Very small impact pressures (as little as 50 psia) resulted from this system without any

*Dilation is the fractional rate of change of volume.

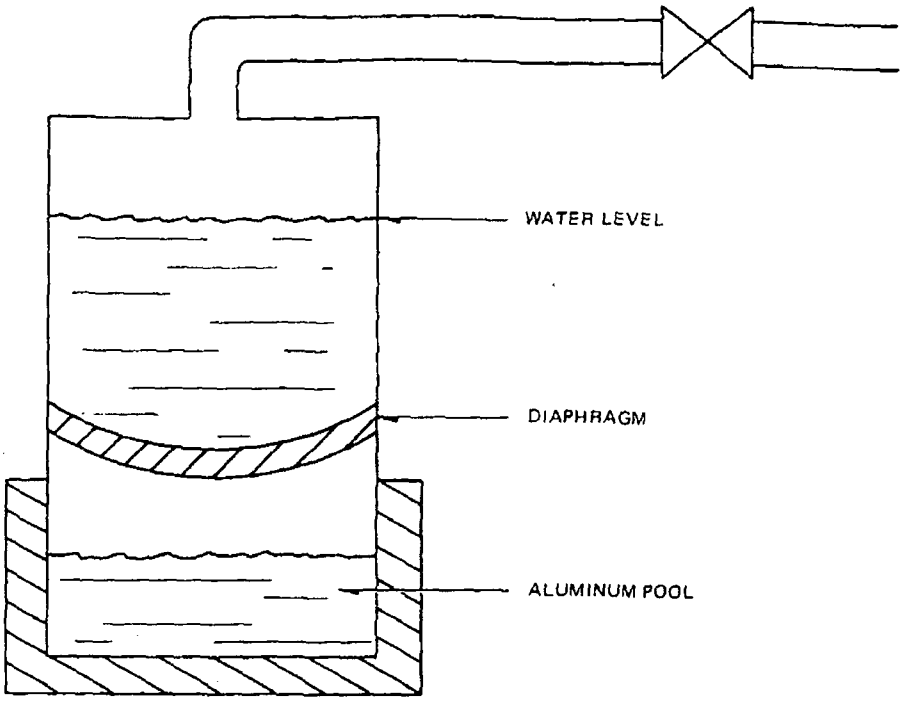


Figure 5-3. Schematic of Molten Aluminum-Water Shock Tube Experiment

large pressure generation. Investigation revealed that the slow rupture of the disc allowed a sizeable jet of water to hit the aluminum surface before the impact of the main water column. The steam produced a cushioning effect, resulting in low impact pressures and no dispersal of the molten aluminum.

Thus the 2900-psia pressure pulse seen in the shock tube experiment (Figure 5-4) combined with the pressure amplification phenomenon discussed by Wright[5.9] explains the destructive pulse experienced at SPERT-1.

Several important conclusions can be made relating the cause and consequences of these incidents and related experiments to a flow blockage incident in a BWR. These are:

a. The cores in all three cases were submerged by a solid water head which, as will be shown below, is much more efficient in transmitting a pressure pulse than the two-phase fluid that exists in a BWR.

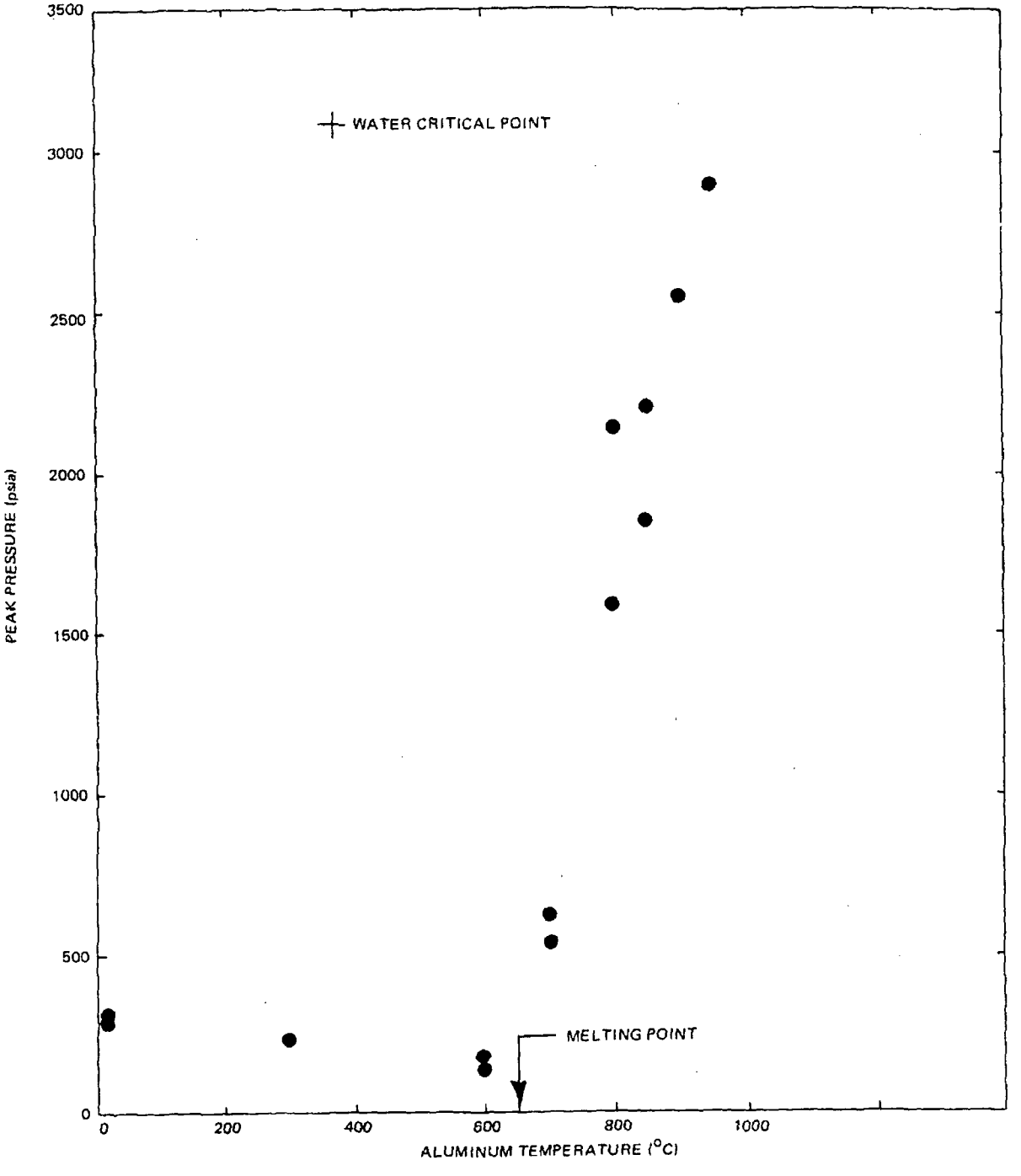


Figure 5-4. Temperature Dependence of the Peak Pressure From Water Impact Upon Aluminum

b. Dispersal of molten material into fine particles is necessary to generate destructive pulses.

c. A mechanism is essential to initiate this dispersal; in BORAX-1 and SL-1 it was the vaporization of the fuel initiated by a power transient on a millisecond time scale and in SPERT-1 the water-hammer impact from the collapsing surface voids dispersed the molten aluminum.

d. If the mechanism initiating dispersal exists, the temperature of the molten material must be much higher than the melting point so that the conversion efficiency of sensible heat energy is high enough to produce a significant amount of high-pressure steam; for $UO_2$ this means that the temperature must be greater than 5000°F.

e. High impact pressures are necessary to disperse molten materials.

f. The presence of steam in contact with molten material will provide a "cushioning effect" such that any impinging water will not be effective in dispersing this material.

The relationships of these observations to a flow blockage incident will be discussed in more detail in the following sections.

### 5.1.2 Pressure Pulses Produced by Rapid Transient Boiling with Solid Surfaces

Another mechanism by which transient pressure pulses have been generated occurs when a fluid undergoes transient heating by another substance. The magnitudes of these pressures are many orders of magnitude less than those seen in BORAX-1 and SPERT-1.

Under isothermal conditions in a single-component two-phase fluid the system pressure is the vapor pressure of the liquid. However, when a fluid undergoes transient heating the conditions are much more complex and only under certain special conditions is the system pressure approximately equal to the vapor pressure of the liquid at the temperature of the heated surface. These conditions were

investigated in experiments at TRW system.[5.9,5.10] The heated surface was a fuel disc immersed in water and contained in a fixed volume capsule. The disc was fission heated in the reflector of the KEWB core with reactor periods on the order of milliseconds. Transients up to 600°C were applied to the surface in about 10 milliseconds. Pressure generation occurred with compression of the water in the small fixed volume. The system pressure approximately followed the water vapor pressure corresponding to the disc surface temperature up to about 300°C. The pressure at this temperature was about 1400 psi. As the disc surface temperature rose above the critical temperature of water at 375°C the pressure was found to decrease. The conclusions reached were that at supercritical temperatures the heat transfer through the water adjacent to the disc surface was sufficiently reduced that the conduction heat losses into the cold water were greater than the heat flux from the disc. The critical pressure of water (3200 psi) could not be reached in these experiments.

Similar experiments were run with an initial load upon the capsule that simulated a solid water head. In this configuration, the water could move away from the heated surface under the pressure developed in boiling as in most systems that have an accessible free surface. As expected, the pressures produced were very modest. Figure 5-2 describes the phenomena that occur under these conditions. After a few milliseconds the high heat transfer of the nucleate boiling phase is terminated and the modest pressure falls to a vacuum as the water moves away. While insulated by the vapor blanket, the surface temperature increases and upon collapse of the vapor blanket a water impact occurs. This process repeats itself with diminishing impact pressures and eventually dies out. As discussed above this is the phenomenon that was hypothesized as being responsible for the delayed dispersal of the molten SPERT-1 core. When an air bubble was introduced in the fixed-volume-capsule experiments, vapor blanketing of the surface occurred very rapidly. The resulting pressures were only a few psi. Conclusions were that with an accessible pressure relief volume near the heated surface, large pressures are difficult to generate.

In these experiments the initial pressure pulse was also correlated with the hydrostatic load on the system as represented by a piston mass. Figure 5-5, reproduced from STL 372-30, shows this relationship. As expected the initial peak pressure decreases as the restraint (piston loading) on the system is lessened. As a

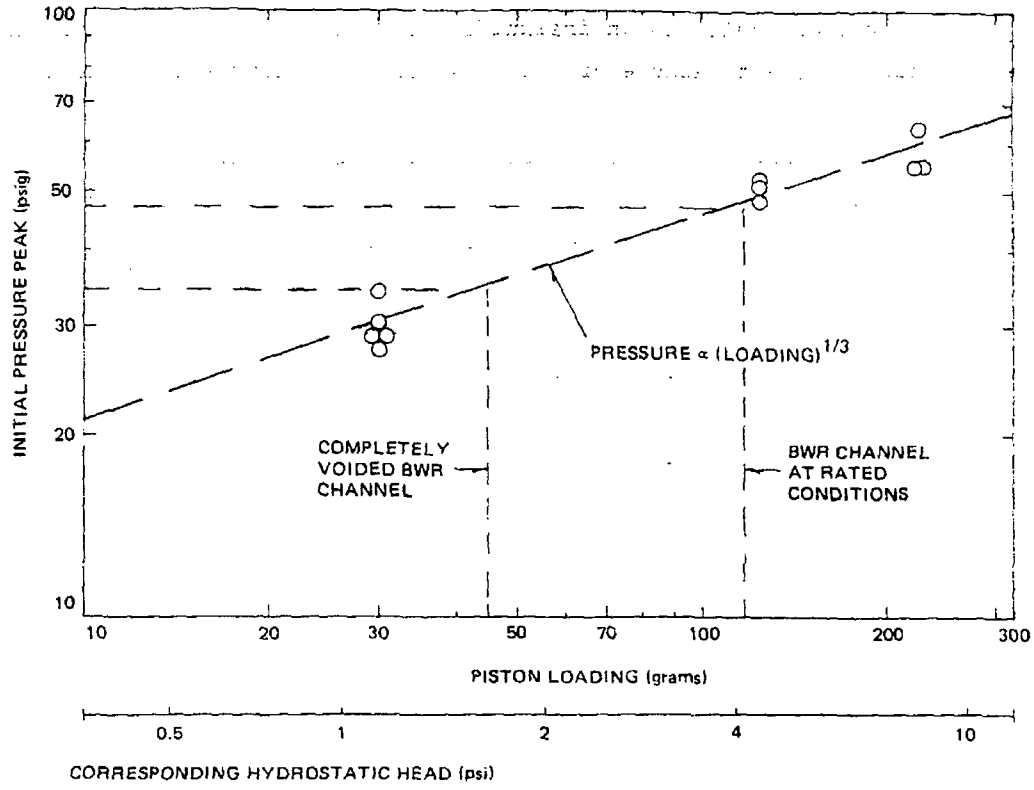


Figure 5-5. Magnitude of Initial Pressure Peak as a Function of Piston Inertial Loading for 5-Millisecond Reactor Period

measure of the relative worths of the various piston loadings in terms of BWR conditions, the hydrostatic head above the bottom of the active fuel in a BWR is also shown in the figure for normal operating conditions and a completely voided channel. The corresponding pressure peak range is between 35 and 45 psi. However, it must be kept in mind that the TRW tests were performed for zero void conditions. And as was shown, the presence of a small amount of voids reduces the peak pressure to a few psi.[5.9,5.10] In a BWR channel operating at rated conditions, the average void fraction is approximately 40% and of course during a flow blockage the void content of the channel is much greater. The rate of temperature increase of the cladding surface during a flow blockage occurs many orders of magnitude more slowly than the transients performed in the above experiments. This lower rate results in merely boiling the coolant away and not in generating pressure

pulses. If by some mystical way the temperature could rise very rapidly (on the order of milliseconds) the presence of the voids in the channel would restrain the initial pressure pulse to an insignificant "few psi", and of course the water-hammer impact is absent because of the presence of a saturated mixture.

Another piece of information which adds to the evidence that pressure pulses will not be produced by the solid surfaces in a BWR is the low conversion efficiency of thermal energy to high-pressure steam. Transient heating experiments of solid surfaces[5.9] have shown that only 0.1% of the total thermal energy goes into high-pressure steam. With this small conversion efficiency it becomes difficult to generate pressures of any magnitude. Considering all of the Zircaloy in a fuel bundle (cladding of 64 rods and the fuel channel) to be cooled from the melting temperature of zircaloy 3371°F to 545°F (the saturation temperature of water at 1000 psia) the amount of energy that would be available for high pressure steam is approximately 50 Btu. This is such a small amount of energy that the difficulty in generating large pressures with the solid surfaces in a BWR is obvious.

To further substantiate the fact that water coming into contact with hot cladding surfaces would not produce appreciable pressures, the General Electric Company performed a "pressure pulse" test in which the pressure rise resulting from water coming into contact with a very hot rod was measured. A schematic of the test configuration is shown in Figure 5-6. The flow to the electrically heated rod was reduced and finally stopped altogether allowing the rod surface to heat up as high as 1960°F in a high-pressure atmosphere. At this point a fast-response valve was opened allowing water to come rushing back into the test section. Transient pressure was measured with transducers whose response times were as low as 10 microseconds. The energy density* in the test section was approximately 40% greater than that in a fuel bundle and the stored energy release rate from the test rod was approximately twice that of a Zircaloy-clad fuel rod. Thus the pressures measured in this test were conservatively higher than would be experienced in a blocked fuel bundle under similar conditions. The maximum pressure measured during the tests was less than 10 psi which occurred when the rod was at 1960°F.

Thus it can be concluded that destructive pressures will not occur when water comes in contact with hot fuel rods in a reactor geometry.

*Stored energy in the cladding per unit of free volume.

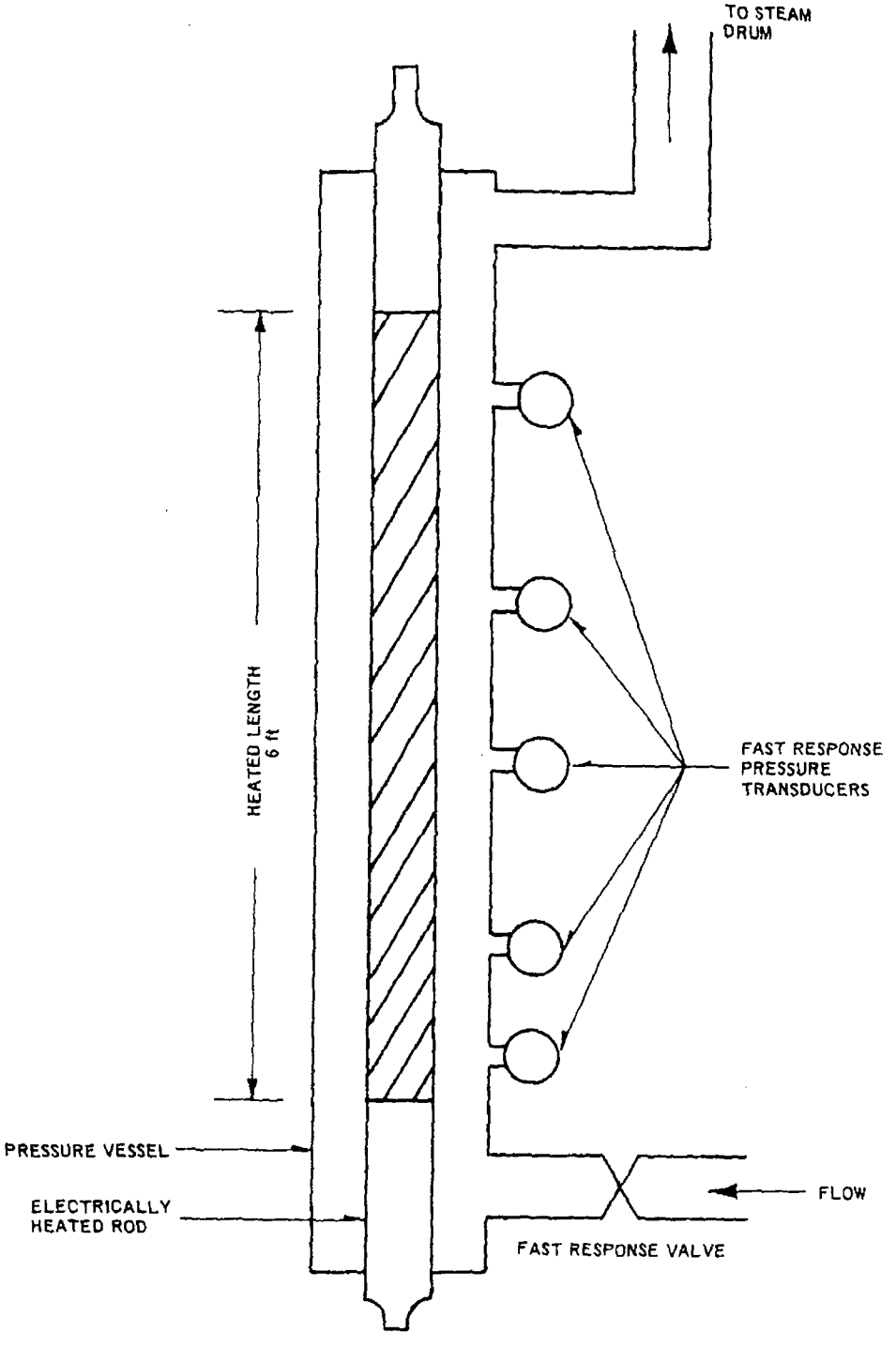


Figure 5-6. Test Configuration Schematic

## 5.2 DISPERSAL MECHANISMS

The one factor that is common to all of the metal/water explosions described in 5.1.1 is that dispersal of the molten material was necessary to generate the destructive pressure pulses. The necessary ingredient for pressure generation is that large amounts of energy must be liberated to the coolant in a very rapid fashion (usually on the order of milliseconds). This can be accomplished only if the molten material is suddenly divided into many small particles. This spearation accomplishes two things which are necessary for rapid heat transfer: (1) the time constant of the particle is very small thereby allowing it to release a large fraction of its heat content rapidly, and (2) the rapid formation of these particles allows the majority of the heat to be released in a short period of time. The combination of these two factors results in a very large amount of heat being liberated in a very short period of time.

In BORAX-1 and SL-1 dispersals were augumented by the fuel reaching vaporization temperatures. In SPERT-1, even though the fuel plates were molten near the time of peak power, the resulting pressure rise was only a modest 35 psi. However, the resulting water-hammer impact caused by the collapse of the surface voids was necessary to disperse the molten plates and augment the heat transferred to the coolant. In the shock tube experiments performed at TRW, large pressures were generated only after the impact by the water column was sufficiently large enough to disperse the pool of molten aluminum. Hence rapid fuel vaporization, collapse of surface voids, and impacting water columns are all mechanisms which could initiate dispersal of molten materials.

As discussed earlier, melting of either the cladding or $UO_2$ will not occur in a flow blockage incident except for the highly unlikely conditions under which the entrance orifice has been blocked off greater than 95%. Under these conditions a limited amount of melting will occur. The molten cladding and fuel or combinations thereof, will tend to form into relatively large droplets and will not exhibit a natural tendency to break up upon being quenched in water. This behavior of molten cladding and $UO_2$ was substantiated by the TREAT flat top transients, which will be discussed in more detail later. Simple melting of the fuel rods due to overpower and flow starvation will not result in the formation of finely dispersed particles that would be capable of generating a pressure increase. In this section, different mechanisms which have

been postulated or known to be responsible for the dispersal of molten materials will be investigated. These mechanisms will be evaluated in terms of whether they could be responsible for dispersing molten material during a flow blockage accident and therefore introduce the possibility for the generation of a pressure pulse.

### 5.2.1 Initial Experimental Investigations and Dispersal Models

Early research work in the field of Fuel Coolant Interaction (FCI) distinguished between fragmentation models in the bulk fluid, free from restraining boundaries, and those which apply in the bulk fluid where a rigid boundary existed. Concerning the former, there generally were four physical mechanisms which were hypothesized to cause the necessary fragmentation and dispersal into the coolant needed to produce an explosion.

1. Frozen Shell

   This hypothesis suggests that the hot fluid will freeze as a shell around the cold fluid. The frozen shell will continue to thicken as heat is transferred between the two liquids until the cold fluid is heated to a point where its vapor pressure is high enough to burst the shell. With this explosion and fragmentation, a thorough mixing of the two fluids will occur, generating a much larger explosion.

2. Weber Number Effect

   Two types of forces are considered when a molten metal sample falls through a fluid, inertia forces and surface tension forces. The effect of the inertia forces, momentum and viscous drag, is to deform and break up the sample, while the surface tension forces tend to counter balance this effect. The ratio of these two forces is known as the Weber Number ($\rho u^2 R/\sigma$). When the Weber Number exceeds a certain critical value, 10 to 20, the inertia forces overcome the surface tension forces and the molten sample fragments into smaller subparticles producing an explosion.

3. Cold Liquid Entrainment

In the liquid entrainment theory, suggested by Brauer[5.16] fragmentation and explosions occur when cold liquid infiltrates fissures in either a freshly frozen crust of hot material or in the incoming jet of hot material and is vaporized. The initial pressure pulse, due to vaporization, would fragment the drop, resulting in greater heat transfer and violent explosions.

4. Violent Boiling

A stable film-boiling regime usually results where a hot molten-metal surface comes in contact with a liquid coolant. The violent boiling theory proposed that fragmentation was caused by the violent force involved with the pulsating collapse and reestablishment of a vapor film during transition boiling.

The above four theories have concerned FCI's in the absence of restraining boundaries. Experimental evidence gathered by Long[5.17] has produced a separate fragmentation hypothesis for fragmentation in the vicinity of a solid restraining surface. Through the Liquid Entrapment Theory, it is postulated that when a molten-metal sample falls through a coolant liquid, but remains molten with sufficient size to entrap coolant against a solid surface, the molten sample may be blown apart due to vaporization of the entrapped liquid coolant under certain conditions. This mechanism should not be confused with the Cold Liquid Entrainment model of Brauer, which requires entrainment of water inside a falling drop of metal, far from any surface.

Anderson and Armstrong[5.18] conducted an experimental study in 1974 to review the early mechanistic models concerning FCI in the absence of restraining boundaries. Using subsurface movies, the Frozen Shell and Weber Number models directly contradicted their experimental results. The resolution of the film interpretation was not fine enough to rule out the Cold Liquid Entrainment and Violent Boiling Hypothesis, but neither was there any direct evidence supporting these mechanisms as the fundamental cause of the explosion. Therefore, a closer examination of these two theories along with supporting experimental data will be made. In addition, a review of Long's experimental investigation into FCI's in the presence of a solid boundary, (Liquid Entrapment Model) will be made. These three theories will then

be applied to a Fuel Coolant Interaction consisting of molten $UO_2$/Zircaloy and water in a BWR and the resulting consequences.

5.2.1.1 "Cold Entrainment Model"

An experimental investigation was conducted by Brauer[5.16] in which a survey of molten metals (aluminum, lead and Wood's Metal) were dropped in liquid water at various temperatures with the objective of obtaining fragmentation of the metal. In more extensive tests by Flory et al[5.19] molten metals such as lead, tin, bismuth, zinc, aluminum, mercury, copper and Wood's Metal were used at diameters ranging from 1/16 to 2 inches in diameter. In general, Brauers results showed that fragmentation did not occur for metal temperatures less than or slightly above the metal melting points or for cooling water temperatures greater than 60°C. It was also found that fragmentation, if it occurred, was more violent at lower water temperatures. Examination of experimental results, showed no evidence supporting the "violent boiling hypothesis" in either series of tests. Brauers results lead him to conclude that molten metal, when coming in contact with a liquid or shortly after, forms a solid shell due to rapid heat transfer from the metal's surface. Due to some mechanism, liquid is trapped inside the shell which rapidly vaporizes and produces internal pressures which finally breaks the shell into many small fragments. A mechanism by which small quantities of quenching liquid gets inside a drop of molten metal has been proposed by Flory et al. This mechanism, supported by tests, is a Helmholtz instability entrapment mechanism. One of the most significant conclusions reached in the tests performed by Flory is the effect of the temperature of the liquid on the amount of fragmentation:

> "The temperature of the quench water has been varied from - 8°C to 100°C in numerous tests. Near the freezing point of water, the violence of fragmentation is not a function of bath temperature, while above about 25°C, the violence and extent of fragmentation decrease rapidly to zero at 90 to 100°C. Tests with several metals dropped into liquid nitrogen at its boiling point gave no fragmentation whatever, giving supporting evidence to the results of the water experiments, namely, that metals will not fragment in a saturated liquid."

This conclusion is significant since in a BWR the coolant is a saturated two-phase mixture. The temperature of even the coldest liquid (which is approximately 20 $Btu/lb_m$ subcooled) is not low enough to cause fragmentation. This 20 $Btu/lb_m$ subcooling corresponds approximately to the 90°C water temperature in Flory's experiment.

Hence the "cold liquid entrainment model" as a mechanism for fragmentation and pressure generation can be completely discounted for a BWR flow blockage incident.

5.2.1.2 "Violent Boiling Hypothesis"

The "violent boiling hypothesis" predicts whether metal fragmentation will occur, whereas the extent of fragmentation is normally assumed to be dependent on the properties of the molten material. This hypothesis has been stated as[5.20]:

> "If the melting point of a metal is within the region of violent boiling (transition or nucleate), it is hypothesized that the metal will suffer fragmentation. If on the other hand, the metal has solidified while in the film boiling regime, then according to the hypothesis fragmentation should not occur."

This criterion, interpreted for metal fragmentation in water, implies that metals which have melting points below the critical temperature of water 375°C (transition to violent boiling occurs near the critical temperature) will suffer fragmentation when the molten metals are quenched in water.

The rationale behind this fragmentation criterion can be described as follows: The classic boiling curve is generally classified into three regimes, namely nucleate, transition, and film boiling, which occur in that order as the difference between the surface temperature and liquid saturation temperature is increased. The film boiling regime is considered hydrodynamically quiet whereas the transition and nucleate boiling regimes are typically characterized by a high degree of turbulence cause by the growth and collapse of vapor bubbles. This turbulence is usually more intense when the bulk liquid temperature is below saturation, a condition known as subcooled boiling. The phenomenon of nucleate boiling cannot occur on a surface whose temperature is higher than the critical temperature of the liquid (for water 375°C or 750°F). Thus, transition boiling changes to film boiling at some temperature above the critical temperature. In the quenching of very hot metals the boiling regimes will proceed in the following order: film boiling, then at a lower temperature the boiling enters a transition region followed by nucleate boiling and finally convective heat transfer without boiling.

The violent boiling hypothesis was investigated by experiments performed at ANL[5.20,5.21] in which uranium (mp 1132°C), nickel (mp 1425°C) and zirconium (mp 1860°C) did not fragment in water. Additional experiments were performed with tin (mp 271°C), bismuth (mp 271°C), lead (mp 327°C), and zinc (mp 420°C) which were heated to 825°C and dropped into 0°C water. The results of these experiments are shown in Table 5-1 which is reproduced from ANL 7152. The metals with melting temperatures above the critical temperature of water (375°C) did not fragment whereas those with melting temperatures below the critical temperature suffered severe fragmentation.

The experiments further indicated that subcooled boiling (<100°C for water) was also necessary for fragmentation. When the water temperature was raised to 60°C, tin, lead, and bismuth did not fragment as they did in 0°C water. These same metals were heated to 600°C and dropped into liquid nitrogen which as a critical temperature of 147°C. No fragmentation occurred which is also consistent with the violent boiling hypothesis. Similar results were also obtained by Ivins[5.22,5.23] with tin and bismuth. Again this upper water temperature threshold for which no violent explosion occurs, agrees with the reported value by Brauer and Flory.

Table 5-1

RESULTS ON DROPPING VARIOUS MATERIALS INTO WATER
REPRODUCED FROM ANL 7152

(Sample volume, ~0.3 cc; height of drop, 2 ft)

| Material | Melting Point (°C) | Sample Behavior for Indicated Drop Temperature (°C) | | | |
|---|---|---|---|---|---|
| | | Water at 0°C | | Water at 60°C | |
| | | Intact | Fragmented | Intact | Fragmented |
| Gold | 1063 | 2600 | - | a | a |
| Silver | 961 | 1900 | - | a | a |
| Aluminum | 660 | 825 | - | 825 | - |
| Zinc | 420 | 825 | - | 825 | - |
| Lead | 327 | - | 825 | 825 | - |
| Bismuth | 271 | - | 825 | 825 | - |
| Tin | 271 | - | 825 | 825 | - |
| Rose's Metal | 96 | - | 600 | a | a |
| Wood's Metal | 70 | - | 600 | a | a |

[a] Experiments not done in 60° water.

The effect of heating the liquid can be caused by a combination of two effects. The formation and collapse of a bubble is typically more violent as the subcooling is increased and, as was shown by Ivins,[5.24] the transition from film to nucleate boiling occurs at lower surface heat fluxes as the water temperature is increased. This latter effect will cause the transition from quiet film boiling to violent nucleate boiling at a lower surface temperature of the molten mass. This lower temperature will result in the molten mass being in a more viscous state and therefore less apt to fragment into small particles.

Application of this hypothesis to molten $UO_2$/Zircaloy-2 water interaction indicates that neither molten $UO_2$ nor Zircaloy-2 will fragment upon being quenched in water. Both the $UO_2$ which has a melting point of 5000°F, and Zircaloy-2 with a melting point of 3371°F will have solidified before the surface temperatures reach the critical temperature of water (750°F). This was further verified in the TREAT flat top experiments (to be discussed later) in which no fragmentation was observed to occur when molten $UO_2$ and Zircaloy-2 were quenched in water.

Exceptions to the violent boiling hypothesis exist as reported by Flory et al. In their experiments, copper which melts as 1087°C, was heated to a temperature slightly greater than its melting point and was dropped into a water bath. The violent boiling hypothesis predicts that, since this temperature is greater than the water critical temperature of 375°C, the copper should have solidified before reaching the critical water temperature and thus no fragmentation should occur. Yet, fragmentation of the copper was reported. Flory et al also state that upon reviewing detailed close-up films of lead and tin, there was no evidence of boiling action at any time. It would appear a second generation model is needed to resolve some of the inconsistencies in these early mechanistic models.

5.2.1.3 "Liquid Entrapment Theory"

Violent interactions between molten metals and liquids have also been experienced by industries that handle molten metals. Accidently dropping a mass of molten metal from a crucible into open troughs of water has in certain cases resulted in the complete destruction of buildings. Handling of liquid metals posed a serious safety hazard until a complete understanding of the problem was

provided by Long.[5.17] In a series of experiments, Long demonstrated that the mechanism which caused the observed explosions was the entrapment of a small amount of liquid beneath the molten mass as it settled on the bottom of the container holding the water.

When a mass of hot metal (solid) is dropped into a vessel of liquid water, there is a considerable amount of steam evolution, hissing, and general agitation but no explosion. The heat transfer between the metal and the water is good enough so that the steam rapidly settles down to a weighted mean temperature (the same elementary technique of the "method of mixtures" for determining heat capacities). If the metal is liquid and falls into a deep pool of water, the same kind of thing happens. To achieve an explosion, the metal must land on the bottom of the containing vessel in a state where at least part of the mass is still fluid — the outside may have cooled and solidified. If the nature of the surface is such that a mass of water is trapped between the molten metal and the bottom, the further cooling of the metal leads to overheating of this water until eventually it blows up with the noise and disruptive violence that characterizes an explosion. If the metal is not hot enough initially, or is cooled by the surroundings before it hits the bottom, or the mass is not large enough, there will be no explosion.

The nature of the surface on which the metal mass comes to rest is of paramount importance. If this solid interface is not readily wetted by liquid water (a hydrophobic surface), it is difficult to obtain the trapping needed for explosion. On the other hand, if the interface tends to by hydrophilic, so as to cling to the water (Figure 5-7), an explosion can be observed under conditions where none would otherwise occur, for example, with a smooth metallic bottom. Proof of this was provided when coating the bottom of the container with materials with little or no affinity for water — oil, grease, tar, or a variety of different paints and other surface finishes — tended to prevent the trapping of water and the kind of explosion considered here.

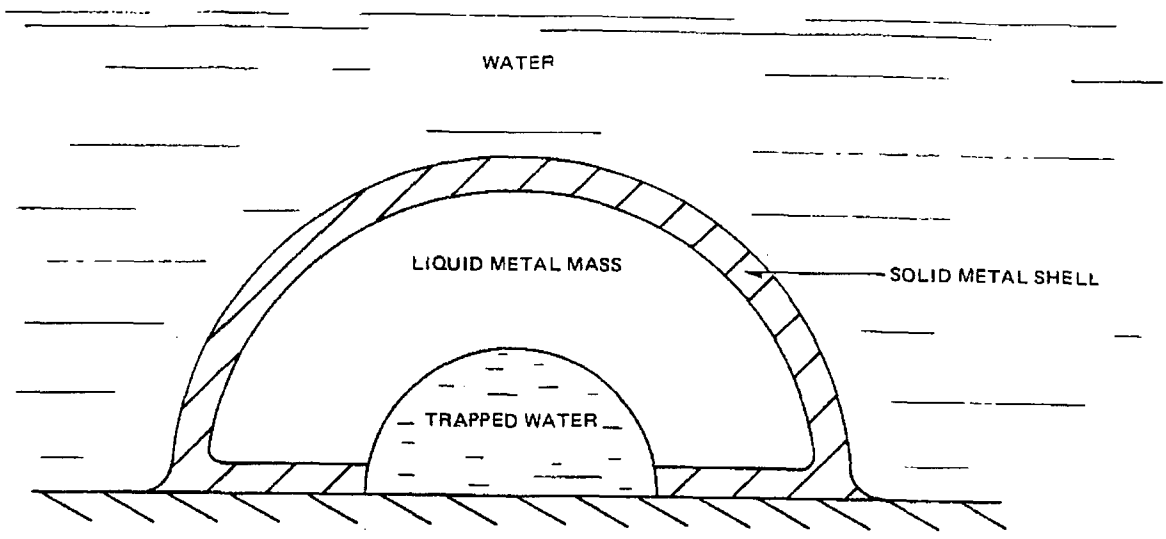


Figure 5-7. Representation of the Mechanism of a Physical Metal-Water Explosion

Long also showed that fine droplets generated by a screen or mesh, which breaks up the mass of molten material into small droplets, could not produce a physical explosion. The reason for this is that the smaller particles solidified more rapidly and because of their smaller size were not capable of entrapping water.

The mechanism for the type of explosions due to liquid entrapment will not be present during a flow blockage accident for a number of reasons. For the unlikely conditions of orifice flow blockage areas greater than 98%, a certain amount of fuel melting will occur as was shown in Section 4. Under conditions such as this, melting will take place in small amounts, e.g., a melting candle. Gross amounts of molten material which would be capable of entrapping liquid are therefore not likely to occur. This fact is supported by tests performed at the General Electric Company in which Zircaloy rods were actually melted.[5.25]

For these tests, a 4-rod and a 9-rod array of simulated fuel rods were inductively heated, allowing the molten Zircaloy to drain through a stainless steel tie plate into a pool of water below. The test configuration is depicted in Figures 5-8 and 5-9. The droplets were measured; a histogram is shown in Figure 5-10. The range of droplet sizes obtained is in general agreement with the predicted droplet size,

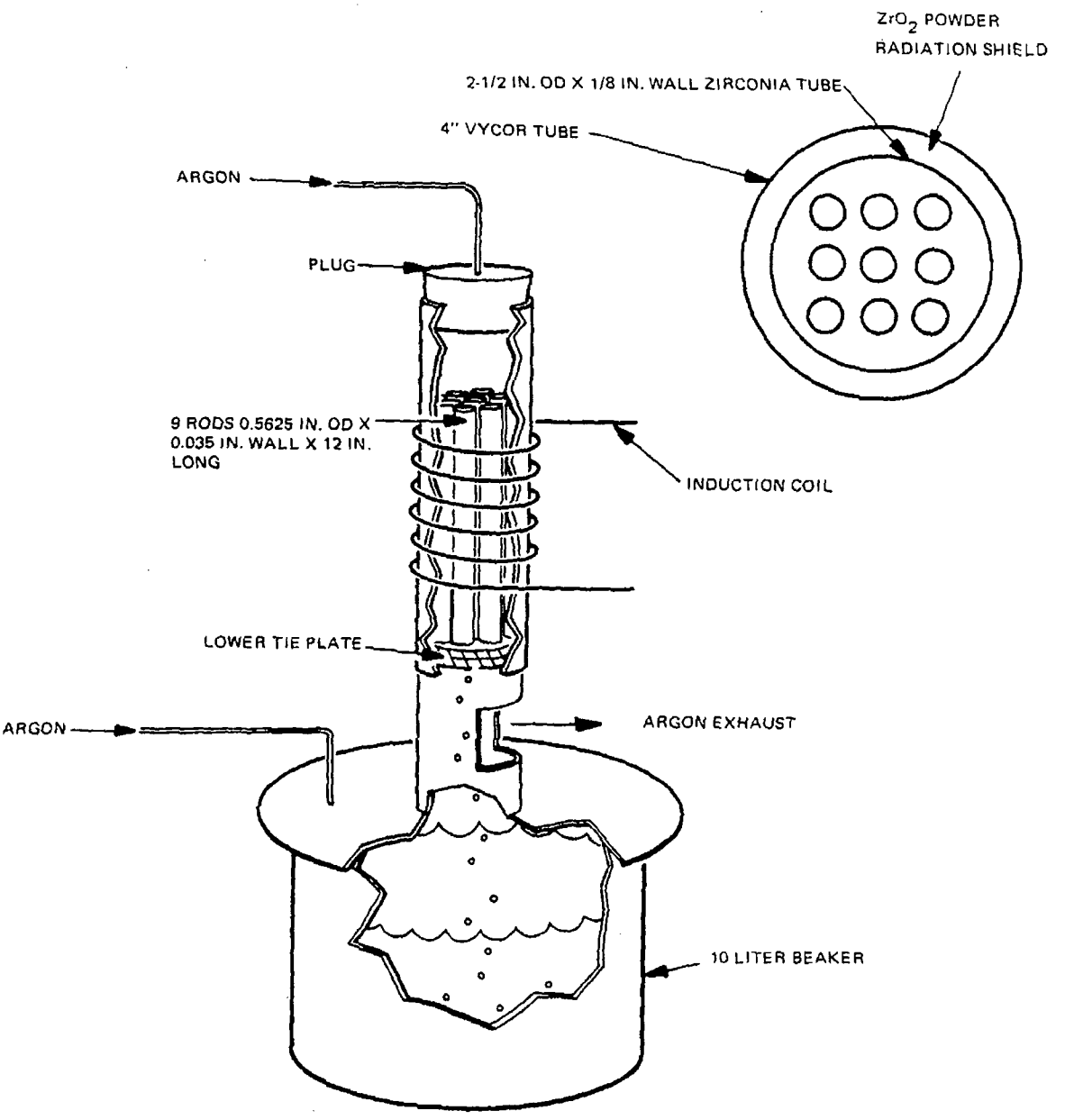


Figure 5-8. Sketch of Induction Heater Droplet Test Section

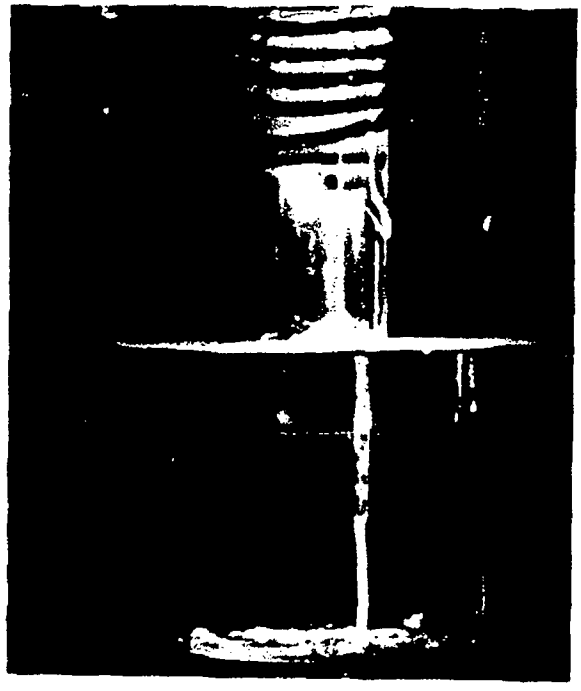

Figure 5-9. Photograph of 9-Rod Droplet Test Section

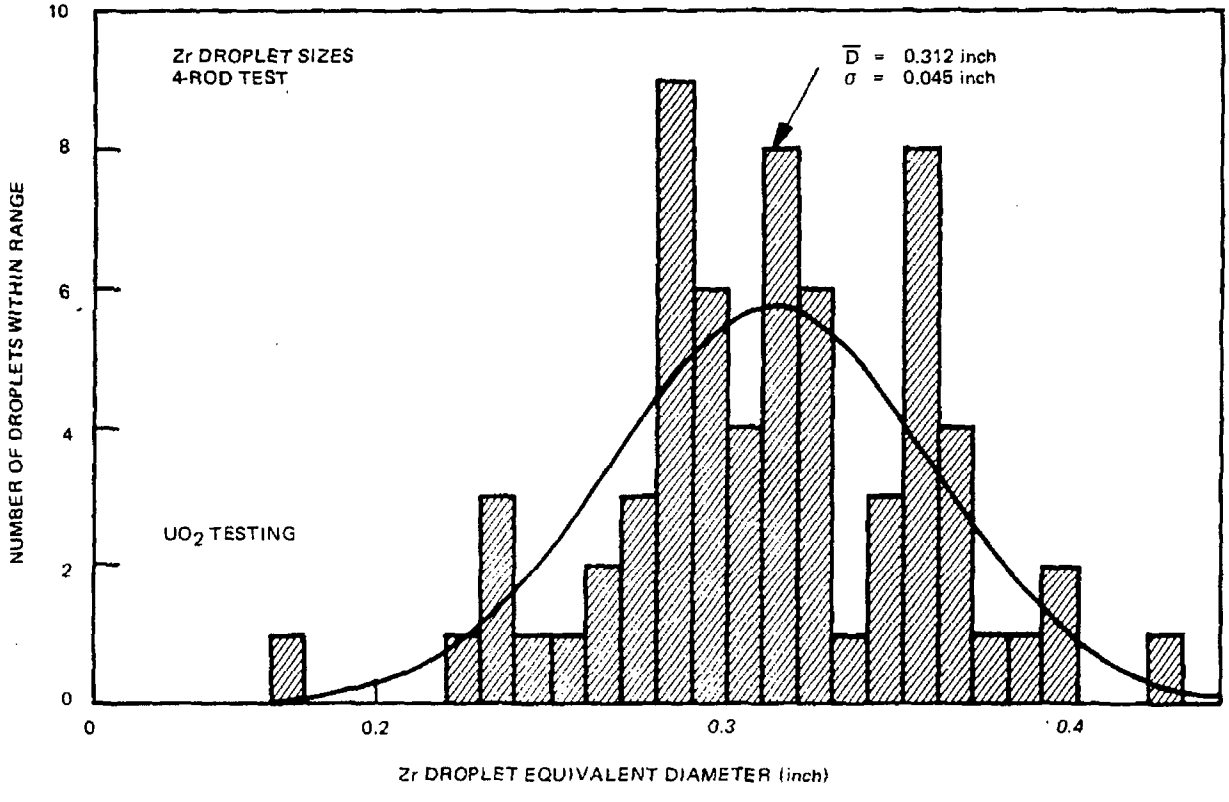


Figure 5-10. Histogram of Zircaloy-2 Droplet Size, Dripping Through a Stainless Steel Tie Plate Into Water

which was obtained simply from the tie plate geometry. The droplets were much too small to entrap any water. There is also evidence[5.26] that as the rate of molten material leaving the rods increases it eventually forms streams rather than discrete droplets. However, this is of an inconsequential nature. Long showed that when 50 pounds of molten metal was poured through holes of various diameters, metal streams smaller than 2-3/4 inches in diameter never resulted in explosions. If molten metal streams occurred in the fuel bundle their diameters would be many orders of magnitude less than this since the diameter of the fuel rod themselves is only 0.483 inches for 8 x 8 fuel. Hence flowing streams of molten fuel rod material in a bundle will not be capable of entrapping water and causing explosions.

Other factors to be considered in evaluating the mechanism of liquid entrapment as a possible source for a destructive explosion during a flow blockage incident are the geometry of the bundle and the hydrodynamic conditions for which fuel rod melting will occur. As can be seen in Figure 3-4 the geometry of the lower tie plate is such that it would be difficult for any water to be trapped upon its surface – the surface upon which the droplets would tend to collect as they left the fuel rods.

It can be concluded that the mechanism of liquid entrapment between a molten material and a solid surface during a flow blockage incident is not possible and it cannot therefore be considered as a possible source for destructive pressure generation in a BWR.

### 5.2.2 Recent Spontaneous Nucleation Model to Describe Fuel Coolant Interaction

A recent mechanistic FCI model has been proposed by Henry and Fauske[5.27] which describes film boiling in a liquid-liquid system. The Spontaneous Nucleation Model is based on analysis[5.27,5.28] and experiments using simulated materials of Freon and Mineral Oil[5.29] and supported by the numerous amount of available tin-water data.[5.30] This model is believed to be the latest state of the art concerning FCI and will be applied to molten $UO_2$/Zircaloy-Water Interactions which could occur during a postulated BWR Flow Blockage.

The basis of this model is the establishment of four criteria, which must be met, in order for an energetic FCI. These criteria are as follows:[5.30]

1. "There must be an initial premixing of the fuel and coolant. This can be accomplished by film boiling being the initial mode of heat transfer between the constituents. This would allow the fuel to nonexplosively become intermingled with the coolant.

2. Direct liquid-liquid contact is required, implying a breakdown in the film layer between the two fluids. This destabilization is dependent upon the surface temperature of the hot fluid.

3. The interface temperature once liquid-liquid contact is achieved must be greater than the spontaneous nucleation temperature for an explosive interaction to occur, but less than the critical temperature of the coolant. This results in fragmentation and mixing of the hot and the cold fluid without delay.

4. For the interaction to escalate to a large scale FCI, the proper inertial constraint is also required. This somewhat nebulous criterion can be thought of qualitatively as a condition where a non-energetic interaction is characterized by the fuel and coolant being driven apart from the initial vapor explosion whereas an energetic FCI is one where fuel and coolant are more fully intermixed."

This model has been based on determining the interface temperature between the coolant and molten fuel when in contact. The interface temperature ($T_I$) at the moment of contact has been proposed by Fauske.[5.31]

$$T_I = \frac{T_H + T_c\alpha}{1 + \alpha} \tag{5.1}$$

where $$\alpha = \sqrt{\frac{K_c\rho_c C_c}{K_H\rho_H C_H}} \qquad \alpha = 0.205 \text{ for Tin-Water}$$

(where subscripts H and C represent the hot and cold liquid, K is the thermal conductivity, $\rho$ is density and C is the specific heat.)

In a liquid-liquid system there is an absence of preferred nucleation sites found at a solid-liquid interface. If a liquid temperature is raised to a sufficient value, fluctuations occur, and there is a finite probability that a cluster of molecules with vapor-like energies can come together to form a vapor embryo of the size of the equilibrium nucleus.[5.32] Spontaneous nucleation refers to homogeneous or gas-free heterogeneous nucleation as a result of density fluctuations in a metastable liquid, rather than nucleation from preferred sites. Due to imperfect wetting of the liquid-liquid surface (wetting is a function of time and temperature) the spontaneous nucleation temperature is in general less than the homogeneous nucleation temperature. For perfect wetting, the homogeneous nucleation temperature is the upper limit of spontaneous nucleation.

Since the capability to identify liquid-liquid contact as a function of time and temperature does not exist at the present time, this model has been based on the homogeneous temperature ($T_{HN}$) as the known upper limit for spontaneous nucleation. For water the homogeous nucleation temperature is 305°C.

The model maintains that $T_I$ must be less than the critical temperature of the coolant ($T_{critical}$). This is due to the fact that if $T_I \geq T_{crit}$, the number of molecules need to make up a vapor bubble decrease rapidly. In addition, when the critical point is reached there cannot be nucleation because the vapor and liquid are the same. Once $T_{crit}$ is exceeded and the coolant contacts the hot fuel, the coolant will enter into film boiling rather than wetting the fuel surface. Thus, the criteria $T_{HN} < T_I < T_{crit}$.

The physical picture of the situation is that the liquid coolant is attempting to wet the hot surface by testing it in the form of coolant drops. The hot surface will wet only when the combination of temperature and drop size are correct. In Figure 5-11, Henry[5.28] varied the drop size parametrically for a Freon-Oil system and found that as the drops get bigger the mode of contact will be film boiling. After the surface has been wet, a large amount of heat can be transferred to the coolant until the homogeneous nucleation point is reached for a sizeable portion of the drop.

At this time a violent nucleation process will fragment the liquid drop, producing a fine liquid spray and the stored high-pressure vapor, which is the incipient shock wave to initiate the reaction. Henry states[5.29]

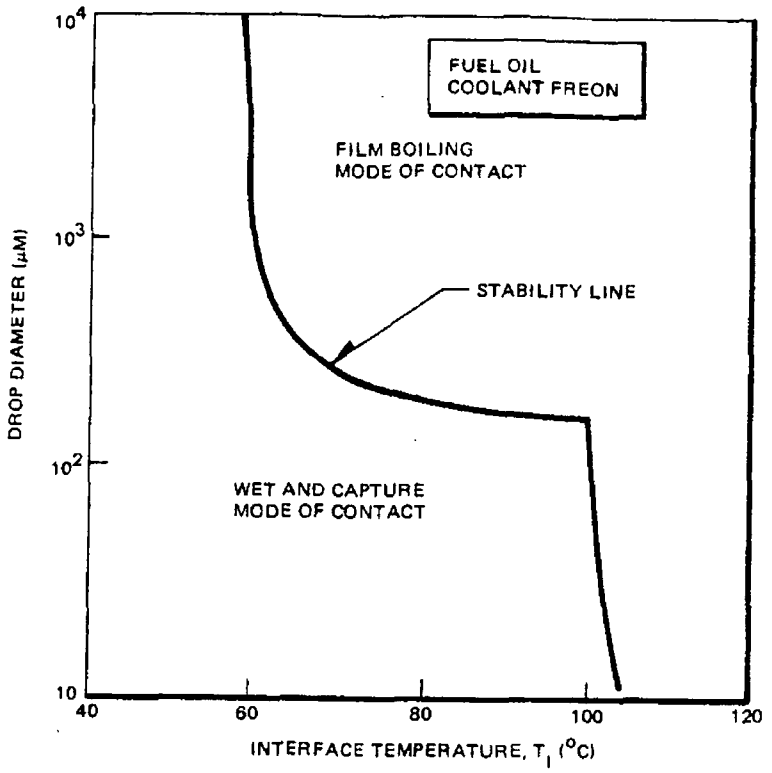


Figure 5-11. Criteria of Wetting of Fuel (Oil) Surface by Coolant[66]

"...the most important aspect is the highly fragmented liquid spray which would be produced as the droplet is ruptured. It is this very fine liquid spray, which is much smaller than the capture size, which can provide the highly fragmented cold liquid material necessary for sustained propagation."

Experimental data for tin dropped into water over a wide range of fuel and coolant temperatures is shown in Figure 5-12.[5.30] The area inside the triangular region represented by circle data points indicate a combination of initial fuel and coolant temperature at which a noticeable FCI occurred.

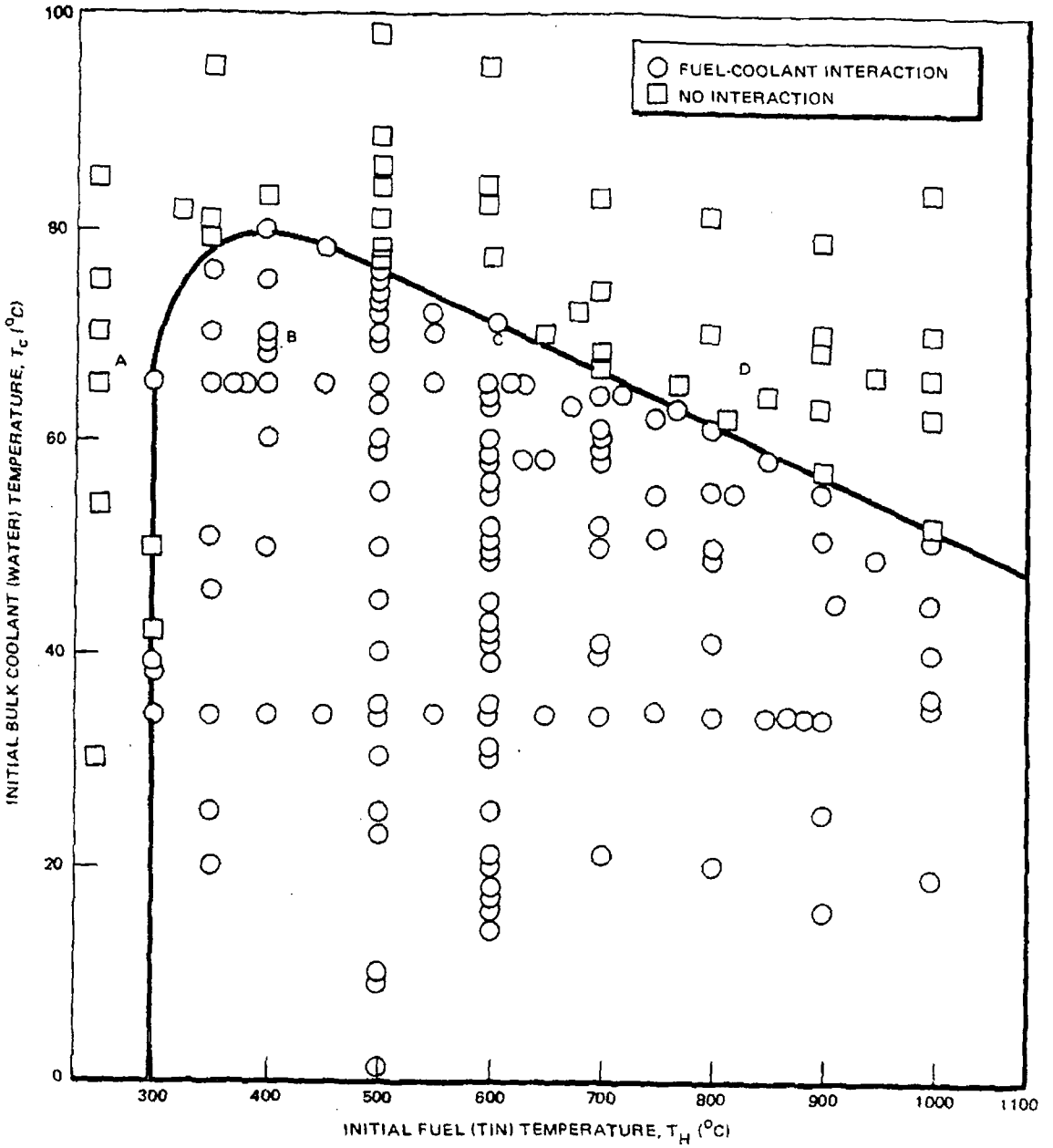


Figure 5-12. Temperature Interaction Zone for 12 gm of Tin

At the boundries of this temperature interaction zone (TIZ) the percentage disintegration fell to zero and no FCI occurred. The melting point of tin ($T_M$) is 271°C. In Figure 5-12, there is no FCI for initial tin temperatures less than 300°C (Region A) due to the tin solidifying upon contact with the coolant water. The bulk temperature of the tin ($T_H$) can be higher than $T_M$ because at liquid-liquid contact the interface temperature decreases immediately, as calculated by equation 5.1. For the tin-water reaction with $\alpha = 0.205$ and $T_I = 271°C$, equation 5.1 determines $T_H$ to be approximately 300°C for coolant temperatures less than 65°C. The homogeneous nucleation temperature of water ($T_{HN}$) is 305°C. For a $T_H \sim 360°C$ as seen in Figure 5-12, the calculated $T_I$ is consistent with the criteria $T_{HN} < T_I$. The critical temperature of water is 375°C. Thus the narrow window in which a FCI can occur with water as the coolant is $305 < T_I < 375$.

In Figure 5-12 Region B corresponds to FCI's that occur spontaneously since the calculated $T_I$ are less than 375°C. The remainder of the interactions shown in Region C correspond to conditions where the molten surface temperature of the fuel cools down below $T_{crit}$ as it is falling through the water bath. Corrandini et al[5.30] saw that as the tin entered the water bath a projection started to grow out of the bulk molten tin. Since the interaction started at this projection, it was postulated that his projection acted as a cooling fin and when $T_I$ became less than 375°C a violent interaction occurred leading to an explosion. Taking tin data in Figure 5-12 at $T_H$ initially equal to 500, 600,700,800,900 and 1000°C, Corrandini et al were able to show that $T_I$ indeed was less than $T_{critical}$ using observed dimensions for both a sphere and fin cooling model.

Thus the criteria of $T_{HN} < T_I < T_{crit}$ is maintained for the tin data. Board et al[5.33] investigated the behavior of an externally trigger interaction at fuel coolant temperatures outside the Temperature Interfaction Zone of Figure 5-12. Using an external pressure pulse at 80°C coolant temperature they were able to obtain a FCI. However, they report the true explosion threshold must be somewhere between 80°C and 95°C since no explosion could be produced even with an external mechanical trigger. (The minimum subcooled temperature of the water in a BWR is 90°C).

At high fuel coolant temperatures near the diagonal of the TIZ (Region D) in Figure 5-12, a thick stable film surrounds the tin when it enters the water, producing film boiling. This produces no interaction and the tin peacefully solidifies and falls to the bottom.[5.30]

As noted there is some difficulty in applying the nucleation model to the tin data due to the molten tin drop deforming when it enters the water. Based on cooling models of the deformed tin, the tin data does appear consistent with the nucleation models criteria. Henry and McUmber[5.29] tested the nucleation model using Freon-Oil experiments in which the cold Freon-22 drop diameter could be controlled and photographed. Using saturated Freon-22 at 0.05 MPa, which corresponds to an initial temperature of -54°C and an initial mineral oil temperature of 205°C, the interface temperature ($T_I$) upon contact evaluated from equation 5.1 is 96°C which is exactly the critical temperature of Freon-22. It should be remembered that from the nucleation considerations, when the interface temperature ($T_I$) upon contact between hot and cold liquids approaches the critical temperature of the cold liquid, film boiling should be generated immediately after contact due to the tremendous nucleation rate. This is exactly what is shown in Figure 5-13 when $T_I$ exceeds the critical temperature of the cold fluid ($T_{crit} \approx 205°C$) and thus vapor explosions are eliminated.

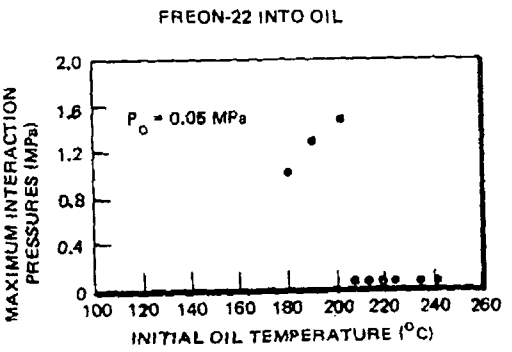


Figure 5-13. Interaction Behavior for Freon-22 and Mineral Oil at High Oil Temperatures

The spontaneous nucleation model to describe a FCI is consistent with interpretation of the tin data,[5.30] Freon-oil data[5.29] and the ANL data of Table 5-1. The interface temperature upon contact between molten $UO_2$ fuel and water, molten stainless steel and water and molten zircaloy and water is much greater than the critical point of the water coolant. With the interaction of $UO_2$ and water, the interface temperature is estimated to be ~1000°C.[5.34] Since $T_I$ is about three times greater than the critical temperature of the water ($T_{crit}$ = 375°C), the explosive potential for this interaction is negligible[5.29] The large scale fuel-water experiments confirm this.[5.34]

5.2.3 Nuclear Excursions

Even though a nuclear excursion is far removed from a flow blockage accident, it is a mechanism which is capable of introducing molten material into the coolant of a BWR. For this reason its potential must be evaluated.

In Section 7 of this report the consequences of a nuclear excursion in a BWR are discussed. However, for the purpose of discussion here all that is necessary are the results of that section. The peak fuel enthalpy experienced by any rod in the reactor for the cold design basis accident is 280 cal/gm. All available SPERT, TREAT, KIWI, and PULSTAR test results show that the prompt fuel rod rupture threshold is about 425 cal/gm. In the range of 200 to 300 cal/gm the fuel rods experience a gradual breakup into large pieces and the fine dispersal of fuel is absent. These tests were usually performed in an enclosed, water-filled capsule at atmospheric pressure, hence the occurrence of a prompt dispersal would result in a pressure spike within the capsule. In Figure 5-14 the pressure pulse generation as a function of the peak enthalpy experienced in the fuel rods is summarized for a large number of tests at the TREAT and SPERT capsule driver core facilities. From this figure it is obvious that the consequences of the design basis excursion analyzed in a BWR are well below the limits of an unacceptable system pressure increase. The peak fuel enthalpy of 280 cal/gm is well below the failure limits that might threaten damage to core internals and structure.

In addition to providing prompt failure thresholds for fuel rods during a nuclear excursion, the TREAT and SPERT tests also indirectly provide information on the interaction between molten $UO_2$ and cladding or combination thereof with water. As

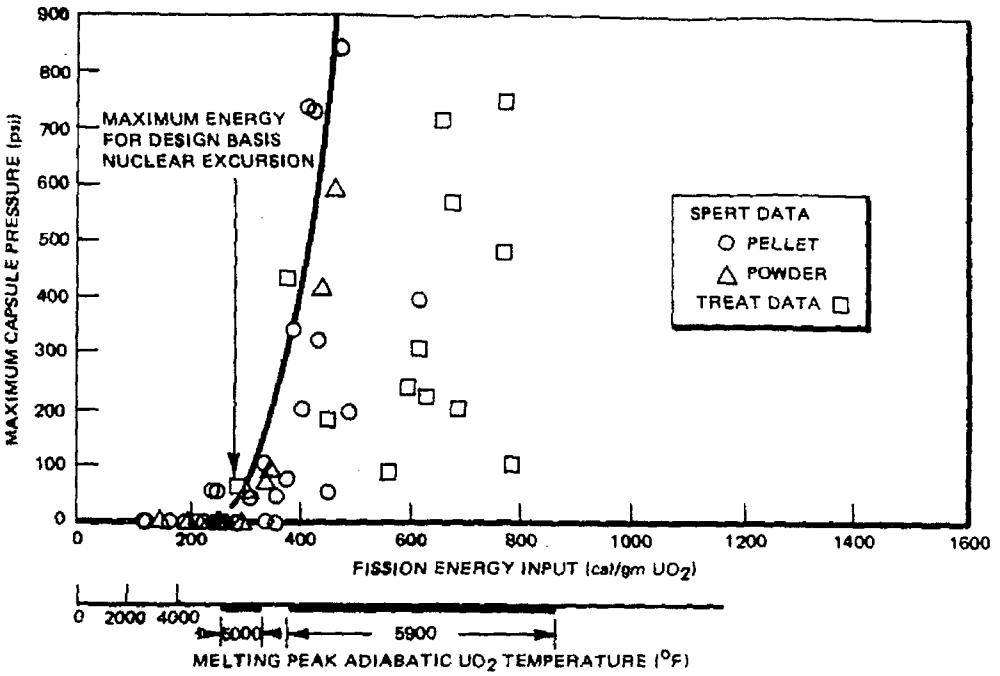


Figure 5-14. ANL and SPERT CDC $UO_2$ Data Summary.

depicted in Figure 5-14 an increase in the fission energy input to the rods increases the temperature of the dispersed fuel and the violence with which failure of the rod occurs also increases resulting in more finely dispersed particles. Even for enthalpies between 300 and 400 cal/gm where the fuel is well within the molten range, very modest pressure increases result as the molten material is dispersed into the water. This is because the violence of the dispersal is not high enough to force division of the molten material into fine enough particles that would be capable of transferring their heat rapidly.

Figure 5-15, a summary of the ANL TREAT tests and SPERT data shows how fine the dispersed molten $UO_2$ must be to generate any significant pressure pulse. Also included in the figure for comparison in the histogram of the Zircaloy-2 droplet test described previously. This comparison clearly indicates that the expected main droplet size is at least 10 times greater than the experimental size for which significant pressure rises are expected to occur. It should also be borne in mind that the particles were rapidly injected (millisecond time scale) into a solid mixture whereas in a case of an overheated fuel rod, melting will take place on a much longer scale (seconds) in a two-phase environment which has been shown to be very ineffective for producing large pressures.

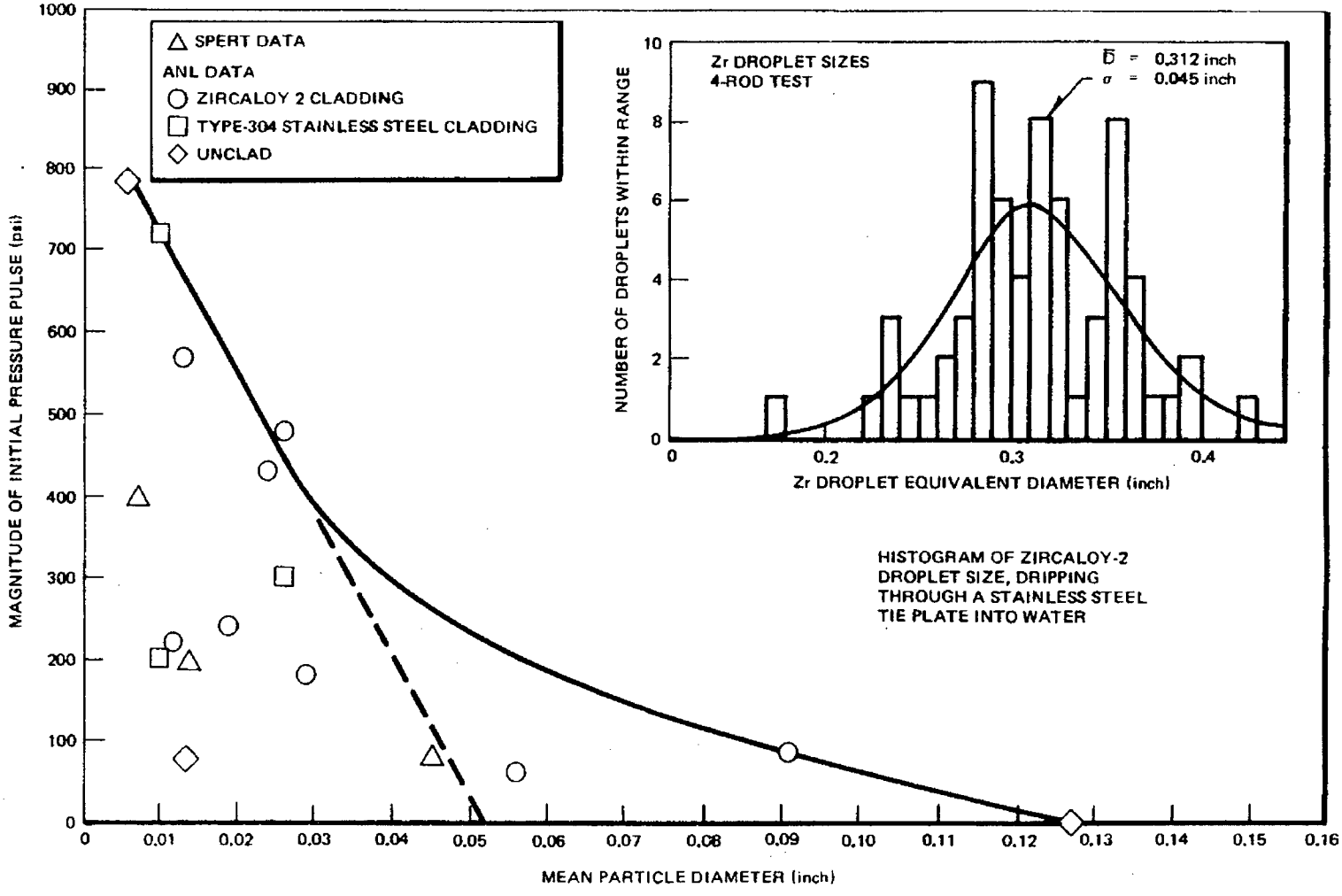


Figure 5-15. ANL Treat and SPERT Tests - $UO_2$ Data Summary

An interesting similarity between these tests and the shock tube tests performed at TRW with molten aluminum can also be made. In the shock tube experiment it was found that the efficiency with which the sensible heat of the molten aluminum was converted into steam energy and mechanical energy increased linearly with increased temperature above the aluminum melting point (Figure 5-4). This means that the temperature of the dispersed metal must be greater than the melting point to produce any significant pressure rise. The same phenomena is evident in Figure 5-14 where the maximum capsule pressure is also seen to be approximately linearly dependent upon the temperature above the melting point of $UO_2$.

Similar conclusions were also drawn by Grund[5.35] from reactivity transients imposed upon 4% enriched $UO_2$ powder fuel rods with Type 304 stainless steel cladding. The rods were subjected to reactivity transients in the SPERT 1 core which resulted in maximum $UO_2$ temperatures of approximately 1800°C. High-speed movies indicated dispersal of $UO_2$ into the water and the ruptured fuel rods exhibited failure characteristics typical of internal pressure buildup. A modest pressure rise of 65 psi resulted and inspection of the fuel rods adjacent to the ruptured specimens failed to show any damage. Dispersal of hot $UO_2$ into the water did not result in any destructive pressure pulse, and as is stated by Grund.

> "...less than 1% of the heat energy in the fuel of the ruptured fuel rods was converted into mechanical energy in the form of pressure generation, and (4) the failure of a fuel rod and consequent dispersal of powdered fuel into the water during a severe power excursion will not necessarily result in pressures sufficiently large to initiate failure of additional fuel rods or seriously damage other reactor components."[5.35]

Similar results were obtained with other tests when the fuel was near melting temperature. Since the fuel in these experiments was already in a powered state and hence finely divided into small particles, the results obtained from dispersing this type of fuel could be expected to be orders of magnitude worse than would be obtained with the pellet-type fuel normally used in BWR's. Hence, with regard to nuclear excursions as a mechanism for dispersal of molten material in a BWR, two conclusions can be drawn:

1. Nuclear excursions in a BWR will not result in the generation of a damaging local pressure pulse since the peak fuel enthalpy is far below the failure threshold.

2. The introduction of molten $UO_2$ and cladding into a solid liquid will not result in a pressure pulse unless it is finely divided and its temperature is well above the melting range.

### 5.2.4 Perforations

The perforation of a fuel rod is caused when the internal gas pressure induces a stress in the cladding greater than the ultimate yield strength. Fuel rod internal pressure can be due to the helium which is backfilled at one atmosphere pressure during rod fabrication, the volatile content of the $UO_2$, and the fraction of gaseous fission products which are released from the $UO_2$. A quantity of $1.35 \times 10^{-3}$ gam-moles of fission gas are produced per MWd of power production. As was shown in Section 4 the temperature of the cladding will reach the melting point before the outer surface of the fuel becomes molten and since the yield strength of Zircaloy-2 cladding decreases very rapidly with temperature, when perforations occur, both the cladding and the fuel will be below the melting point and perforation would only result in rupture of the cladding and release of fission products, not in dispersal of molten rod material. Even if it were possible to disperse $UO_2$ by this perforation mechanism the consequences would be insignificant as was shown by Grund, as well as in the TREAT and SPERT tests described in the above section. The pressure rise would be far less than the 65 psi seen in Grund's tests or the TREAT and SPERT tests for a flow blockage accident since the presence of a large amount of voids in the channel reduces the peak pressure considerably as discussed in Section 5.1. Therefore, fuel rod perforations can be eliminated as a potential for dispersing fuel and generating any significant pressure rise.

### 5.2.5 Experimental Results on Contact between Molten $UO_2$/Zr-2 and $H_2O$

Nuclear excursions and perforations in a BWR have been shown not capable of dispersing fuel that would result in the generation of large pressure pulses. It also has been established that the mere melting of the fuel rods for high degrees of blockage will not produce the finely divided particles necessary for high pressure production. When applying the Spontaneous Nucleation Model based on tin,

Freon-oil and ANL data for molten $UO_2$/Zircaloy and water interactions, the theory predicts the explosive potential is negligible. However, it remains to be verified experimentally that large quantities of molten $UO_2$ and Zircaloy-2 will show no natural tendencies to fragment into fine particles and initiate a vapor explosion upon being quenched in water. This section addresses such experimental verification.

Perhaps one of the most realistic tests performed that most closely simulates the slow fuel melting and slumping that would be experienced by a BWR fuel bundle for a high degrees of blockage are the "flat top" transients performed at the TREAT facilities.[5.36] The experimental technique consisted of loading an autoclave (which is essentially an instrumented, stainless steel pressure vessel) with a fuel rod cluster and water and exposing the entire assembly to a neutron flux in the TREAT reactor. The fuel rod cluster consisted of three fuel rods which were located above a pool of water at atmospheric pressure. Each rod contained 10 sintered $UO_2$ pellets clad with Zircaloy 2 with a diameter of 0.42 inch by 5-5/8 inches long. The fission heat generated in the 10%-enriched $UO_2$ during a flat top transient caused meltdown of the fuel rods which then collapsed into the pool of water below. In a "flat top" transient the fission heating remains reasonably constant for a major part of the transient. In these three experiments, the duration of this constant heating period was 12, 32, and 50 seconds. The water below the rod cluster was heated from the ambient 30°C to a value of 100°C just before the transient was initiated. Thus a 1-atmosphere steam environment was provided for the fuel rods located immediately above the water level.

The conditions under which these tests were conducted were very similar to, if not exactly the same as, those which would be experienced for high degrees of flow starvation in a BWR fuel bundle. The constant heating periods over which the fuel rods undergo melting are very comparable to those predicted in Section 4. The steam environment and the saturated pool of water are the type of fluid conditions present in a BWR. Hence, for all practical purposes the melting of the fuel rod cluster could be considered as being caused by a flow blockage incident. There are no technical reasons why the results of these tests would be different from a flow blockage incident in a BWR with area blockages greater than 95%.

The results of these tests are shown in Figure 5-16. Conditions of the fuel are given in Table 5-2. It is noteworthy that in no test was there recorded a pressure spike when the molten $UO_2$ and Zircaloy 2 entered the water. It is also interesting to note that the particle size is in close agreement with the results obtained from the GE molten droplet tests (Section 5.2.1.3). In each of the three tests, all of the molten material was found to have entered the water. The slow pressure rise seen in the curves is simply due to the slow heating of the steam and water in the enclosed autoclave. The behavior of the molten $UO_2$ and Zircaloy-2 entering the water is thus no different from the quenching action that normally occurs when a bar of molten steel is quenched in water. An important conclusion was reached in this experiment which is as follows:

> "A very significant observation, based upon the particle-size distribution of the residues, is the absence of large quantities of very fine particles. This is a particularly encouraging result, since it suggests that molten $UO_2$ (and $UO_2$ - Zr $ZrO_2$ mixtures) do not exhibit a marked tendency for spontaneous subdivision on being quenched in water. It is also noteworthy that the pressure time traces show no "spike" pressure rises, which suggests that no steam explosions or very violent boiling occurred as the molten fuel material entered the water pool, at least for the small scale experiments performed in this study."[5.37]

This natural tendency for molten $UO_2$ not to fragment upon being quenched in water is also supported by tests performed by Aerojet-General Corporation.[5.38] In these tests molten uranium was dropped into water and reaction rates as well as pressure time histories were measured. Molten samples up to 227 grams were dropped into the water without any significant pressure rises resulting. The resulting average particle sizes for these tests were greater than 0.4 inch in diameter. It was concluded from these tests that the reaction of molten $UO_2$ with water is neither violent nor self sustaining at the experimental temperatures. These results agree with Gibby's[5.39] in which molten $UO_2$ was dropped into water with the bath temperature varied from 30 to 250°C. No explosion was recorded for this water temperature variation.

Large scale $UO_2$-water experimental were carried out by Amblard et al[5.34] in the CORRECT II set up and consisted of dropping approximately 1 kg of molten $UO_2$ into a bath of cold water at ambient temperature and pressure. No large pressure spikes were generated but fragmentation of the fuel did take place. However, the smallest fragment was 0.080 inch which agrees with particle sizes seen in the TREAT and GE tests.

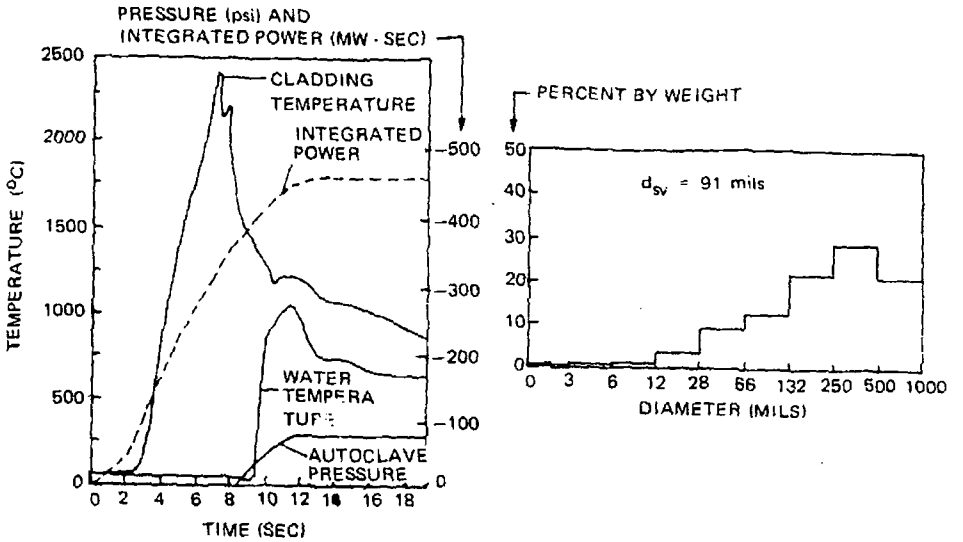


a. EXPERIMENT CEN-217S 12-SEC FLAT TOP TRANSIENT

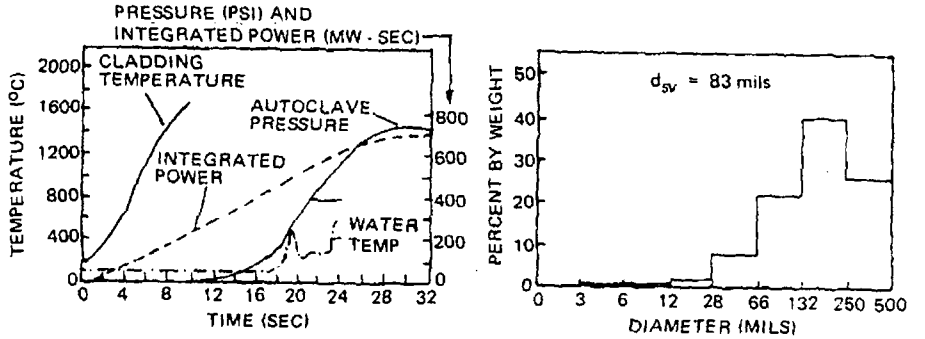


b. EXPERIMENT CEN-217S 32-SEC FLAT TOP TRANSIENT

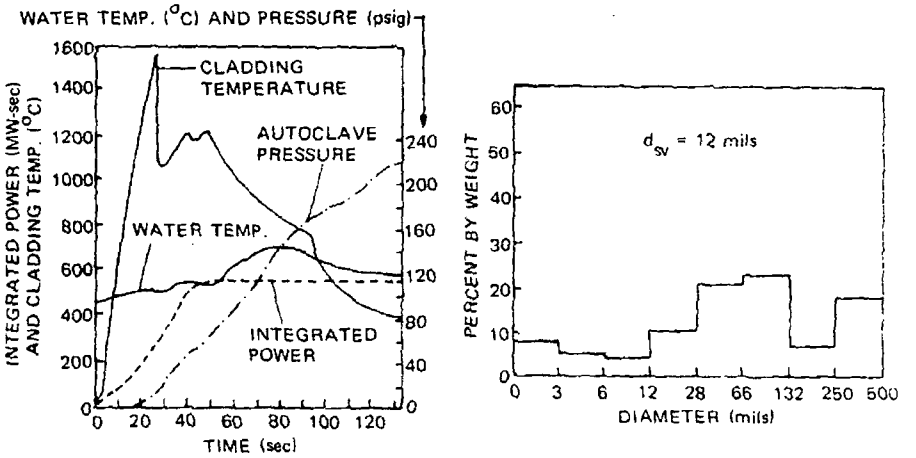


C. EXPERIMENT CEN-223S 50 SEC FLAT TOP EXPERIMENT

Figure 5-16. Results of Treat Flat Top Experiments

Table 5-2

CONDITIONS OF FUEL AT THE TIME OF RECORDING THE MAXIMUM CLADDING TEMPERATURE IN TREAT FLAT TOP EXPERIMENTS (REPRODUCED FROM ANL 7325)

| Experiment Number | Average (Constant) Heat Generation Rate (kW/ft) | Peak Recorded Cladding Temperature ($^{o}C$) | Energy Deposit in Fuel (cal/gm $UO_2$) | Adiabatic Fuel Temp ($^{o}C$) and Physical State of Fuel |
|---|---|---|---|---|
| CEN-217S | 40 | 2430 | 360 | 3300 (fuel fully melted) |
| CEN-220S | 20 | 1670 | 240 | 2800 (fuel partly melted) |
| CEN-223S | 11 | 1570 | 285 | 2850 (Fuel Fully melted) |

The TREAT flat top transients along with the Aerojet test and experimental tests of Gibby and Amblard et al provide overwhelming evidence that the presence of molten $UO_2$, Zircaloy-2 or combinations thereof during conditions of high flow starvation in a BWR fuel bundle will not result in a destructive pressure pulse that would propagate the accident throughout the core. Contact between molten fuel rods and water will not result in fine dispersal of the molten material nor will it generate any significant pressure rise.

## 5.3 REVIEW OF ACTUAL FLOW BLOCKAGE ACCIDENTS IN THE NUCLEAR INDUSTRY

As stated in section 3 of this report, some flow blockage accidents have indeed occurred in operating reactors. The occurrence of these incidents clearly indicates that flow blockages by foreign objects are within the realm of possibility. This subsection reviews actual flow blockage accidents and the resulting consequences. To relate the consequences of these accidents to a BWR, only those accidents which have occurred in water-moderated, water-cooled reactors will be reviewed in detail. In particular, flow blockage accidents at the Materials Test Reactor (MTR) and Engineering Test Reactor (ETR) near Idaho Falls will be reviewed.

### 5.3.1 Flow Blockage in the MTR

On November 13, 1962, a piece of dislodged gasket material from the MTR primary coolant system caused a significant flow restriction in at least two flow channels of a standard MTR fuel element.[1.3] A visual examination of this material in the fuel assembly indicated that it was black rubber with an asbestos or fiber glass binder. The gasket material caused a flow reduction of approximately 30%. The accident was immediately detected by in-core instrumentation and an increase in radiation levels around the reactor proper and in the process water building. The damage was found to consist of one fuel plate which had partially melted, resulting in the loss of approximately 10.5 grams of metal containing an estimated 0.7 gram of fissionable material. The fact that melting was caused by a flow reduction of only 30%, which is different from that predicted for a BWR, is attributed to the fact that the thermal hydraulic conditions in MTR are very much different from a BWR.

The consequences of this incident were minimal. Contamination of the primary coolant system was not severe, nor were any personnel overexposures received. There was no evidence to indicate that the introduction of molten material to the coolant generated any sort of pressure pulse. Thus, the only item of any consequence associated with this flow blockage accident was that the reactor had to be shut down and inspection initiated, in addition to cleaning up the system.

### 5.3.2 Flow Blockage in the ETR

On December 12, 1961, the Engineering Test Reactor experienced fission breaks in six fuel elements as a result of a flow blockage in one quadrant of the core. Eighteen separate fuel plates, distributed among six fuel elements, were found to have melted in varying degrees. Approximately 12.4 grams of U-235 contained in 134 grams of alloy were lost. Examination of the core after shutdown revealed the cause of these fission breaks to be the presence of considerable amounts of foreign materials blocking off coolant to several fuel elements. The material was identified as Lucite from a sight box which had escaped detection during prestartup inspections and checks.[1.4]

Hydraulic and thermal analysis after the accident revealed that the normal flow through the damaged fuel assemblies was reduced by 65%. Again the difference between this value and that predicted for a BWR is due to the differences in the thermal-hydraulic conditions. Reactor instrumentation also indicated that some of the coolant channels in the six melted fuel elements were "chugging". There was a cyclic filling of the channels with steam expelling the water and a subsequent refilling of the channels with water. Hot-cell inspection also revealed that the molten fuel alloy flowed down the coolant channel and solidified in a cooler section. Another important aspect which concerns the possible propagation of a flow blockage accident through the generation of a pressure pulse was revealed when inspection of the fuel plates in the damaged elements revealed that there was no deformation that would have indicated an explosive metal-water reaction took place when the fuel plates melted.

As in the MTR flow blockage accident, the consequences of the ETR flow blockages were also inconsequential. No overexposures of serious health physics problems were encountered during or subsequent to the fission breaks. There was also no indication that an explosive metal-water reaction was present that could have possibly propagated the accident. These results are consistent with the TREAT flat top transients,[5.36] Aerojet tests,[5.38] large scale $UO_2$/Zircaloy experiments, and SPERT tests - all of which indicate that there is no serious explosive metal/water reaction with molten UO2 that has not been finely dispersed. Another significant item of note was that the coolant chugging phenomenon that occurred did not generate any pressure pulse. In fact this chugging provided additional cooling to the top half of the fuel assembly by providing intermittent nucleate boiling conditions to locations where film boiling normally would have occurred.

## 5.4 CONSEQUENCES OF INTRODUCING MOLTEN MATERIALS INTO A BWR AS A RESULT OF A FLOW BLOCKAGE INCIDENT

In the above sections a wide and varied wealth of experimental information was presented demonstrating that partial fuel rod melting in a BWR will not lead to unacceptable conditions. This fact will be further substantiated in this section by analytically demonstrating that destructive pressure pulses are not possible for conditions of high flow starvation during which molten (or near molten) material could possibly be introduced into the fuel channel.

For transient pressures to be produced in fluid systems, a volume expansion must first occur. The magnitude of the pressure increase produced by this volume expansion is strongly dependent on the resistance offered by the fluid and the system against which this volume is expanding. The nature of this resistance can be different depending on whether the system behaves inertially or acoustically; in other words, whether the volume expansion is fast or slow in comparison with the acoustic length of the system divided by the velocity of sound.

In an inertial system the rise time to peak pressure is significantly longer than the time for a pressure disturbance (wave) to be transmitted to and return from the system's free surface, the wave being transmitted throughout

the fluid at sonic velocity. In the case of an acoustic system, the rise time of the pressure pulse is much less than the time for the pressure wave to be transmitted to and return from the system boundary. Considering the case where the heating period, $\tau$, is much longer than the acoustic period of the system, 2 h/c, such as in an inertial system, $\tau >> 2$ h/c, where h is the distance to the nearest free surface and c is the sonic velocity in the coolant, the pressure change, $\Delta P$, can be determined by the inertial acceleration of the coolant's resistance, $\rho h$, or

$$\Delta P = \frac{\rho h \, d^2x}{g_c \, dt^2}, \qquad (5.2)$$

where x is a measure of the interface between the expanding region and the coolant load. This is diagramatically described below.

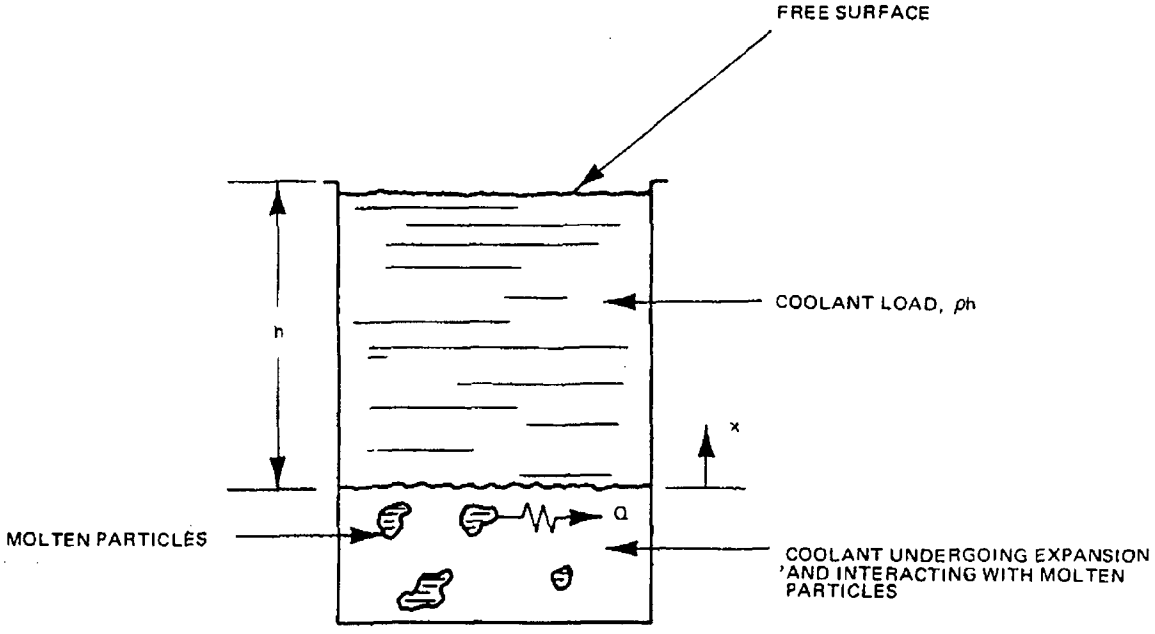


In the case of the system behaving acoustically, the heating period is much less than the acoustic period, $\tau << 2h/c$, and the pressure change can be expressed as,[5.40]

$$\Delta P = \frac{\rho C}{g_c} \frac{dx}{dt} \qquad (5.3)$$

In the inertial type of system any pressure disturbance is effectively transmitted throughout the fluid instantaneously; therefore, all the system boundaries interact with the pressure-generating source and can alter it. In the case where a free surface exists, the pressure is relieved almost as fast as it is generated. This was seen in experiments in which hot particles were injected into a coolant through a free surface. These experiments demonstrated that appreciable pressures could not be generated because of the pressure relief afforded by that free surface. However, in the acoustic system the pressure at the source essentially rises instantaneously and then is slowly transmitted through the fluid at sonic velocity. During the initial stages there is no dynamic communication between the boundaries of the system and the source so that the pressure rise is virtually unaffected. Acoustic pressure pulses are usually very large; the pressure pulses seen at SPERT-1, BORAX-1, SL-1, and the shock tube experiments at TRW were typical of acoustic pressure pulses. It is therefore appropriate that prior to determining the magnitude of a pressure rise that might occur during a flow blockage incident the first step is to determine whether the fuel channel will behave acoustically or inertially. Another important factor to be considered in determining the magnitude of these pulses is that the quantitative results will be strongly dependent upon the assumption used for an effective heat transfer rate. Unfortunately experimental data are not available for estimating this quantity; however, by approaching the problem parametrically, an order of magnitude of the expected pressure rise can be obtained.

In transferring heat from hot particles to a liquid that is a relatively good conductor, such as water, two types of resistance to the heat flow can occur: (1) the conduction of heat from the surface of the particle across the surface film to the body of liquid, and (2) the conduction of heat from the interior of the particle to its surface. In the case of small particles, the first type of resistance controls the heat transfer rate from the surface, whereas for large particles the second type controls.

For the case where the heat transfer is controlled by conduction from within the particle, consider a sphere of radius $R_0$ at a uniform temperature $T_0$, suddenly cooled to a constant temperature of $T_s$ as by a liquid at temperature

$T_s$. The expression for the fraction of heat initially in the sphere above the liquid temperature $T_s$ that is transferred to the liquid as a function of time is given by,[5.41]

$$\frac{Q}{Q_0} = 1 - \frac{6}{\pi^2} \sum_{n=1}^{\infty} \left(\frac{1}{n^2}\right) \exp\left[-\left(\frac{n\pi}{R_0}\right)^2 \frac{k}{C_p \rho} t\right] \tag{5.4}$$

where

$Q/Q_0$ = fraction of heat transferred,
$R_0$ = radius,
$t$ = time,
$k$ = thermal conductivity of sphere,
$C_p$ = specific heat capacity of sphere,
$\rho$ = sphere density.

The assumptions associated with this expression are that the thermal conductivity of the sphere is small compared with the surface heat transfer coefficient, and the sphere density, specific heat, and thermal conductivity are constant.

For the case in which the heat transfer is controlled by the surface film on the particle, the expression for the fraction of the heat initially in the sphere above the liquid temperature $T_s$ that is transferred to the coolant as a function of time is given by

$$\frac{Q}{Q_0} = 1 - \exp\left(-\frac{3}{R_0} \frac{h}{C_p \rho} t\right) \tag{5.5}$$

The assumption here is that the thermal properties of the sphere are constant and that the thermal conductivity of the particle is large compared to the film heat transfer coefficient.

The effect of particle size and heat transfer coefficients on the heat rate to the coolant can be assessed by comparing the time to transfer heat from $UO_2$ particles of different diameters. This is shown in Figures 5-17, 5-18, and 5-19, where equations (5.4) and (5.5) were used to determine the time to transfer 10, 50, and 90% of the available heat from particles of various diameters. Both the conditions for which the heat transfer is controlled either by the $UO_2$ thermal diffusivity or the surface film are shown. The following thermal properties were used for these plots:

$$\rho = 600\ lb_m/ft^3$$
$$C_p = 1.18\ Btu/lb_m \cdot {}^\circ F$$
$$k = 1.45\ Btu/h \cdot ft \cdot {}^\circ F$$

To determine whether the fuel channel will behave acoustically or inertially, the acoustic period of the channel relative to the time required for the particles to transfer their heat must be compared. In Figures 5-17, 5-18, and 5-19 the range of possible acoustic periods is shown for various fluid conditions in the channel. This range defines the maximum amount of time in which the effective heat transfer from particles of $UO_2$ to the coolant would need to take place to generate a high acoustic pressure pulse. Hence to generate an acoustic pressure pulse the effective heat transfer to the coolant that results in pressurization would have to take place in less time than that defined by the cross hatched area in the figures. This range was conservatively calculated by assuming that the pressure relief surface was at the top of the channel and the generating source was located at the bottom. The acoustic time can be calculated by

$$\tau = 2h/c \qquad (5.6)$$

where

$h$ = distance from pressure generating source to free surface,

$c$ = sonic velocity of the mixture

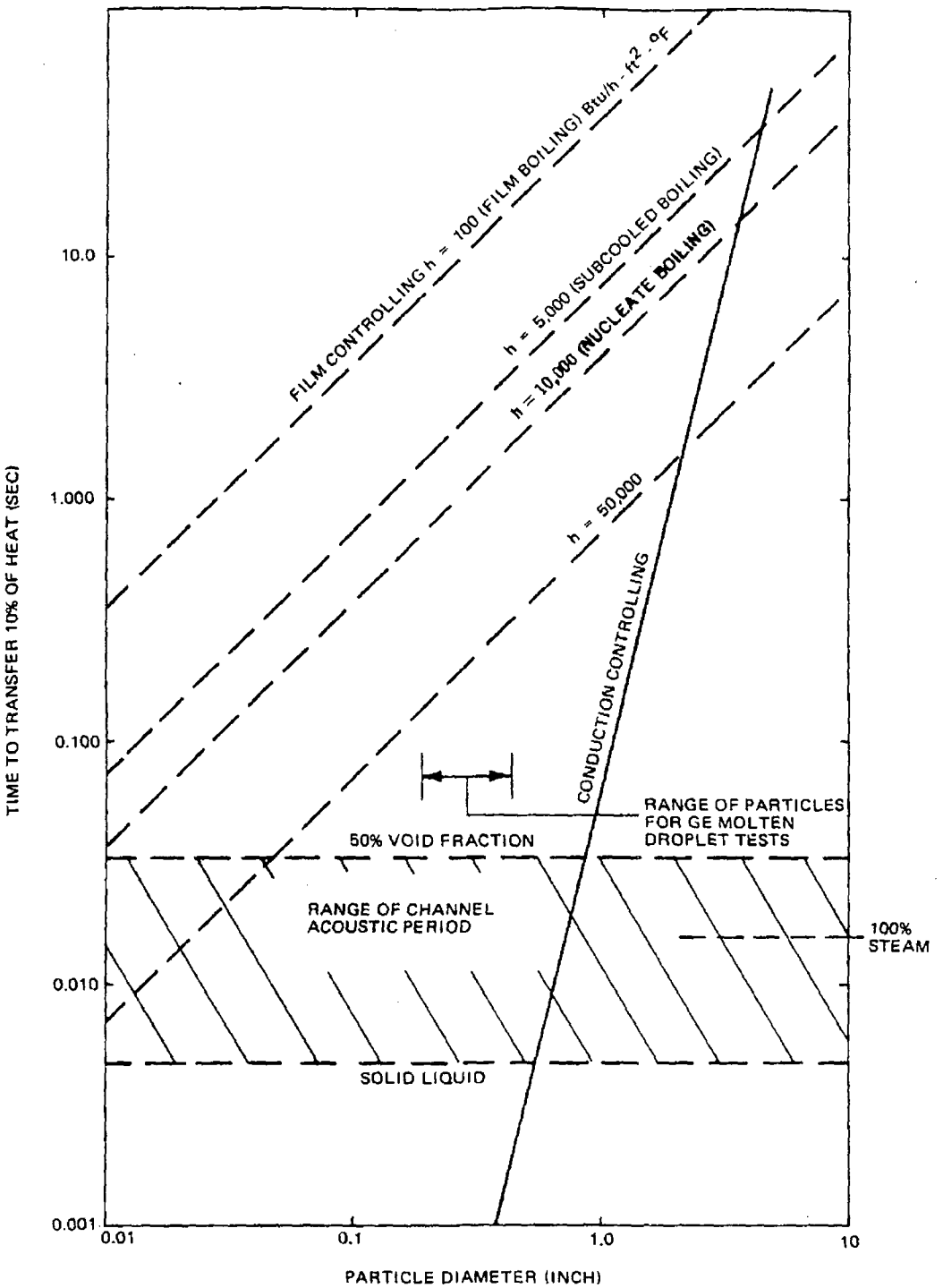


Figure 5-17. Time to Transfer 10% of Available Energy from Particles of Various Diameters

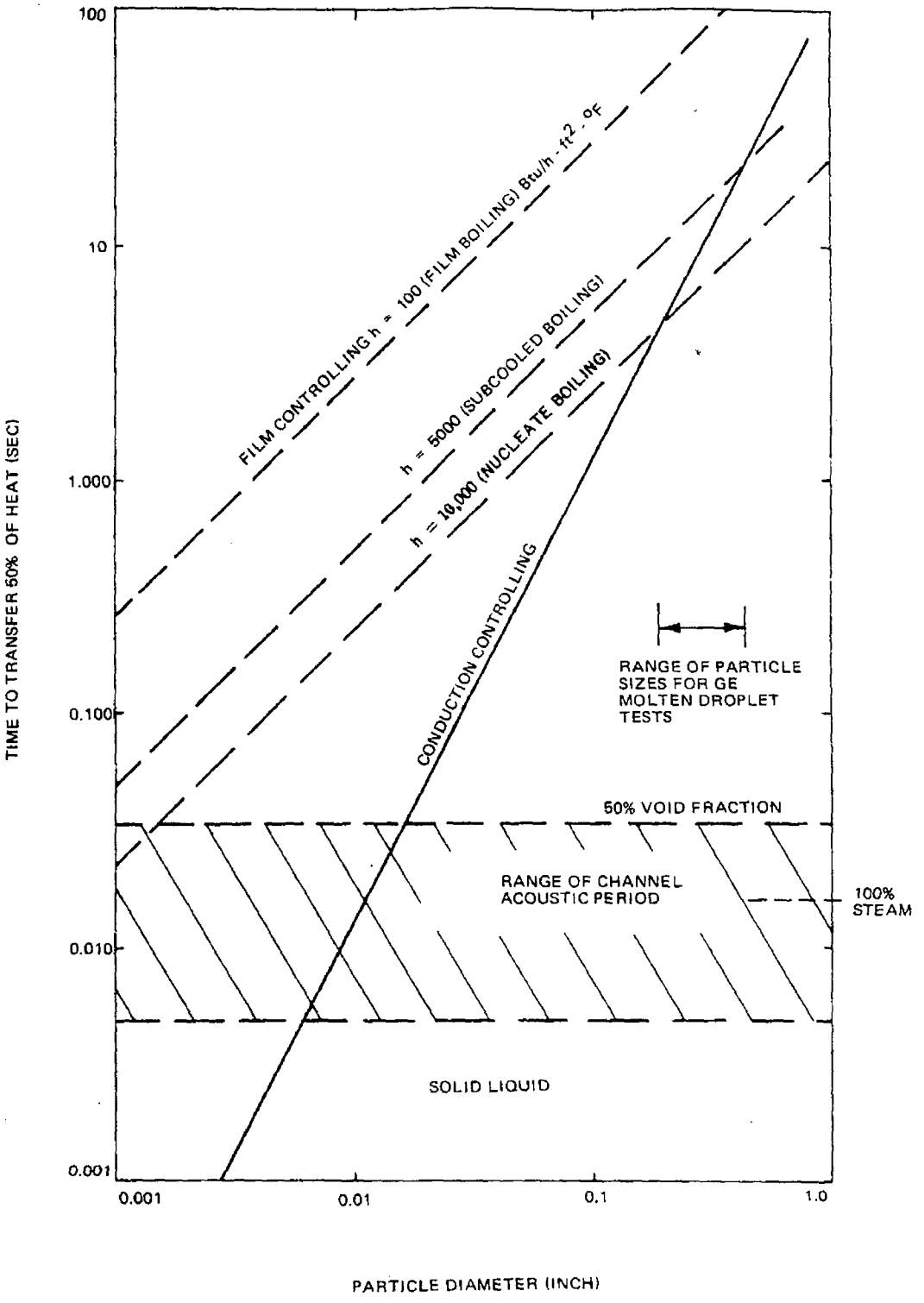


Figure 5-18. Time to Transfer 50% of Available Energy from Particles of Various Diameters

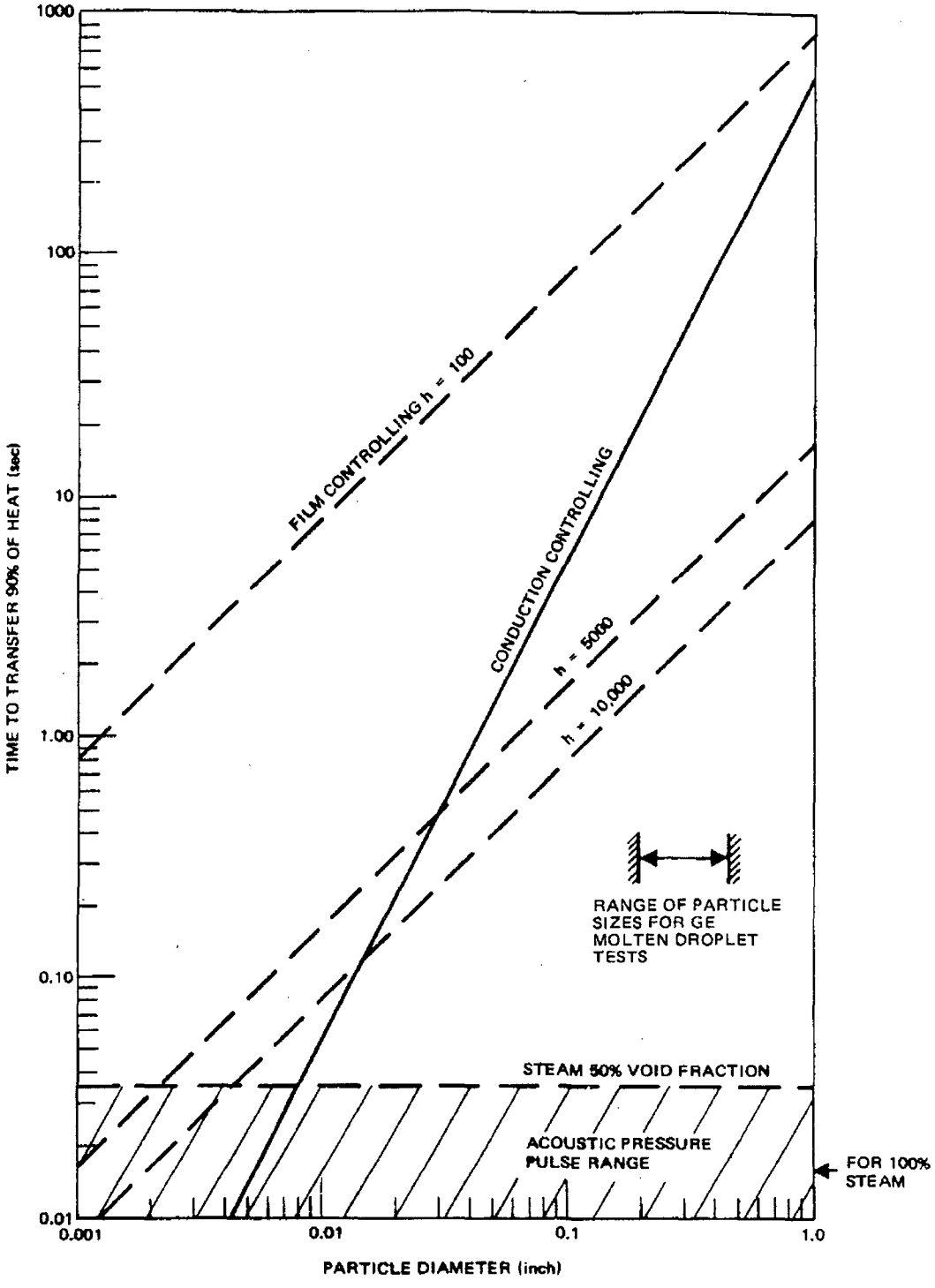


Figure 5-19. Time to Transfer 90% of Available Energy from Particles of Various Diameters

Assuming the channel to be completely filled with liquid gives the shortest times as,

$$\tau = \frac{2 \times 12.5 \text{ ft}}{5000 \text{ ft/sec}}$$

$$= 5.0 \text{ msec.} \qquad (5.7)$$

The longest time is given by assuming the channel is filled with steam at 50% void fraction. This gives the lowest sonic velocity at 1000 psia,[5.42]

$$\tau = \frac{2 \times 12.5 \text{ ft}}{700 \text{ ft/sec}}$$

$$= 35.6 \text{ msec.} \qquad (5.8)$$

For steam the acoustic period will fall between these values with a period of approximately 16 msec.

The actual acoustic time can actually fall anywhere within this range depending upon what the coolant conditions are in the channel. For conditions under which melting will occur, the flow in the channel must be reduced below 10% of rated and at these conditions the major part of the channel will be filled with pure steam. The acoustic period is then expected to be approximately 16 msec. Another factor which must be considered is the efficiency necessary to produce large pressures with molten materials. In the TRW shock tube experiments this efficiency varied from 0.05%, which did not cause a pressure rise, to 40% which generated a 2900 psi pulse. Figures 5-17, 5-18, and 5-19 encompass this range of efficiencies. Included in these figures is also shown the range of expected particle sizes obtained from the GE molten droplet tests. It is apparent that for the expected range of particle sizes the heat transfer is much too slow to generate acoustic pressure pulses. For low efficiencies the heat transfer is limited by the film heat transfer coefficient whereas for high efficiencies the heat transfer rate is limited by the conduction through the particles. Even assuming low efficiencies for pressure generation and an excellent nucleate boiling coefficient of 50,000 Btu/hr-ft$^2$-°F, which is not to be expected in a high steam environment, the particle sizes

would have to be less than 20-30 mils to fall within the acoustic pressure pulse generating range. In the TREAT tests, particles of this size resulted on only after fuel rods were subjected to energy inputs greater than 400 cal/gm. It therefore seems highly improbable that particles of this size could be a result of the slow "candle dripping" type of melting that a rod would experience for conditions of high flow starvation and no scram.

Since the heat transfer rate ot the coolant is too slow for the generation of an acoustic pressure pulse, a conservative estimate of the inertial pressure rise can be made by considering the system shown on the following page.

From Newton's second law the following equation can be written for the fluid undergoing acceleration,

$$- F_c - F_f - \frac{Mg}{g_c} + PA = \frac{M\, d^2x}{g_c\, dt^2} \tag{5.9}$$

where

$M$ = mass of coolant being accelerated,
$x$ = displacement of coolant,
$t$ = time,
$P$ = driving pressure created by expanding volume,
$A$ = cross sectional area of coolant,
$F_c$ = opposing force offered by the compressibility of gas,
$F_f$ = opposing frictional or viscous force acting on coolant.

$$g_c = 32.17 \frac{\text{lbm - ft}}{\text{lbf - Sec}^2} = 1.0 \frac{\text{Kg - m}}{\text{N - sec}^2}$$

By neglecting gravitational, frictional, and compressibility effects, Equation (5.9) can be simplified to,

$$PA = \frac{M\, d^2x}{g_c\, dt^2} \tag{5.10}$$

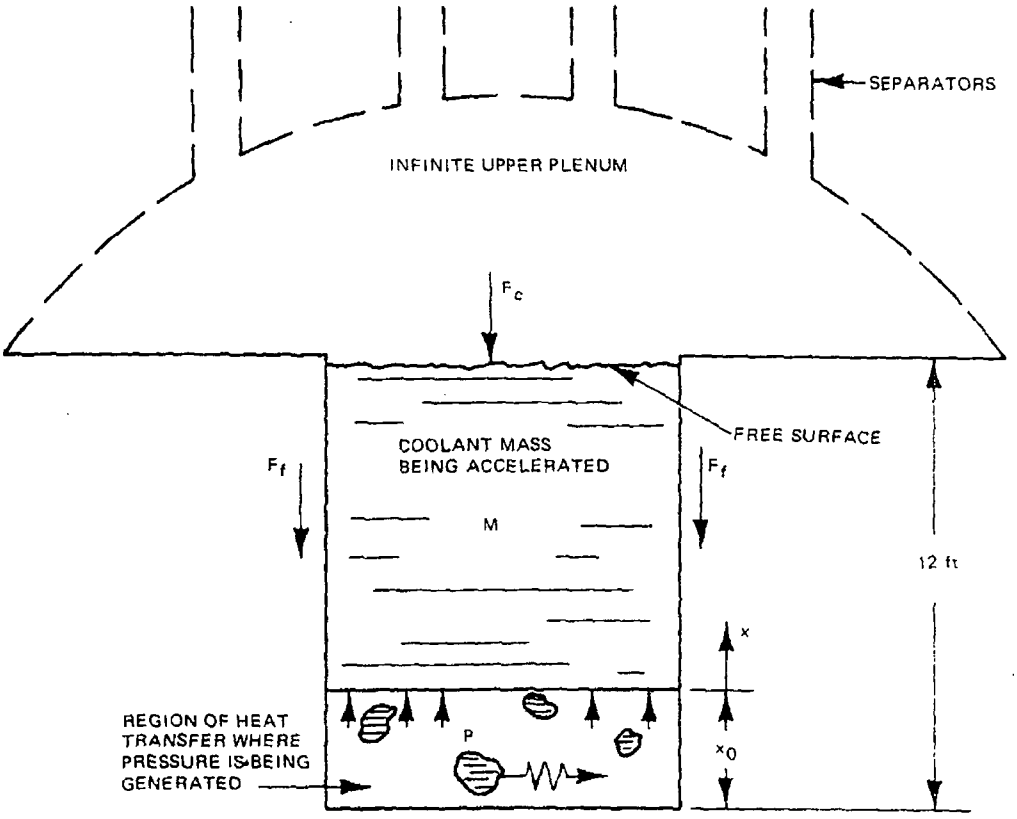


Assuming the driving steam to be a perfect gas,

$$PV = mRT \tag{5.11}$$

where

m = mass of evaporated steam,
T = steam temperature,
R = gas constant,
V = volume of expanding steam.

This assumption is highly conservative since it results in a higher pressure at a given temperature and specific volume than predicted by steam tables.

Assuming that the steam generation rate is constant,

$$m = ct \tag{5.12}$$

where c is the rate of steam generation, Equation (5.9) can be written

$$\left[\frac{RTcg_c}{M}\right]\frac{t}{x} = \frac{d^2x}{dt^2} \tag{5.13}$$

Integrating and satisfying the initial conditions of x = 0 and dx/dt = 0 at t = 0 gives the following solution for x,

$$x = \left[\frac{4RTcg_c}{3\ M}\right]^{1/2} t^{3/2} \tag{5.14}$$

The pressure in the active region where heat transfer is occurring can now be described by

$$P = \frac{mRT}{V} \tag{5.15}$$

where V is described as the initial volume plus the volume increase produced by the moving coolant load boundary, x, or

$$V = A(x_o + x) \tag{5.16}$$

Substituting Equations (5.12), (5.14), and (5.16) into (5.15) gives the pressure rise as a function of time or

$$P_{rise} = \frac{\alpha t}{x_o + \beta t^{3/2}} \tag{5.17}$$

where

$$\alpha = \frac{cRT}{A}$$

$$\beta = \left[\frac{4}{3}\frac{RTcg_c}{M}\right]^{1/2}$$

By maximizing Equation (5.16) we find that the peak pressure occurs at

$$t_{max} = \left(\frac{2x_0}{\beta}\right)^{2/3} \tag{5.18}$$

This peak pressure is

$$P_{max} = \frac{\alpha}{3}\left[\frac{2}{x_o^{1/2}\beta}\right]^{2/3} \tag{5.19}$$

Equation (5.19) applies as long as the peak pressure occurs before the bottom of the accelerated coolant has reached the top of the fuel channel, at which time pressure relief will be achieved because of the large volume offerred by the large upper plenum. From Equation (5.14) the time for the coolant to reach the top of the channel is,

$$t_{limit} = \left(\frac{12 - X_0}{\beta}\right)^{2/3} \tag{5.20}$$

Therefore, for Equation (5.19) to apply, $t_{max}$ must be $\leq t_{limit}$ or $x_0$ must be $\leq 4$.

In determining the rate at which energy is released from the molten fuel one of two techniques can be used. The first is that all the molten fuel, regardless of the amount, is in the form of spherical droplets of various diameters. The second is that particle diameter is allowed to vary as the amount of molten fuel increases by assuming that the number of individual particles remains approximately constant. The first of these assumptions is a reasonable assumption for small amounts of fuel melting. However, as the amount of liberated molten fuel increases it cannot be expected that it would remain in the form of individual particles. A more reasonable assumption would be that the molten fuel would tend to coalesce, forming larger droplets as the amount of molten fuel increases. For this reason, the peak channel pressure obtained from Equation 5.19 has been plotted in Figure 5-20 for various numbers of particles rather than as a function of particle size. In Figure 5-21, the average particle size for various amounts of molten $UO_2$ is shown. This technique correlates well with the results of the molten droplet tests performed at GE in which approximately 1 pound of Zircaloy-2 was melted, resulting in an average particle size of 0.312 inch.

The energy liberated was the heat of fusion for $UO_2$ plus the sensible heat contained from 5000 to 550°F. The time required for this energy transfer which is dependent on the particle size was obtained from Figure 5-19 for the case of nearly 100% energy transfer. From this the steam generation rate, c, could also be determined. As an example, for a 1-pound mass of molten $UO_2$ broken up into 500 particles of 0.2 inch in diameter, the time to transfer approximately 100% of its heat is 20 seconds (from Figure 5-19). The generation rate of steam is thus determined as

$$c = \frac{w}{h_{fg}} \frac{(C_p \Delta T + \Delta h)}{t}$$

where

$w$ = mass of $UO_2$ undergoing cooling,

$C_p$ = specific heat capacity,

$\Delta T$ = total temperature change,

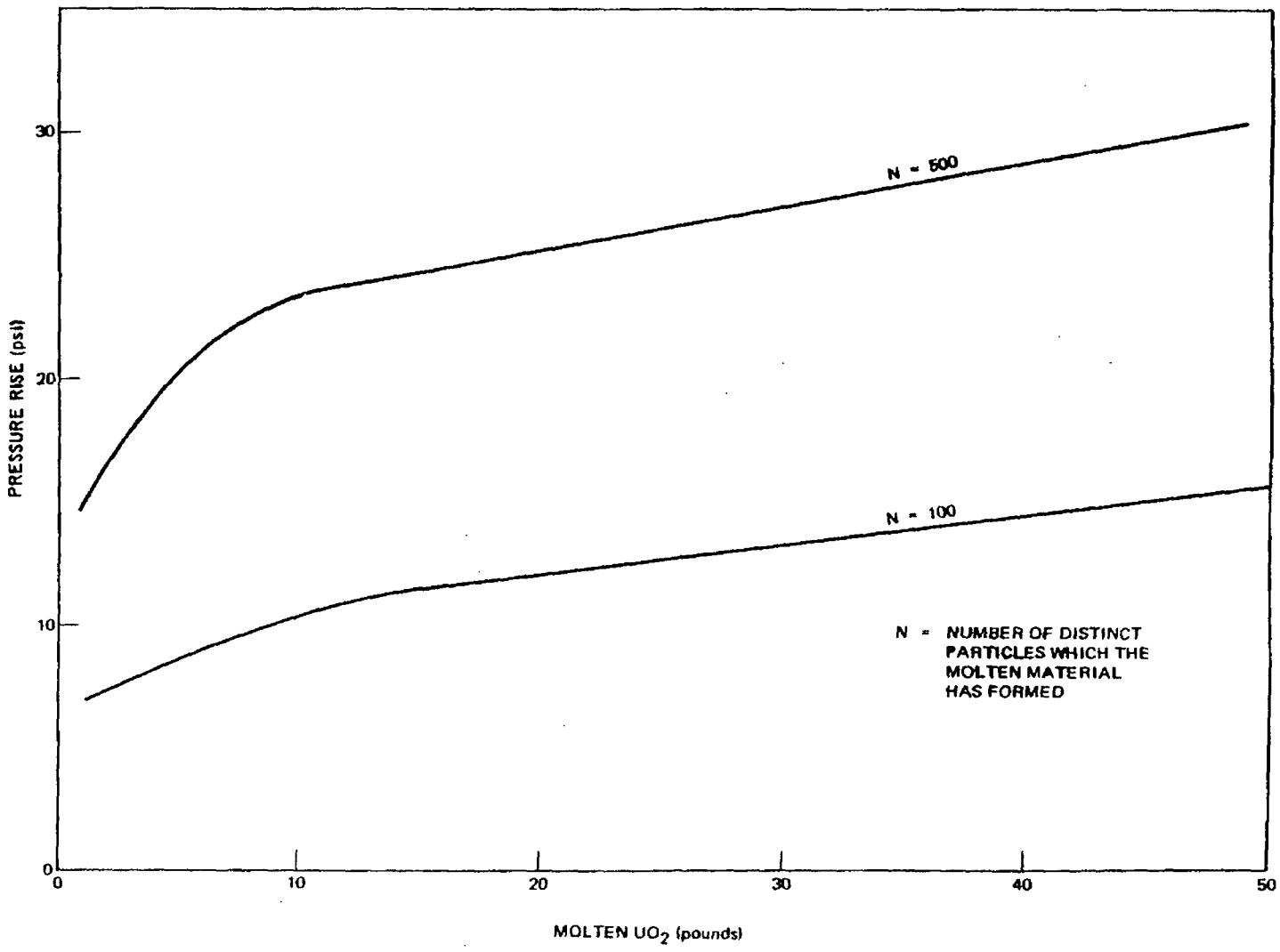


Figure 5-20. Internal Channel Pressure Rise Resulting from Various Amounts of Molten $UO_2$ Being Liberated

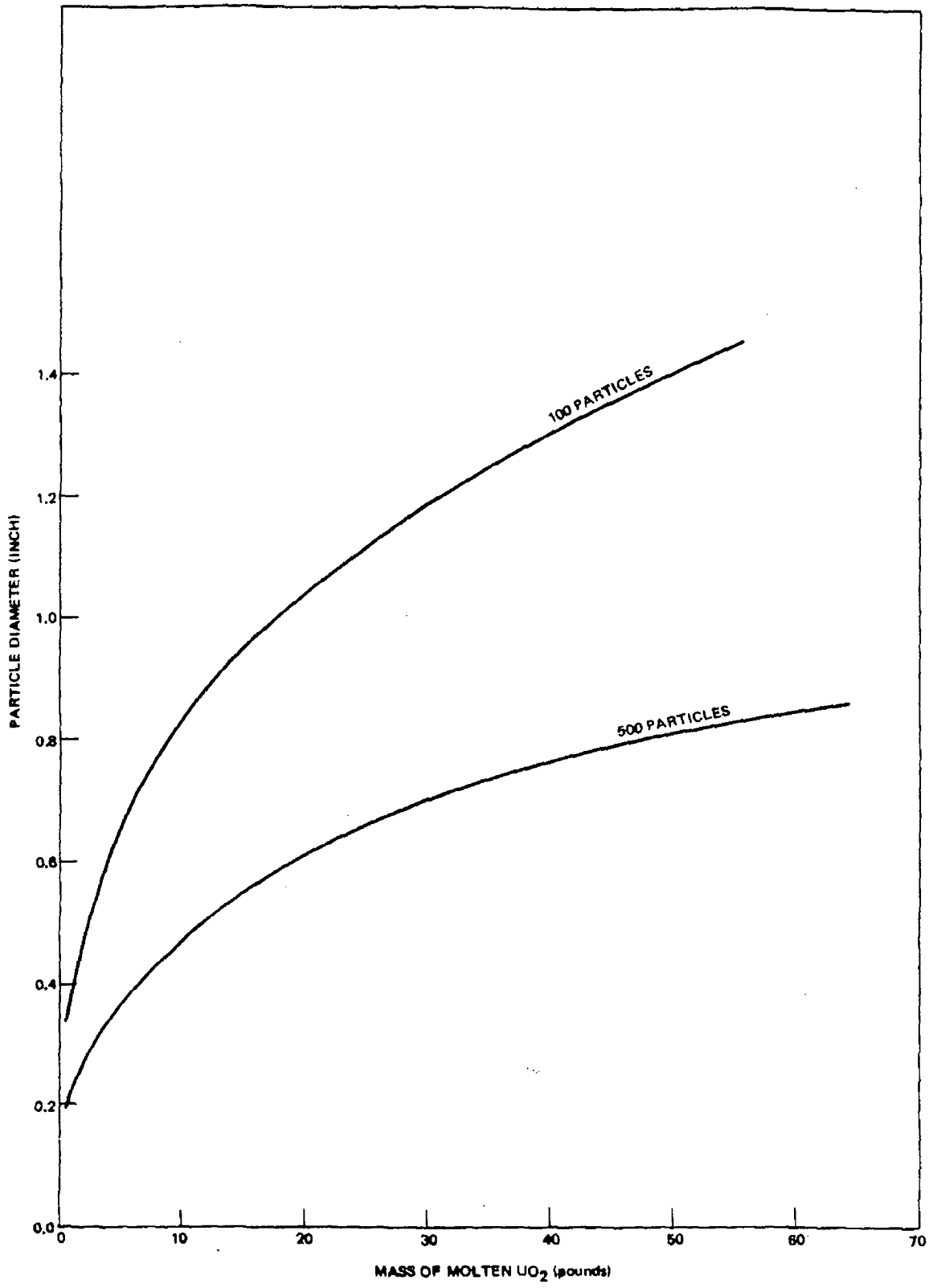


Figure 5-21. Average Particle Size of Molton $UO_2$

$\Delta h$ = heat of fusion,

$h_{fg}$ = liquid heat of vaporization,

$t$ = total time for heat transfer to take place.

$$c = \frac{[1.18\ (5000 - 550) + 125]\ 0.9}{650\ (20)}$$

$$c = 0.375 \text{ lb/sec}$$

With this generation rate the maximum pressure reached in the channel is approximately 14 psi.

As the amount of molten $UO_2$ increases the resulting pressure rise increases, but not very rapidly. The reason for this is the $UO_2$ tends to form into larger droplets whose heat transfer rates are slower. The upper limit of 500 particles is based on the smallest particle size (0.2-inch diameter) obtained from the molten droplet test occupying all the free flow area in a fuel assembly. Hence approximately 500 particles of 0.2-inch diameter will occupy all of the free flow area. This is considered as an upper limit. Of course, as the amount of molten fuel increases it would be expected that the number of particles would also decrease because more of the fuel would come into contact with other molten fuel, thereby coalescing and forming larger droplets.

The actual pressure rises are expected to be even less than that shown because of the conservative assumptions made in the analysis such as: the small heat reaction zone ($x_0$ = 1 ft), the perfect gas relationship, and the fact that the quantities of molten $UO_2$ were assumed to be introduced into the coolant instantaneously whereas they would actually be introduced over a relatively long period of time, thereby decreasing the steam generation rate and the pressure rise. The effects of this pressure rise on the fuel assembly and adjacent channels is covered in the following section.

Summarizing, we find that acoustic pressure pulses cannot be generated because the heat transfer rate is not fast enough and that the resulting inertial pressure rises will be of a very modest nature.

## 5.5 CONCLUSIONS

This section considered the consequences of introducing molten materials into a BWR-type environment. Nuclear excursions and the loss-of-coolant accidents are not capable of initiating such an event because of the safety systems provided in a BWR reactor. The only event capable of bringing about such a condition is a flow blockage incident in which the flow area has been blocked off by more than 95%.

Propagation of this accident is the area of most concern and since the only mechanism capable of initiating such events is the generation of a large pressure pulse resulting from the interaction of molten $UO_2$/Zircaloy and water, it became essential to investigate the potential of such interactions.

Several events, both experimental and accidental, which resulted in the generation of destructive acoustic pressure pulses, were examined. The conclusion reached in reviewing these incidents was that the dispersal of the molten material into finely divided particles was necessary to generate destructive acoustic pulses. The latest state of the art mechanistic model to describe a Fuel Coolant Interaction, The Spontaneous Nucleation Theory, was applied to the interaction of molten $UO_2$/Zircaloy and water. This model is based on analysis and criteria necessary for a FCI and have been confirmed with Freon-Oil and Tin-Water experimental data. Analyses showed that the explosive potential for a $UO_2$/Zircaloy-Water interaction is negligible. Experimental tests by various investigators with molten $UO_2$ and Zircaloy, or combinations thereof, were shown not to exhibit natural tendencies of subdivision upon being quenched in water. Tests performed at General Electric in which a Zircaloy-2 bundle was melted demonstrated that simple melting due to overheating would not produce particles small enough to generate acoustic pressure pulses, therefore eliminating the possibility of generating destructive pressure pulses. Tests at GE also demonstrated that pressure pulses with hot surfaces are not possible.

Since the possibility of acoustic pulses was eliminated, a conservative analysis was performed to evaluate the magnitude of the inertial pressure rise that possibly result. These pressures were found to be very modest (< 30 psi) and, therefore, offered no threat to adjacent channels or other reactor core

components. The consequences of introducing molten materials into a BWR environment as a result of a high degree of flow blockage will not jeopardize the integrity of the reactor components nor will it lead to conditions which would propagate the accident.

# 6. INTEGRITY OF A FUEL CHANNEL SUBJECTED TO INTERNAL PRESSURE RISES

In the preceding section, the severity of molten metal/water interactions in a BWR were investigated. It was shown that large acoustic pressure pulses were not possible because the necessary phenomena were not present, namely the fine division of the molten particles, the absence of a pressure relief surface, and the high heat transfer rates. However, it was shown by a conservative analysis that modest pressure rises may occur when water re-enters the channel and makes contact with the molten $UO_2$/Zircaloy mixture after a major blockage. Considering a maximum flow blockage, which would result in the maximum amount of fuel damage to the assembly, there are two possible sources of re-entering water: (1) the object causing the blockage could be suddenly removed, allowing coolant to enter the bundle through its normal path or (2) as was shown in Section 4.4 if the molten fuel makes contact with the channel wall, the material will melt through the wall, allowing water from the inter-channel region to enter the bundle. Thus, the thermal transient which the fuel rods are undergoing at the time would effectively be terminated by the cooling provided by the re-entering water. During this initial quenching phase the pressure rise which occurs within the channel is due to the steam generation. This type of pressure rise was shown to be very modest (Figure 5-20), even for large amounts of molten $UO_2$.

It can be postulated that if the coolant water is re-entering the blocked bundle due to removal of the object causing the blockage (i.e., (1) above), the most adverse consequence is a breach of the channel wall. This would simply result in the ingress of additional coolant water. If the coolant water is re-entering the blocked bundle due to a breach in the channel wall (i.e. (2) above), a small pressure pulse could be transmitted to adjacent assemblies. Even assuming that the total energy of the pressure pulse is transmitted to a single adjacent channel, the integrity of the adjacent channel will not be jeopardized.

# 7. CONSEQUENCES OF A NUCLEAR EXCURSION

## 7.1 DESIGN BASIS ACCIDENT

One of the mechanisms that could result in expulsion of molten fuel to the coolant and therefore create a potential for a destructive pressure pulse is a nuclear excursion.

The worst nuclear transient which the fuel in a BWR can experience is a control rod drop accident. The direct effects of this accident, considered as a design basis accident by the General Electric Company, have been evaluated in detail[7.1-7.6] and for this reason will not be discussed here. The results of these evaluations are that the peak enthalpies experienced during the accident are far below 425 cal/gm, which is estimated to be the threshold for immediate rupture of fuel rods due to $UO_2$ vapor pressure as shown in Figure 5-14. There are no damaging pressure pulses as a result of the rod drop accident, and the only damage expected would be failed fuel cladding. The analysis therefore demonstrates that the direct effects of a nuclear excursion in a boiling water reactor will not result in molten fuel being released to the coolant.

The effects of a nuclear excursion on a flow blockage due to cladding swelling are evaluated below.

## 7.2 POTENTIAL FLOW BLOCKAGE AS A CONSEQUENCE OF A NUCLEAR EXCURSION

In the unlikely event that a nuclear excursion occurs in a BWR, there is a potential for the consequences of that excursion to be augmented by a flow blockage. This could occur if the excursion took place at a time when the decay power in the core was still substantial. The excursion itself would be turned around by Doppler effects and completely shut down by scramming of control rods. However, if coolant is prevented from reaching the rods, the decay power may continue to add heat to the fuel and raise its temperature after the excursion.

The design basis nuclear excursion accident analyzed in a BWR has been discussed earlier. If the decay heat is not removed after the transient, it is possible that fuel melting will occur. This condition of fuel melting with no coolant flow has been analyzed earlier and the fact that an excursion leads to this condition does not alter the results of that analysis. However, there is reason to believe that this condition would not arise from an excursion accident.

The mechanism by which a channel could become blocked as a result of an excursion is cladding swelling. The cladding becomes very hot during and after an excursion, even with adequate cooling. If adequate pressure exists internal to the fuel rods, the cladding strength may be exceeded and permanent deformation of the cladding could occur. This behavior during a transient has been observed experimentally in both the SPERT IV Capsule Driver Core,[7.7] and in TREAT.[7.8,7.9]

7.2.1 Analysis

The circumferential cladding strain required to completely block flow in a bundle is ∿69%.

This strain must occur in every rod in the bundle and it must occur at the same axial position on every rod. The power distribution in a bundle and the normal variations in cladding properties would combine to make complete blockage highly improbable. Also, the experimental evidence shows that the blockage would not take place. Experiments have been performed at General Electric that verify the conclusion reached above. Those experiments were to study rod failures during a loss of coolant. The particular phase of that study that is of interest to this analysis involved a bundle of zirconium heater rods heated up without coolant and with internal gas pressure. The gas pressure was designed to simulate the pressure that would result from fission products in a fuel rod. The results of these tests are provided in Reference 7.10. Figures 7-1 and 7-2 show the condition of the heater rods after the test.

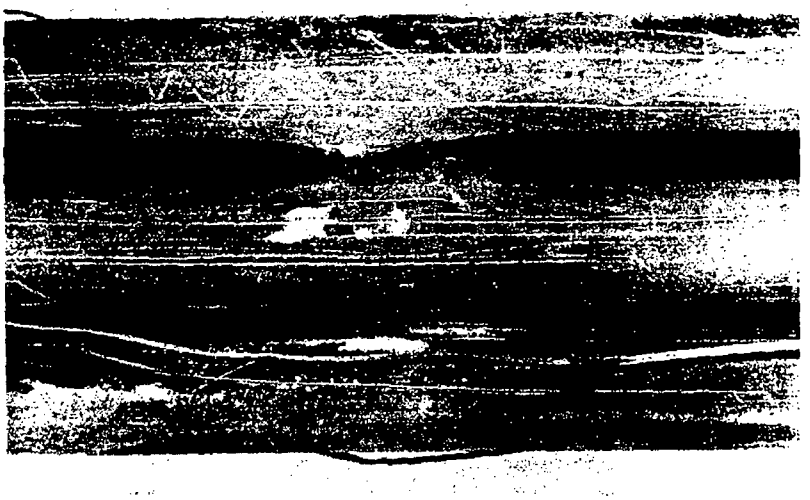

Figure 7-1. Test 1, Rods B, E, and H — 8 Inches Below Upper Spacer

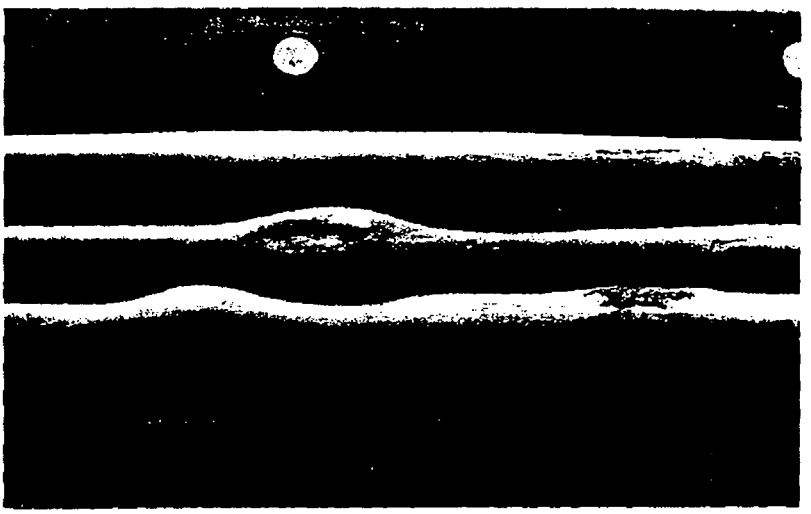

Figure 7-2. Test II, Rods B, E, and H — 6 Inches Below Center Spacer

The blockage observed in the tests amounted to ∿11% at the plane of maximum deformation. The observed cladding temperatures were somewhat less than those experienced in a nuclear excursion. Figure 7-3 shows the temperature history of the cladding on a fuel pin tested with SPERT IV Capsule Driver Core.[7.11] This particular temperature history was observed on a fuel pin with an energy deposition of 262 cal/gm which is comparable to the maximum energy obtained in the design base accident in a BWR.

The deformations observed in SPERT and TREAT have not been enough to completely block a channel. The tests in TREAT[7.8,7.9] were done in a sodium environment and may not be directly applicable to BWR's. The swelling in those tests was about one percent. The SPERT tests[7.12] are more representative of conditions in a BWR. Figure 7-4 shows a fuel pin after transient irradiation in SPERT.

The fuel pin in Figure 7-4 had an energy input of 194 cal/gm and the cladding experienced a growth of 22%.* The measured internal pressure was 200 psig which is approximately the same as the pressure used in the bundle tests at General Electric. A similar type pin subjected to an energy input of 260 cal/gm which had been pre-irradiated to about 3000 mwd/T experienced a maximum deformation of 20%. Internal pin pressure was measured to be about 100 psig.

These fuel pins were subjected to energies that are similar to the peak enthalpies that would be experienced in the design basis accident in a BWR.** Since the shape of the power burst in SPERT IV is very similar to that of a BWR, these tests are representative of expected transient behavior of BWR fuel.

---

*Due to more recent data it was concluded that this gross swelling was caused by CO formed due to the fact that the fuel was fabricated with a paraffin binder which is not used in BWR fuel. Although the new test data show some swelling it is much less than 22%.

**These pins also had paraffin binders (see footnote above).

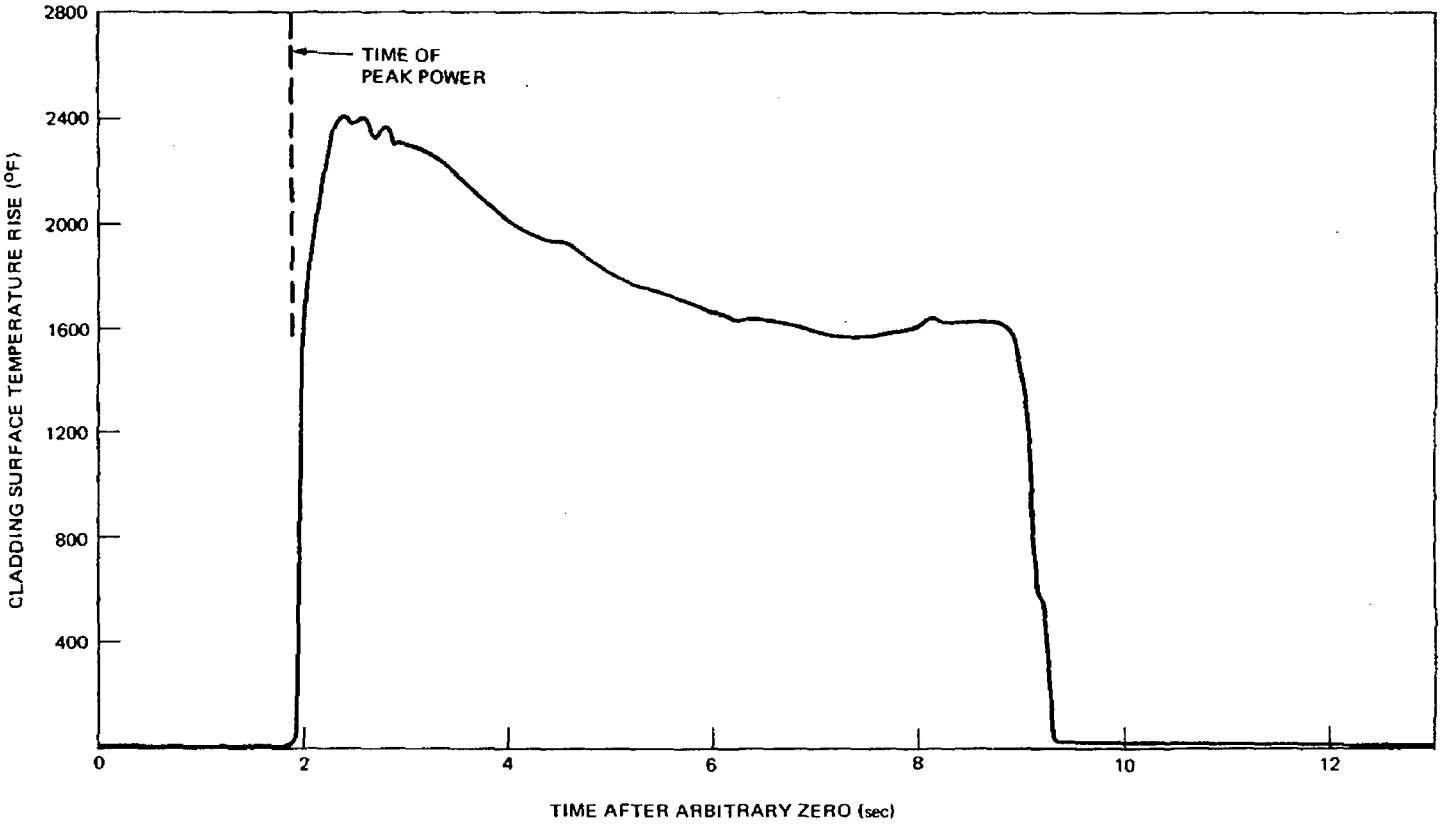


Figure 7-3. SPERT IV Test No. 518 262 cal/gm $UO_2$

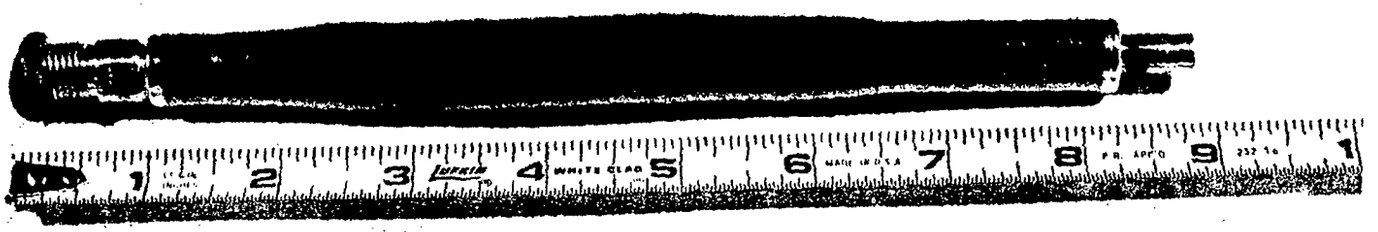


Figure 7-4. SPERT IV Run 484 SE-8

Another consideration in evaluating the extent of cladding deformation is irradiation effects. During the life of the fuel the cladding becomes less ductile due to the neutron flux environment. This reduced ductility prevents large deformations because the cladding cracks and relieves the driving pressure inside before it deforms excessively. The cladding may reach temperatures in excess of annealing temperature during an excursion but the time available for the annealing to take place is quite short. As can be seen in Figure 7-3 the cladding reaches peak temperatures in about 0.5 second. It is unlikely that irradiation effects can be annealed out in that time. If the strength of the cladding has not been exceeded at the time of peak temperature it certainly won't be exceeded later as the cladding is cooling. The net result of this effect is that the cladding in an operating BWR should experience even less deformation than was observed in the experiments discussed above.

### 7.2.2 Conclusions

The experimental evidence and consideration of irradiation effects show that a nuclear excursion would not cause sufficient flow blockage to increase the severity of the accident. Some blockage could occur but the coolant would continue to flow and easily carry away the heat in the fuel.

# 8. RADIOLOGICAL ASPECTS OF FLOW BLOCKAGE EVENTS

The key points contained in this section are:

a. Noble gas release rates from the fuel of between 0.05 and 0.20 percent of the bundle total noble gas inventory per second have been calculated to result in main steam line radiation monitor (MSLRM) trip which would initiate reactor scram and isolation for the most severe case of complete orifice blockage. Fuel melt of the hottest axial plane of all rods in the bundle is calculated to occur within about a ten second time span. This alone is sufficient to cause MSLRM trip.

b. The total time increment between initial release of sufficient noble gas from melted fuel to cause MSLRM trip and completion of reactor scram has been calculated to be within 13 seconds (between 8.5 and 12.5 seconds).

c. The offgas pretreatment monitor sensitivity is sufficient to indicate the occurrence of flow blockage events which result in cladding failures. The time increment to detection and alarm is about 2 minutes followed by the time for operator action.

d. The offsite radiological consequences have been estimated based on conservative assumptions and are small fractions of 10CFR100 offsite dose guidelines.

## 8.1 FUEL FAILURE RADIATION DETECTION SYSTEMS

### 8.1.1 General Considerations

Fuel bundle coolant flow reductions due to flow blockage will for most events result in no fuel damage. Fuel damage, ranging from cladding failure to fuel melting, will result in direct release of fission products from the fuel, with the rapidity and quantity of release generally directly related to the rate of occurrence and overall severity of fuel rod damage.

As a function of severity, fission product release would characteristically involve prompt noble gas release, followed by halogen release, and in the worst damage case by the release of other fission products. The most significant flow blockage events are expected to occur when the reactor is operating at high power. Normal water-steam partitioning or carryover factors would apply. Thus transfer to steam would involve essentially all of the noble gases released, approximately 1% of the halogens & 0.01% of other fission products. The transfer of noble gases to the steam provides the transport mechanism for detection of any significant fuel damage.

On a typical BWR there are a number of radiation monitoring systems which are capable of indicating an abnormal release of fission product activity. However, for the purpose of this event those systems which would provide the most rapid response are the Main Steam Line Radiation Monitors which input to the Reactor Protection System and the Steam Jet Air Ejector Monitors which are part of the Offgas Treatment System.

### 8.1.2 Main Steam Line Radiation Monitors

The purpose of the Main Steam Line Radiation Monitors (MSLRM) is to provide prompt detection of any core damage event which results in the significant release of noble gases. As a part of the Reactor Protection System, the MSLRM provide prompt reactor scram and main steam line isolation.

The MSLRM operate in the presence of the normal high level Nitrogen-16 activity in the steam, which is of the order of 100 curies per second at rated power for large BWRs. The trip point is normally set at about 3 to 7 times the N-16 background radiation level. Due to the lower average gamma decay energy of noble gases released from failed fuel, releases on the order of a few kilocuries per second are necessary to cause MSLRM trip and initiation of the protection system. Thus the MSLRM would probably not react to the noble gas releases associated with cladding defects, expected to be below a curie per second per fuel rod cladding defect. The MSLRM would promptly react to a massive noble gas release that would occur as soon as fuel melting started.

At rated power the noble gas transit time from core midplane to the MSLRM is within 9 seconds for the typical large BWR. Detection, scram, and steam line isolation follows within approximately 4 seconds.

### 8.1.3 SJAE Offgas Monitoring System

The SJAE offgas monitoring system, which also serves as the pre-treatment monitor on augmented offgas treatment systems, provides routine core surveillance by detection of low-level emissions of noble gases. A two minute holdup period is provided to allow for the decay of N-16 and other short half life fission products and activation products. In normal operation, an alarm trip setting of several times the offgas level is established to provide prompt operator warning of any significant change. With expected fuel performance, any change associated with an increase of the order of 1-10 curies per second would be promptly alarmed.

Upon the occurrence of an alarm, operator action would be initiated and, if necessary, power reduction or reactor shutdown, depending upon the level of the increase indicated.

Thus for any flow blockage event which results in significant cladding failure, alarm and control is available from the offgas monitoring system. Noble gases reaching the condenser would enter the offgas treatment system as long as SJAE steam is available. If reactor shutdown occurs, offgas system isolation would retain the stored gases for decay. Halogens and other fission products reaching the condenser would flow to the offgas system, or would be initially retained in the condenser air space or in the condensate.

### 8.1.4 Fuel Noble Gas Inventory

As the majority of fission product noble gases are of short half-life, during power operation the fuel noble gas inventory reaches approximately 75% of its equilibrium value after an hour's operation, and about 98% in a day. Thus the principal source term inventory is not significantly influenced by period of operation prior to the occurrence of the flow blockage event.

At rated power the noble gas inventory of an average fuel bundle is $1.8 \times 10^6$ curies (see Table 8.1). The inventory would be somewhat less for a bundle operating for less than 1 day.

### 8.1.5 Main Steam Line Radiation Monitor Response to Fuel Melting

The detection and shutdown sequence has been evaluated for the low probability event of complete orifice flow blockage. This degree of flow blockage is predicted to lead to melting of fuel. For this event, once fuel melting in the hottest rod in the bundle starts, the melting will increase across the bundle as well as axially. Considering the action in the initially hottest six inch axial node, the fuel node melt from start to completion will occur within approximately ten seconds. This six inch node corresponds to about 4 percent of a total rod length. Considering the noble gas inventory in this node only, and ignoring melting in other axial nodes which would soon follow, the average release rate over the first ten second period would be $7.5 \times 10^3$ curies per second. When the monitor trip is set at three times normal N-16-background, a noble gas release of about $1.1 \times 10^3$ curies per second is required for a trip signal. This corresponds to 0.06% of the bundle noble gas inventory being released per second (0.6% over ten seconds). When the monitor is set for a trip at seven times background, a noble gas release of about $3.2 \times 10^3$ curies per second is required (0.18% of the bundle inventory per second). Therefore the release of the fission gases in the highest powered axial node is sufficient for the MSLRM to trip and initiate scram and isolation.

The noble gas "gap" inventory available for release from a fuel rod upon cladding failures during a fuel heatup transient has been estimated to be as much as 3 percent of the total rod noble gas inventory (see Rasmussen report[8.1]). This estimate is an upper bound. In addition, the isotopic distribution of a gas inventory is predicted to have higher fractions of long-lived noble gas than are contained in the fuel itself. This would cause less MSLRM response per curie than for the rod noble gas mixture released upon fuel melt because of the lower energy level of the longer lived isotopes. If the release of 3% of the inventory from 12 fuel rods were to occur over several seconds the MSLRM would detect this release, scram the reactor and isolate the vessel.

However, it is considered more likely that the "gap" inventory would be less than 3% and would be released over a longer time period resulting in the inability of the MSLRM to detect cladding failure.

### 8.1.6 SJAE Offgas Monitor Response to Cladding Failure

For the event where the assumed flow blockage provides bundle flow sufficient to prevent fuel melting, but not enough to prevent boiling transition, cladding oxidation and fragmentation is expected to occur after some period of time.

The noble gas inventory in an average fuel rod is about 30,000 curies. In terms of reference to the two minute decay at the SJAE monitor, this is equivalent to about 10,000 curies per rod.

At two minutes decay, release of 1% of the inventory of a single rod is equivalent to 100 curies. As indicated previously, the SJAE monitor normally would respond sharply to a sudden increase of 1-10 curies per second (and perhaps 0.1 curies per second most of the time). Therefore if the 100 curies did in fact leave the fuel rod in a period less than 10 seconds, the SJAE monitor provides the desired alarm to operating personnel. The failure of more than one fuel rod would provide additional activity for monitor response.

## 8.2 RADIATION DETECTION SYSTEM EVALUATION

As a result of a flow blockage in excess of 95%, fuel rod failures are expected and some failures may result from blockages between 79% and 95%. The purpose of this evaluation is to define the magnitude of fuel failures and fission product release required to activate the steam line and offgas radiation monitor trip levels.

The description of the fuel fission product release is given in Section 8.1. A summary of the other basic assumptions and conditions used in evaluating the monitor performance is as follows:

a. Normal reactor separation factors are assumed to be constant during the flow blockage event. Hence, only fission product noble gases were considered in evaluating radiation monitor response.

b. The isotopic distribution of noble gases in the main steam lines is defined in Table 8.1, corrected for radioactive decay to the point of monitoring.

c. The N-16 concentration leaving the reactor vessel is considered to be the design basis value of 50 μCi/g of steam (Reference 8.2). This is equivalent to 0.5 $Ci/ft^3$. Steam flow conditions are $2.0 \times 10^6$ g/s.

d. The steam dome volume is 6300 $ft^3$ ($6.4 \times 10^6$ g of steam at 1000 psi).

e. The main steam line detector response to N-16 and noble gas mixtures were evaluated based on the steam line-detector geometry: cylindrical steam lines of schedule 80 pipe with an assumed monitored length of 20 feet with the detectors located at the midpoint of the monitored length. The steam line diameter is 28 inches with a wall thickness of 1.42 inches. Calculations were made using a shielding code which accounted for energy dependent buildup effects.

f. The activity concentration at the off-gas monitor is based on a turbine air inleakage of 50 scfm. The sample flow rate to the monitor has been adjusted to result in a two minute transit delay to the monitor, and the monitor high level alarm is set at 3 times the normal full power value.

### 8.2.1 Radiation Monitor Response Evaluation

The full power background levels of the radiation monitors were calculated in terms of relative response between noble gases and N-16 for the steam line monitor and in terms of mR/hr of noble gas for the offgas monitor. The trip levels for the steam line monitors have been 7X full power steady-state background levels on older BWRs with the NRC now requiring 3X background levels on BWRs receiving operating licenses. The alarm levels for the off-gas monitor are commonly 3X full power background levels.

#### 8.2.1.1 Main Steam Line Radiation Monitors

The relationship between the release rate from the fuel and the noble gas concentration in the steam lines was estimated as follows:

a. The noble gas release was assumed to occur uniformly over a given time interval (establishing a release rate).

b. The release rate from the bundle contributes to a buildup in the steam dome balanced by steam flow to the main steam lines and radioactive decay.

c. The noble gases leaving the bundle mix uniformly in the entire steam dome volume prior to transport from the vessel.

The approach allows a conservative estimate of the noble gas concentration in the steam lines as a function of time. It predicts an increase in steam line activity concentration during the period of release followed by a decrease in concentration after the release is terminated.

For the noble gas isotopic distribution identified in Table 8.1 corrected for decay to the MSLRM location, 0.28 $Ci/ft^3$ in the steam lines in the region of the main steam line monitors is estimated to be required to give response equal to the full power N-16 background response. This was found to be practically independent of the distance between the detector and the steam line surface for distances between 5 and 20 feet.

Table 8.1

MSLRM RESPONSE TO THE VARIOUS NOBLE GASES

| Isotope | Half-Life | Fraction of Total Response | Cumulative Fraction of Total Response | Bundle Inventory ($10^4$ Ci) |
|---|---|---|---|---|
| Kr-91 | 8.6 sec | 0.007 | 0.007 | 9.3 |
| Xe-140 | 14 sec | 0.017 | 0.024 | 12.7 |
| Kr-90 | 32 sec | 0.104 | 0.128 | 12.2 |
| Xe-139 | 40 sec | 0.157 | 0.285 | 19.1 |
| Kr-89 | 3.2 min | 0.228 | 0.513 | 10.8 |
| Xe-137 | 3.8 min | 0.045 | 0.558 | 24.0 |
| Xe-138 | 14 min | 0.203 | 0.761 | 23.0 |
| Xe-135m | 16 min | 0.010 | 0.771 | 4.7 |
| Kr-87 | 76 min | 0.047 | 0.818 | 5.9 |
| Kr-88 | 2.8 hr | 0.159 | 0.977 | 8.8 |
| Kr-85m | 4.4 hr | 0.005 | 0.982 | 3.5 |
| Xe-135 | 9.2 hr | 0.008 | 0.990 | 3.6 |
| Xe-133 | 5.3 day | 0.007 | 0.997 | 26.9 |
| | | | | total = 179. |

The combination of isotopic distribution, gamma-ray abundances and gamma energies are such that 97% of the steam line radiation monitor response would be due to nuclides whose half-lives are less than or equal to that of 2.8 hr Kr-88 and 75% of the response would be due to nuclides with half-lives less than or equal to that of 14.2 min Xe-138. This has the important consequence that the monitoring sensitivity is relatively independent of the length of operating time at any given power. The relative response to the isotopic distribution at the steam line monitor is given in Table 8.1.

Table 8.2 presents the magnitude of the total noble gas release required to generate main steam line monitor trip as a function of the duration of the release. Note from Table 8.2 that the Ci release needed for trip does not increase directly with the duration of the release for the times considered. For example, release over a 10 sec period requires just 2.4 times the release over a 2 sec period.

Table 8.2

FISSION PRODUCT RELEASE FOR MAIN STEAM LINE MONITOR TRIP

| Duration of Release (sec) | Total Ci Release for 3X BKG Trip* | Total Ci Release for 7X BKG Trip |
|---|---|---|
| 1 | $3.9 \times 10^3$ | $1.16 \times 10^4$ |
| 2 | $4.4 \times 10^3$ | $1.33 \times 10^4$ |
| 5 | $6.4 \times 10^3$ | $1.83 \times 10^4$ |
| 7.5 | $8.4 \times 10^3$ | $2.51 \times 10^4$ |
| 10 | $1.06 \times 10^4$ | $3.18 \times 10^4$ |

*For example, the release rate for 3X BKG trip levels is $3.9 \times 10^3$ Ci/sec for a 1 sec release, $2.2 \times 10^3$ Ci/sec for a 2 sec release and $1.3 \times 10^3$ Ci/sec for a 5 sec release.

8.2.1.1.1 Time to Accomplish Protective Action

The time between release of a sufficient quantity of noble gases from the fuel to cause a reactor scram and isolation and completion of these protective actions has been estimated based on the following estimates:

a. Transport time from hottest fuel node to core exit for complete flow blockage - 1 to 2 seconds.

b. Transport time from core exit to main steam line (MSL) entrance (plant size dependent) - 4.0 to 5.5 seconds.

c. Transport time from MSL entrance to MSL radiation detectors - 1 second.

d. MSLRM and reactor protection system response time to initiation of scram and isolation - 0.5 to 1 second.

e. Completion of scram after initiation (control rods fully inserted) - 2 to 3 seconds.

f. Completion of main steam line isolation valve closure after initiation - 3 to 5 seconds.

Thus reactor shutdown is estimated to occur between 8.5 and 12.5 seconds after release of sufficient quantities of noble gas from the fuel. Reactor vessel isolation occurs between 9.5 and 14.5 seconds.

8.2.1.2 Off-Gas Pre-Treatment Radiation Monitor

For the purpose of expressing fuel performance off-gas release rates are defined in terms of the sum of the release rates of the six longer-lived noble gases.† As a worse case, it is assumed that the full power (SJAE) release rate for the sum of these six nuclides will not exceed $10^6$ μCi/s with an isotopic distribution characterized by a "b" value of 0.6.* This is 2.5 times the design basis value and approximately a factor of 10 greater than average operating conditions thereby providing a very conservative background level.

Previous evaluation of this monitor, Reference 8.3, has shown that the response may be expressed by the empirical relation:

$$\sum_{1}^{6} (R_i) = K \cdot F \cdot E \qquad (8\text{-}1)$$

where:

$\sum_{1}^{6} (R_i)$ = μCi/s of the six nuclides measured at the monitor location, effectively 2-min delay from the SJAE.

F = Off-gas flow, SCFM

E = Monitor Response, mR/h

K = Calibration Factor

†4.4h Kr-85m, 76m Kr-87, 2.80h Kr-88, 5.27d Xe-133, 9.16h Xe-135, 14.2m Xe-138.

*The fission gas activity distribution is commonly represented by $A_i = K \cdot Y_i \cdot \lambda_i^{-b+1}$ Reference, 8.4 where $A_i$ is the μCi/s of the $i^{th}$ nuclide, K and b are constants, and $Y_i$ and $\lambda_i$ are the corresponding fission yields and decay constants.

For the purpose of this analysis, F was taken as a relatively high value of 50 SCFM air downstream of the offgas recombiner. The "K" factor is a function of "b" and, for "b" equal to 0.6, has an average value of 0.48. For the conditions stated, the background reading of the monitor would be:

$$E = \frac{10^6}{(0.48)\ (50)} = 4.2 \times 10^4 \text{ mR/hr} \qquad (8\text{-}2)$$

Thus, the radiation level required to trip the alarm to 3 times operating level corresponds to $1.25 \times 10^5$ mR/hr. For this assumed level, the increase in the fission gas radiation field required to trip the monitor would be $1.25 \times 10^5 - 0.42 \times 10^5$ or $8.3 \times 10^4$ mR/hr.

The actual Ci/s corresponding to a radiation level of $8.3 \times 10^4$ mR/hr depends upon the nuclide distribution. Considering either a recoil, "b" = 0, or equilibrium source, "b" = 1, as the two extremes, "K" has average values of 0.09 and 1.5, respectively. From Equation (8-1), an increase of $8.3 \times 10^4$ mR/hr requires an increased release rate for the sum of the six nuclides of 0.37 Ci/sec for a recoil source and 6.3 Ci/sec for an equilibrium source. The distribution of noble gases in Table 8.1 is an equilibrium distribution. From Table 8.2 it can be observed that the off-gas pre-treatment radiation monitor will alarm at releases roughly 200 to 2000 times *below* the level required for main steam line radiation monitor trips.

## 8.3 RADIOLOGICAL CONSEQUENCES

The off-site radiological assessment of a flow blockage event is based on *very conservative NRC* design basis type assumptions similar to the assumptions made for the evaluation of a postulated control rod drop accident.[8.5]

a. 100% of the noble gases and 50% of the iodines contained in the bundle are released to the reactor coolant.

b. One tenth of the iodines and 100% of the noble gases reach the turbine and condenser.

c. 100% of the noble gases and 10% of the iodines (due to partitioning and plate-out) remain airborne for leakage from the turbine and condenser.

d. The turbine and condenser leak at a rate of 1.0%/day with the effects of radioactive decay accounted for during holdup in the turbine and condenser.

e. Leakage from the turbine and condenser is released directly to the environment without credit for holdup in the turbine building.

f. Accident meteorological conditions with an exclusion area X/Q of $1.0 \times 10^{-3}$ sec/$m^3$ (0 to 2 hrs) and a low population zone X/Q of $5.0 \times 10^{-5}$ sec/$m^3$ (0 to 30 days).

The calculated off-site doses are then

| | Inhalation (REM) | Whole Body (REM) |
|---|---|---|
| Exclusion Area | 0.5 | 0.1 |
| Low Population Zone | 1.1 | 0.03 |

Even based on the above very conservative source terms, the resultant exposures are small fractions of 10CFR100 guidelines.

## 9. REFERENCES


1.1 Letter from Mr. Olan D. Parr (USNRC) to the attention of Dr. G. G. Sherwood (GE) dated December 20, 1976; Subject: Request for additional information on GE Topical Report NEDE-20944-P, "BWR/4 and BWR/5 Fuel Design," Request No. 231.13.

1.2 McCarthy, Jr., W.J. Jens, W.H., "Enrico Fermi Fast Breeder Reactor", Nuclear News 10, No. 11 (Nov. 1967).

1.3 Dykes, J.W., Ford, J.D., Hoopingarner, K.R., "A Summary of the 1962 Fuel Element Fission Break in the MTR," IDO-176064 (February 1965).

1.4 Keller, F.R., "Fuel Element Flow Blockage in the Engineering Test Reactor," IDO-16780 (May 10, 1962).

3.1 Consumers Power Company, Big Rock Point, Docket No. 50-155, May 1 - Oct 31, 1963

3.2 Wooley, J.A., "Three-Dimensional BWR Core Simulator", NEDO-20953 (May 1976).

3.3 Martin, C.L., "Lattice Physics Methods", NEDO-20913 (July 1976).

3.4 "Analytical Model for Loss-of-Coolant Analysis in Accordance with 10CFR50 Appendix K - Volume II", NEDO-20566, Page II-60, 1975.

4.1 "General Electric Thermal Analysis Basis Data, Correlation and Design Application", NEDO-10958-A (January 1977).

4.2 "Analytical Model for Loss-of-Coolant Analysis in Accordance with 10CFR50 Appendix K" NEDO-20566, 1975.

4.3 Submittal from General Electric (A.J. Levine, Manager, Project Licensing 1, Safety and Licensing) to USNCR (Dr. D.F. Ross, Assistant Director for Reactor Safety, Division of Systems Safety). "General Electric (GE) Loss of Coolant Accident (LOCA) Analysis Model Revisions - Core Heatup Code CHASTE05," (January 27, 1977)

4.4 Baker, L. and Just, L.C., "Studies of Metal Water Reactions at High Temperatures, III. Experimental and Theoretical Studies of the Zirconium - Water Reaction," ANL-6548, p. 7 (May 1962).

4.5 Dougall, R.S. and Rohsenow, W.M., "Film Boiling on the Inside of Vertical Tubes with Upward Flow of Fluid at Low Qualities," MIT Report 9079-26. Date Cambridge, Mass., September, 1963.

4.6 "Chemical Engineering Division Seminannual Report," January-June, 1966, ANL-7225 (July 31, 1966).

4.7 Zuber, N., "Hydrodynamic Aspects of Boiling Heat Transfer," USAEC Report AECU-4439, 1959.

5.1 Dietrich, J.R., "Experimental Investigation of the Self-Limitation of Power During Reactivity Transients in a Subcooled Water-Moderated Reactor - Borax-1 Experiments - 1954," AECD-3668 (1955).

5.2 "Final Report of SL-1 Recovery Operation," May 1961 - July 1962, J.F. Kunze, ed., IDO-19311 (1962).

5.3 Kunze, J. F., Bills, C. W., "Correlation of Nuclear and Mechanical Effects in the SL-1 Incident," Trans. ANS. 5, No. 1, p 154 (1962).

5.4 Miller, R. W., Spano, A. H., Dugone J., Wieland, D. D., and Houghtaling, J. E., "Experimental Results and Damage Effects of Destructive Tests," Trans. Am. Nuclear Soc. 6, No. 1, p 138 (June 1963).

5.5 Miller, R. W., Sola, A., and McCardell, R. K., "Report of the SPERT 1 Destructive Test Program on An Aluminum Plate Type, Water-Moderated Reactor," IDO-16883 (1964).

5.6 Baker, Jr., L., "Metal Water Reactions," Nuclear Safety, 7 p 75 (1965).

5.7 "Kinetic Studies of Heterogenous Water Reactors," 1963 Annual Summary Report, STL-6312 (December 30, 1963).

5.8 "Kinetic Studies of Heterogenous Water Reactors," 1964 Annual Summary Report, STL-372-13 (December 30, 1964).

5.9 "Kinetic Studies of Heterogenous Water Reactors," 1965 Annual Summary Report, STL-372-30 (December 1965).

5.10 "Kinetic Studies of Heterogenous Water Reactors," 1966 Annual Summary Report, STL-372-50 (December 1966).

5.11 "Kinetic Studies of Heterogenous Water Reactors," Quarterly Progress Report for period ending June 1965. STL-372-22 (July 31, 1965).

5.12 "Kinetic Studies of Heterogenous Water Reactors," Quarterly Progress Report for period ending September 1965, STL-372-27 (October 30, 1965).

5.13 "Kinetic Studies of Heterogenous Water Reactors," Quarterly Progress Report for period ending September 1966 - STL-372-47 (October 31, 1966).

5.14 Wrentz, L. G., "In-Pile Capsule Measurements of Steam Void Formation in Millisecond Power Excursions," Trans. Am Nucl. Soc., 7 No. 1 p 149 (1964).

5.15 Wright, R. W., "Pressure Pulses in Rapid Transient Boiling," Trans. Am. Nucl. Soc., 6, No. 2, p 338 (1963).

5.16 Brauer, F. E., "Metal/Water Explosions," Nuclear Science & Engineering, 31, No. 3 (March 1968).

5.17 Long, George, "Explosions of Molten Aluminum in Water - Cause and Prevention," Metal Progress, 71 (1957).

5.18 Anderson, R. P. and Armstrong, D. R., "Comparison between Vapor Explosion Models and Recent Experimental Results", AICHE Symposium Series No. 138, Vol. 70, 31, (1974).

5.19 Flory, K., Paoli, R., Mesler, R., "Molten Metal-Water Explosions," Chemical Engineering Progress, 65, No. 12 (December 1969).

5.20 "Chemical Engineering Division Semi Annual Report July - December 1965," ANL-7125 (May 1966).

5.21 "Reactor Development Program Progress Report," ANL-7152 (January 1966).

5.22 "Reactor Development Program Progress Report," ANL-7478 (July 1968).

5.23 "Reactor Development Program Progress Report," ANL-7527 (December 1968).

5.24 "Reactor Development Program Progress Report," ANL-7438 (March 1968).

5.25 Ianni, P. W., "Metal-Water Reactions-Effects on CORE Cooling and Containment," APED-5454 (March 1968).

5.26 Rodgers, S. J., and Kennedy, G. E., "Fission Product Release During a Simulated Meltdown of a PWR Type Core," MSA Research Corp. Report No. 63, Index No. NP 7071 (October 1958).

5.27 Henry, R. E. and Fauske, "Nucleation Characteristics in Physical Explosions", Proc. Third Specialists Mtg. on Sodium/Fuel Interaction in Fast Reactors. Tokyo, Japan, PNC N251 76-12, Vol. 2, 595 (March 1976).

5.28 Henry, R. E. and Fauske, H. K., "Energetics of Vapor Explosions", ASME Paper No. 75-HT-66, presented at National Heat Transfer Conf., San Francisco, Ca. (August 1975).

5.29 Henry, R. E. and McUmber, L. M., "Vapor Explosion Potentials Under Hypothetical Accident Conditions", American Nuclear Society Topical Meeting - Thermal Reactor Safety, Sun Valley, Idaho, July 31-Aug. 4, 1977.

5.30 Corradini, M., Rohsenow, W. M., and Todreas, N. E., "Application of Spontaneous Nucleation Theory to Tin-$H_2O$ Interactions", MIT, September Nuclear Engineering Report #COO-278 1-IITR (January 1977).

5.31 Fauske, H. K., "Some Aspects of Liquid-Liquid Heat Transfer in Explosive Boiling". Proc. Fast Reactor Safety Mtg., Beverly Hills, Ca., CONF-740 401-P2, 992 (April 1974).

5.32 Collier, J. G., "Convective Boiling and Condensation", McGraw-Hill Book Company (1972).

5.33 Board, S. J., Farmer, C. L. and Poole, D. H., "Fragmentation in Thermal Explosions", Int. J. Heat Mass Transfer, Vol. 17, 331 (1974).

5.34 Amblard, M., Berthoud, G., Lackme, C., and Scott, E., "Experimental Results of Contact between Molten $UO_2$ and $H_2O$ Statement of Thermal Interaction Models", Paper presented at the OEDC CSNI Specialists Mtg. on the Behavior of Water Reactor Fuel Elements under Accident Conditions, Spatind, Norway (September 1976).

5.35 Grund, J. E., "SPERT-1 Experimental Investigations of Potentially Destructive Reactivity Additions to an Oxide Core," Trans ANS. 7, No. 1 (June 1964).

5.36 "Chemical Engineering Division semi Annual Report," July - December 1966, ANL-7325 (July 31, 1966).

5.37 "Reactor Development Program Progress Report," ANL-7286 (December 1966).

5.38 Higgins, H. M., "The Reaction of Molten Uranium and Zirconium Alloys with Water," Aerojet General Corporation, AGC-AE-17 (April 30, 1956).

5.39 Gibby, R. L., "Reaction of Molten $UO_2$ with Water", Battelle Northwest Laboratory Report No. BNWL 362 (January 1967).

5.40 Cole, R. H., "Underwater Explosions," Princeton University Press, Princeton, New Jersey (1948).

5.41 "Reactor Development Program Progress Report," ANL-7595 (July 1969).

5.42 Moody, F. J., "A Pressure Pulse Model for Two-Phase Critical Flow and Sonic Velocity" General Electric Company, APED 5579, January 1968.

7.1 Dietrich, R.A., "The Mechanical Effects of Reactivity Transients," APED-5455 (January 1968).

7.2 Wood, J.E., "Analysis Methods of Hypothetical Super-Prompt Critical Reactivity Transients in Large Power Reactors," APED-5448 (April 1968)

7.3 Brammer, H.A., Wood, J.E., and McWhorter, R.J., "Nuclear Excursion Technology," APED-5528 (September 1965, Revised August 1967).

7.4 Paone, C. J. and Woolley, J. A., "Rod Drop Accident Analysis for Large Boiling Water Reactors," Licensing Topical Report, March 1972 (NEDO-10527).

7.5 Stirn, R. C., Paone, C. J., and Young, R. M., "Rod Drop Accident Analysis for Large Boiling Water Reactors," Licensing Topical Report, July 1972 (NEDO-10527 Supplement 1).

7.6 Stirn, R. C., Paone, C. J., and Haun, J. M., "Rod Drop Accident Analysis for Large Boiling Water Reactors, Addendum No. 2, Exposed Cores," Licensing Topical Report, January 1973 (NEDO-10527, Supplement 2).

7.7 Miller, R.W., Lussie, W.G., "The Response of $UO_2$ Fuel Rods to Power Bursts, 9/16-Inch OD, Pellet and Powder Fuel, Zircaloy Clad" IDO-ITR-104 (April 1969).

7.8 Hanson, J.E., Field, J.H., "Experimental Studies of Transient Effects in Fast Reactor Fuels Series III, Pre-Irradiated Mixed-Oxide ($PuO_2$ - $UO_2$) Irradiations Final Report, Transient Irradiations," GEAP-4469 (July 1967).

7.9 "Sodium-Cooled Reactors Fast Ceramic Reactor Development Program Thirtieth Quarterly Report February - April 1969," GEAP-10028 (May 1969).

7.10 Leonard, J.E. Duncan, J.D., Rao, A.S. and Cipolla, R.C., "Emergency Core Cooling Tests of an Internally Pressurized Zircaloy-Clad, 8x8 Simulated BWR Fuel Bundle," Licensing Topical Report, NEDE-20231-PA, April 1976.

7.11 Miller, R.W., Lussie, W.G., "The Response of $UO_2$ Fuel Rods to Power Bursts, Detailed Tests on 5/16-Inch OD, Powder Fuel, Zircaloy Clad Rods," IN-1302 (IDO-ITR-106) (June 1969).

7.12 Schraub, F.A., Bock, R.G., "Fuel Failures During Simulated Loss-of-Coolant Conditions," APED-5479 (March 1968).

8.1 "Reactor Safety Study," WASH-1400 (NUREG-75/014), Appendix VII, USNRC, 1975.

8.2 "BWR Turbine Equipment N-16 Radiation Shielding Studies," D.R. Rodgers, NEDO-20206, December 1973.

8.3 "Performance of an Off-Gas Monitor System," R. S. Gilbert. H. R. Helmholz, NEDM-12239, September 30, 1971.

8.4 "Technical Deviation of BWR 1971 Design Basis Radioactive Material Source Terms," NEDO-10871, J. M. Skarpelos, R. S. Gilbert, March 1973.

8.5 USNRC Standard Review Plan 15.4.9, Appendix, "Radiological Consequences of Control Rod Drop Accident (BWR)", NUREG-75/087, 1975.